UNIVERSITY OF CALIFORNIA,
IRVINE

Brain Computer Interface Design for Robot Assisted Neurorehabilitation

DISSERTATION

submitted in partial satisfaction of the requirements
for the degree of

DOCTOR OF PHILOSOPHY

in Mechanical and Aerospace Engineering

by

Sumner Lee Norman

Dissertation Committee:
Professor David J. Reinkensmeyer, Chair
Assistant Professor Beth A. Lopour
Associate Professor Zoran Nenadic
Professor Ramesh Srinivasan

2017

DEDICATION

To

the shoulders of giants

∴

TABLE OF CONTENTS

LIST OF FIGURES

LIST OF TABLES

ACKNOWLEDGEMENTS

I would like to thank Dr. David J. Reinkensmeyer whose greatest strength as a professor is his “assist-as-needed” approach to both robotics and advising. Dave, thank you for your continuing leadership and example. Your insight, guidance, and kindness made my journey to a PhD an incredible experience. I would like to thank Ramesh Srinivasan, Zoran Nenadic, and Beth Lopour, who all played major roles in demystifying the art of multivariate time series analysis.

I would like to thank my colleagues in the Biorobotics lab and beyond. Specifically, I would like to thank Justin Rowe, whose patience and willingness to help are second to none. I would like to thank Albert Sans and Jaime Duarte, great friends and lab-mates always ready with an espresso with a side of conversation. I would like to thank Diogo Schwerz, Oliver Stoller, and Joan Aguilar for their friendship and our enlightening discussions on a broad range of topics in- and outside the realm of research.

This project would not have been possible without the support of the National Science Foundation Graduate Research Fellowship that allowed me to pursue an exciting new line of research. I’d like to thank Sue & Nick Alexopoulos and everyone at ARCS foundation who, in addition to funding my work, introduced me to some truly incredible people. Finally, I’d like to thank the UCI Graduate Division for the Public Impact Fellowship and the opportunity to write/edit for National Public Radio: The Loh Down on Science, opportunities that gave me the chance to bring this important research, and science like it, to the public eye during a critical era where science and technology advocacy is more important than ever.

I would like to thank my parents, Annie and Stewart, who encouraged me to pursue an education at all costs and supported my ambitions every step of the way. Finally, I would like to thank my wife, Krissta. You are the life force behind this work. Thank you.

CURRICULUM VITAE

EDUCATION

Ph.D., Mechanical and Aerospace Engineering August 2017
University of California: Irvine
NSF fellow, ARCS scholar, Public Impact fellow, Commencement Speaker 2017

M.S., Mechanical and Aerospace Engineering December 2014
University of California: Irvine

B.S., Mechanical Engineering May 2012
University of Utah
High Honors, Undergraduate Research Scholar, FE Certification

EXPERIENCE

University of California, Irvine September 2012-August 2017
Ph.D. Candidate, Control Systems - Biorobotics

- Led an interdisciplinary research collaboration investigating brain-computer interface technology for use in robotics & human-machine interfaces.
- Developed robot controllers and algorithms for upper extremity exoskeletons to enhance human sensorimotor learning.
- Integrated robotic hardware and gaming software subsystems with new robot controllers.
- Designed and implemented four clinical trials/experiments, including writing standard procedures for physicians, physical therapists, engineers, and scientists.
- Developed a new neural-network model of motor learning and fused its fundamental findings with hardware/software design and clinical trial design of experiments.
- Designed and assembled wearable devices and high-precision robotics for basic science.

Journal of NeuroEngineering and Rehabilitation January 2015-August 2017
Editorial Board Member

- Contributed to improving impact factor by 45% through a new selective review process. JNER is now the #3 ranked journal in Rehabilitation and #12 ranked journal in Biomedical Engineering.
- Facilitated review and publication of approximately 400 scientific paper submissions annually.
- Reviewed academic papers as an editorial board member, associate editor, or peer reviewer.

National Public Radio (NPR) April 2016-May 2017

Managing Editor & Writer, "The Loh Down on Science"

- A syndicated radio minute available on 89.3 FM in Los Angeles and as an NPR podcast.
- Managed the production of over 200 scripts from a team of 18 writers, ensuring scientific accuracy and script quality throughout production.
- Contributed 20 broadcast scripts on scientific news with appeal to a non-technical audience.
- Completed a 10-week science communication course (UC Irvine), sharpening written & oral presentation.

University of Utah May 2011- September 2012

Research Assistant, Haptics and Embedded Mechatronics

- Designed, built, and published experimental results of an upper extremity haptic robot.
- Conceived an infrared tracking system to compensate for human error using haptic feedback.
- Designed and assembled a new calibration base for high-precision devices.

Brigham Young University May 2010 – September 2010

Research Assistant, Condensed Matter Physics

- Used crystallography theory and computational modeling to simulate x-ray diffraction experiment results.
- Validated real-world single crystal x-ray crystallography data against computational models.

AWARDS AND HONORS

Graduate Hooding Commencement Speaker, UC Irvine	2017
Public Impact Fellowship Distinguished Fellow, UC Irvine	2016
BCI Meeting 2016 Student Travel Award, BCI Society	2016
Neuromuscular Plasticity Scholar, University of Florida	2016
Graduate Student Research and Travel Grant Award, UC Irvine	2016
Data Science Initiative Scholar Award, UC Irvine	2015
Dean's Award, 2015 AGS Symposium, UC Irvine	2015
ARCS Fellowship Award, Orange County Chapter	2014
National Science Foundation Graduate Research Fellowship Award	2012
Tau Beta Pi Engineering Honors Society	2010
Tuition Waiver Scholarship, University of Utah	2009
New Century Scholarship, University of Utah	2007

SCIENCE & TECHNOLOGY COMMUNICATION

Graduate Research Advocacy Day Apr 2017
Sacramento, CA
Represented the University of California, advocating the importance of research to California lawmakers. Advocated for a $9 million budget-line appropriation to fund 900 new PhD students across the UC system.

AAAS Catalyzing Advocacy in Science and Engineering Apr 2017
Washington, D.C.
As one of two elected students, participated in a three-and-a-half-day workshop to explore tools for effective science communication and civic engagement within the structure and organization of Congress, the federal budget, and appropriations processes. Conducted meetings with elected Members of Congress.

Neural Interfaces Plenary Speaker Jun 2016
Baltimore, MD
Session: "*Using Targeted Neuroplasticity to Trigger Widespread Beneficial Plasticity*", North American Neuromodulation Society/Neural Interfaces Conference (NANS-NIC). NANS-NIC provided AMA PRA category 1 continuing education credits for physicians.

UC Innovation & Entrepreneurship Day May 2016
Sacramento, CA
Successfully advocated for the Innovation and Entrepreneurship (I&E) Assembly Bill (AB 2664): Investing in Innovation and Economic Growth which proposed a $22-million-dollar investment to more than double the current state investment in I&E programs at the University of California. Meeting with state lawmakers, representing the UC school system, led to its eventual success passing in the house.

Congressional Robotics Caucus & Congressional Inventions Caucus Nov 2015
Rayburn House Office Building/Eisenhower Executive Office Building, Washington, D.C.
Represented UC Irvine alongside Carnegie-Melon as national leaders in robotics and innovation at the congressional robotics caucus and inventions caucus. Met with national lawmakers including congressional members and the Office of Science and Technology Policy at the White House to promote research and the impact of science funding at the national level.

Course on Science Communication March–June 2015
University of California: Irvine. Irvine, California, USA
Participated in a ten-week program that emphasized science communication to lay audiences, with a focus on public speaking and science advocacy. Offered a part-time position at NPR at the conclusion of the course.

PUBLICATIONS

Journal Articles

J1. Norman, S.L., McFarland, D.J., Miner, A., Wolpaw, J.R., Wolbrecht, E., Reinkensmeyer, D.J. (in preparation). Training Sensorimotor Rhythms Improves Robot Assisted Movement Therapy after Stroke.

J2. McFarland, D.J., Norman, S.L., Sarnacki, W.A., Wolbrecht, E., Reinkensmeyer, D.J., Wolpaw, J.R. (in preparation). BCI-based Sensorimotor Rhythm Training Can Affect Individuated Finger Movements.

J3. Norman, S.L., Wolpaw, J.R., Reinkensmeyer D.J. (in preparation). Using Targeted Neuroplasticity to Improve Motor Recovery after Neurological Injury. *Neural Networks*.

J4. Norman, S. L., Dennison, M., Wolbrecht, E., Cramer, S.C., Srinivasan R., & Reinkensmeyer, D. J. (2016, January). Movement Anticipation and EEG: Implications for BCI-Contingent Robot Therapy. *IEEE Transactions on Neural Systems and Rehabilitation Engineering, 24(8), 911-919.*

J5. Norman, S. L., Doxon, A. J., Gleeson, B. T., & Provancher, W. R. (2014). Planar Hand Motion Guidance Using Fingertip Skin-Stretch Feedback. *IEEE transactions on haptics*, *7*(2), 121-130.

Conference Articles & Abstracts

C1. Jin, B.J., Zhong, H., Norman, S.L., de Lucena D.S., Roy, R.R., Gerasimenko, Y., Reinkensmeyer, D.J., Lu, D.C., & Edgerton, R. (Accepted 2017, June). Combination of Epidural Stimulation, Serotonergic Agonist, and Rehabilitative Training Promotes Forelimb Recovery in Cervical Spinal Cord Injured Rats, *Neuroscience 2017*.

C2. Norman, S.L., Lobo-Prat, J., Reinkensmeyer, D.J. (2017, July). How do strength and recovery interact after stroke? A computational model for informing robotic training, *International Conference on Rehabilitation Robotics 2017*.

C3. McFarland, D.J., Norman, S.L., Sarnacki, W.A., Wolbrecht, E.T., Reinkensmeyer, D.J., Wolpaw, J.R. (2016, November). BCI-Based Sensorimotor Rhythm Training Can Affect Individuated Finger Movements, *Neuroscience 2016*.

C4. Norman, S.L., McFarland, D.J., Sarnacki, W.A., Wolpaw, J.R., Wolbrecht, E.T., Reinkensmeyer, D.J. (2016, May). Sensorimotor Rhythms During Preparation for Robot-Assisted Movement, *BCI Meeting.*

C5. Norman, S.L., Sarigul-Klijn, Y., & Reinkensmeyer, D.J. (2016, April). Design of a Wearable Robot to Enable Bimanual Manipulation after Stroke. *Southern California Robotics Symposium 2016*.

C6. Aguilar, C., Shanta, O., Tran, T., Reinkensmeyer, D.J., & Norman, S. (2015, October). Towards a Low-Cost Alternative for BCI-aided Neurorehabilitation: A Comparison of the Emotiv Epoc to a Clinical EEG System. *American Society of Neurorehabilitation 2015 Annual Meeting Abstracts*.

C7. Norman, S.L., Dennison, M., Srinivasan, R., & Reinkensmeyer, D.J. (2015, April). Movement Anticipation and EEG: Implications for BCI-Contingent Robot Therapy. *Neural Engineering, 2015. Conference Proceedings. 7th International IEEE EMBS Conference on.* IEEE, 2015.

C8. Maughan, N. M., Norman, S., Robertson, D. G., & Campbell, B. J. (2011, October). Defect-induced diffuse scattering in microporous aluminophosphate-5. In *APS Four Corners Section Meeting Abstracts* (Vol. 1, p. 3004).

C9. Maughan, N., Norman, S., Robertson, D., & Campbell, B. (2010, October). Framework defects in microporous materials. In *APS Four Corners Section Meeting Abstracts* (Vol. 1, p. 2003).

MENTORSHIP

Mentor - Physical Medicine & Rehabilitation Clinicians

Alex Miner, MD — February 2017 – current
Physical Medicine & Rehabilitation, UC Irvine School of Medicine

Alessandro Bragetti, MD — December 2016- March 2017
Physical Medicine & Rehabilitation, UC Irvine School of Medicine

Mentor - Undergraduate Students

Camilo Aguilar — November 2014-December 2015
Electrical Engineering, University of California Irvine

Omar Shanta — November 2014-December 2015
Electrical Engineering, University of California Irvine

Thuong Tran — November 2014-December 2015
Mechanical Engineering, University of California Irvine

TEACHING

University of California, Irvine — March 2015 – June 2017

Teaching Assistant, Mechanical Systems & Robotics

This third-year level course (>300 students/year) covered theory and experiments on control systems, filters, amplifiers, structural resonance, and vibration. Topics were covered with an emphasis on their use in building robots and mechatronic devices. A final project saw the design and construction of a robot for a class competition. Duties involved lab design, instruction, grading, and occasional lecture instruction.

TECHNICAL SKILLS (selected)

	Most Experienced		**Experienced**
Languages	MATLAB	C++	Python
	SolidWorks	Visual Basic	R
	BCI2000 (C++)	Mathematica	
	Simulink Real-Time	Git	
	Mercurial		
Techniques	Neural Networks	Machine Learning	AI - Tensor Flow
	Computational Modeling		
	Electrophysiology Analysis		
Software/OS	SolidWorks	Linux	
	Adobe Creative Suite	Cluster Computing	
	Microsoft Office		
	OS X		
	Windows		
Subjects	Mechatronics (Robotics)	Thermodynamics	
	Numerical Methods	Heat Transfer	
	Solid-state physics	Fluid Dynamics	
	Dynamics	Material Science	
	Control Systems		

PARTICIPATION IN WORKSHOPS

Data Science Initiative Introduction to R *January 2016*
University of California: Irvine. Irvine, California, USA

Introduction to Linux and Cluster Computing *October 2015*
University of California: Irvine. Irvine, California, USA

ASU Rehabilitation Robotics Workshop *February 2015*
Arizona State University. Tempe, Arizona, USA

EU-COST School on Computational Methods for Neurorehabilitation *January 2015*
European Network on Robotics for Neurorehabilitation. Obertauern, Austria

ASU Rehabilitation Robotics Workshop *February 2013*
Arizona State University. Tempe, Arizona, USA

ABSTRACT OF THE DISSERTATION

Brain Computer Interface Design for
Robot Assisted Neurorehabilitation

By

Sumner L. Norman

Doctor of Philosophy in Mechanical and Aerospace Engineering

University of California, Irvine, 2017

David J. Reinkensmeyer, Chair

Stroke is the number one cause of movement disability in the world. In recent years, robotic assistance has empowered people with stroke to complete intensive movement therapy in motivating environments, thus matching or bettering the motor recovery attainable with traditional therapy. Yet, motor deficits remain stubbornly persistent, especially for those with severe impairments.

Brain-computer interfaces (BCI) are a technology that can facilitate direct communication between the brain and an external device. BCIs have already been used to control robotic prostheses to replace lost function. The premise of this dissertation is that, with the right tools and knowledge, BCIs could also help restore function to those with movement disability after a neurologic injury. In this dissertation, I investigate use of a BCI to help individuals with a stroke shape their brain activity while moving the fingers with assistance from a robotic orthosis, with the goal of guiding activity-dependent plasticity in the brain to drive motor recovery. The working hypothesis is that appropriately shaping brain activity will improve finger movement ability and provide a therapeutic benefit after stroke.

First, I present a computational model of motor learning that uses a neural network to simulate the motor cortex after a stroke and during subsequent finger force recovery.

These simulations suggested that BCI-based interventions should target perilesional motor areas, thus restoring normative network recruitment during finger movement, and that targeted training should make up about 20% of total limb use to maximize recovery.

In a study of unimpaired people completing a robot-assisted movement task, I identified a key confound of BCI-contingent robot-assisted therapy, showing that robot assistance can affect the BCI even when the participant is passive, which may hinder motor learning. I also present a potential design approach for both the robot and the BCI to avoid this confound.

I then explore BCI methodological considerations in two experiments with impaired and unimpaired people moving in a robot-assisted environment. Key results included that bipolar EEG recordings and finger extension movements led to the best models correlating brain state with ensuing movement and are thus most conducive to BCI-based training.

The culmination of this work is the design of a BCI-robot rehabilitation paradigm, which I tested in a study with eight people with severe impairment after a chronic stroke. Participants participated in four weeks of a therapy protocol that determined the effect of BCI-based sensorimotor rhythm control on finger extension performance. Here, we found that BCI training can improve subsequent movement performance – a result never before found for individuals with a stroke. The training also produced therapeutic benefits, indicating its viability as a future rehabilitation intervention. Finally, looking to the future of BCI-robot therapy, I present low-cost alternatives for BCI signal acquisition and wearable robotic devices.

CHAPTER 1: INTRODUCTION

Movement is the only method we have to interact with the world and with each other. All communication, whether writing, speaking, or gesturing, is facilitated through movement. After a neurologic injury, this world can be diminished. With an interface between brain and robot, this world could be restored – or even expanded.

1.1 STROKE

Stroke is the leading cause of disability in the world (Feigin et al., 2014; Lopez, Mathers, Ezzati, Jamison, & Murray, 2006), affecting over 700,000 people in the US each year (Broderick et al., 1998). A stroke occurs when blood flow to the brain is interrupted, either by a blockage or when blood vessels burst. The affected neurologic circuitry often causes a deficit in descending neural pathways. For example, damage to motor areas will affect movement in the form of paresis and/or spasticity. Indeed, about 80% of people with acute stroke experience functional motor deficits (Gresham et al., 1995). After a neuro-motor injury, activities of daily living (ADLs) become more difficult. As a result, less than half of stroke survivors return to work. Functional impairment is also a significant contributor to post-stroke depression (Teasell, Foley, Bhogal, & Speechley, 2003).

To some extent, these deficits are reversible. After injury, a massive reorganization of cortical and sub-cortical function occurs, especially in areas related to movement (Cramer & Crafton, 2006), a phenomenon referred to as neuroplasticity. Although a significant portion of motor function recovery is spontaneous, motor practice can enhance the effects of neuroplasticity (Calautti & Baron, 2003). People with stroke typically undergo several months of motor therapy rehabilitation with the hope of improving their ability to move, a process driven by the brains inexorable ability to reorganize itself through neuroplasticity.

The amount of function a person can recover during traditional movement therapies is limited, and varies greatly (Teasell et al., 2003). One potential limiting factor is the amount of movement therapy available to people with stroke. A systematic review of 123 randomized clinical trials (RCTs) demonstrated that intensity and task specificity are likely the main drivers of effective motor therapy following stroke (Janne Marieke Veerbeek et al.,

2014). And yet, the number of task-specific upper extremity movements during a typical stroke rehabilitation session averages just 32 repetitions (Lang, MacDonald, et al., 2009), far fewer than is thought to be necessary for functional recovery (Kleim & Jones, 2008).

1.2 ROBOT ASSISTED MOTOR REHABILITATION

Robot-assisted therapy has been suggested to assist people with stroke in training high quality movements with a high number of repetitions, with the expectation that the increased activity can improve therapy outcomes (Kahn, Zygman, Rymer, & Reinkensmeyer, 2006; Krebs, Volpe, Aisen, & Hogan, 2000; P. Lum, Reinkensmeyer, Mahoney, Rymer, & Burgar, 2002; Reinkensmeyer, Emken, & Cramer, 2004; Sanchez Jr et al., 2005). Robotic therapy has also been suggested to use active-assisted movements to help a patient complete a movement they couldn't normally complete independently, and active-resisted movements in higher-level patients to strengthen movement synergies (P. Lum et al., 2002). A systematic review found that upper arm robot-assisted therapies can significantly improve motor function after stroke (Kwakkel, Kollen, & Krebs, 2007). However, many therapy robots are currently complex and come at a substantial financial cost. Therefore, for such devices to be clinically justified, their efficacy must match or exceed that of the standard of care. Indeed, many robot-assisted protocols have exhibited therapy outcomes that were comparable to, or better than, similar amounts of intensive training without robot assistance (Lotze, Braun, Birbaumer, Anders, & Cohen, 2003; P. S. Lum et al., 2005; Volpe et al., 2005; Volpe et al., 2008).

The mechanisms behind robot-assisted therapy's efficacy are under continuing investigation. One important question is whether sensory engagement alone, without overt movement intention, is enough to aid motor outcome after therapy. In a key study, robot-assisted training that required patient volition, measured by electromyography (EMG), showed therapy outcomes exceeding that of an equal number of passive, robot-induced movements (Hu, Tong, Song, Zheng, & Leung, 2009). Thus, we can conclude that an important factor for ensuring the effectiveness of robotic therapy is active effort by the patient, a view shared by the field (Hidler et al., 2009; Hornby, Campbell, Zemon, & Kahn, 2005; Kaelin-Lang, Sawaki, & Cohen, 2005; Lotze et al., 2003). Even so, it is difficult to ensure patient

engagement. Physically assisting in movement with a robot can trigger slacking by the motor system, which is an automatic and subconscious reduction in patient effort (Israel, Campbell, Kahn, & Hornby, 2006; Reinkensmeyer et al., 2004; Reinkensmeyer, Wolbrecht, et al., 2012; Brendan Wesley Smith, 2017; Wolbrecht, Chan, Reinkensmeyer, & Bobrow, 2008). Thus, it is important when designing robotic therapy systems to develop methods that encourage patient engagement and effort during the therapy and prevent slacking, since robotic assistance may, in some cases, innately encourage slacking.

1.3 BRAIN COMPUTER INTERFACE

Brain computer Interface (BCI) technology, sometimes called a brain-machine interface, is a system that records neural or neural-population activity, and transmits those signals to a decoder that can provide a direct communication channel from the brain to an external device (Wolpaw, Birbaumer, McFarland, Pfurtscheller, & Vaughan, 2002). BCI technology has already proven its substantial utility in people with devastating neurologic disorders. For example, people with advanced amyotrophic lateral sclerosis (ALS) or a brainstem stroke, who can be "locked in" with no ability communicate on their own, can use a BCI to communicate with family, friends, and caretakers once again (Daly & Wolpaw, 2008).

Beyond replacing lost function, BCI can also guide activity-dependent plasticity in the brain by providing feedback on specific neural networks; to wit, several BCI interventions have shown promise to promote adaptive plasticity (Cramer et al., 2011). Brain imaging-based interventions promote adaptive plasticity by providing feedback to the patient, e.g. a visual cursor on a screen, to induce behavioral learning through operant conditioning. A protocol that bases its feedback to the patient on an electrical analog of functional activity in the CNS of that patient is known as neurofeedback, a process first attempted in 1968 (Wyrwicka & Sterman, 1968) and in humans shortly thereafter (Kamiya, 1969). Neurofeedback protocols have since been extended to induce long-term functional and structural changes in specific CNS networks, a process now known as "targeted neuroplasticity" (Sitaram et al., 2016; Wolpaw, Braitman, & Seegal, 1983).

It is not clear how interventions can restore normative biological function to the brain (Cramer et al., 2011). However, evidence suggests that beneficial reorganization of the

sensorimotor system after stroke is dependent on the type and amount of motor training provided (Cramer et al., 2011; Kiper et al., 2016). Still, the optimal targets and dosages for enhancing adaptive plasticity (i.e. plasticity associated with a gain in function) are unclear (L. G. Cohen et al., 1997). Further, it is possible to elicit maladaptive plasticity (i.e. plasticity associated with a loss of function or other negative consequences) (Nudo, 2006). Thus, attempts to improve motor recovery using targeted neuroplasticity have produced mixed results. For example, Ramos-Murguialday et al. found modest improvements in motor outcome compared to a control group in an electroencephalography (EEG)-based BCI that triggered movement in a hand orthosis for people with chronic hand impairment after stroke (Ramos-Murguialday et al., 2013). A similar study used a magnetoencephalography (MEG)-based BCI but found no significant improvement in clinical scales used to rate hand function (Buch et al., 2008). There have been no studies of fMRI-based targeted neuroplasticity that have shown clinical or functional motor improvement after a stroke.

For many people with severe paralysis after stroke, moving their impaired limb is difficult, if not impossible, even after traditional movement therapy. A potential use for BCI is in the practice of motor imagery (MI). That is, the practice of mental rehearsal of a physical movement task at the cerebral level without any physical demands (Jackson, Lafleur, Malouin, Richards, & Doyon, 2001). In an MI paradigm, the therapy is directly targeting the stroke impaired brain with the goal of affecting function in the impaired limb. BCIs most commonly consider changes in the sensorimotor rhythm (SMR) to detect MI. For example, normative physiological SMR modulation includes a down-regulation of power in the mu (8-13 Hz) and beta (13-30 Hz) frequency bands preceding movement, a phenomenon known as event-related desynchronization (ERD) (Pfurtscheller & Aranibar, 1977; Pfurtscheller & Lopes da Silva, 1999). However, movement related signals are known to be significantly smaller in amplitude (Fu, Daly, & Cavusoglu, 2006) and more spatially distributed (Cramer et al., 1997) in people with stroke than in those without impairment. Despite these confounding effects of stroke, in this document I will show that people with stroke can learn to control a BCI over the course of multiple EEG recording sessions and with similar success rates to people without neurologic injury.

1.4 COMPUTATIONAL MODELING

Although targeted neurofeedback has experienced significant growth and promising results in recent years, it has not yet reached its full potential. This is, in part, due to the complexity and cost of brain imaging techniques in clinical practice. Computational models of motor learning might therefore be useful for predicting principles of adaptive plasticity during motor rehabilitation that can be later validated in a clinical setting. However, despite a large body of computational modeling in neuroscience, only a handful of models exist that have attempted to model the mechanisms underlying sensorimotor rehabilitation. A recent review compares these models (Reinkensmeyer et al., 2016). For example, a model by Han et al. (Han, Arbib, & Schweighofer, 2008) used a population vector framework to simulate reinforcement and error-based learning of a bilateral limb task. The authors work predicted a threshold level of motor recovery that, if surpassed, allowed the model's spontaneous activity to bootstrap future recovery, a phenomenon the authors call a "virtuous cycle". In another model of reinforcement learning, Reinkensmeyer et al. (Reinkensmeyer, Guigon, & Maier, 2012) employed a simplified corticospinal (CS) neural network with inherent stochastic noise to simulate finger extension force recovery after stroke. The model used a reinforcement learning algorithm to optimize CS activation patterns. The network predicted several experimental observations of motor recovery after stroke including exponential recovery, latent residual capacity, and shift of motor activity to secondary motor areas.

1.5 GOALS OF THE DISSERTATION

The marriage of a BCI system's ability to target neuroplasticity in the brain, and a robotic system's ability to affect real-world movements, have the potential to greatly impact the field of stroke rehabilitation and, in time, the everyday lives of people living with movement disability after stroke. In this document, I address the need for investigation into the mechanisms behind BCI and robot-assisted movement environments and how one might affect the other.

In Chapters 2 and 3, I address this problem by simulating motor learning after a stroke using a computational model based on a neural network architecture that is generalizable to other motor tasks and neurologic injuries. In Chapter 2, I use this model to

elucidate potential mechanisms that could allow targeted plasticity to enhance movement recovery after a stroke. In Chapter 3, I use the model to gain insight into how targeting strength versus coordination could affects motor recovery. In Chapter 4, I describe a key potential confound of robot-assisted movement on BCI-contingent therapy using an experiment with unimpaired people in a robot-assisted movement environment – that is, robotically assisting in movement in a predictable way when a person is a passive can cause changes in brain activity similar to when they are active. In Chapter 5, I explore potential means of solving this confounding issue using data-driven approaches to identifying patient engagement in a motor task. In Chapter 6, I explore several ways of approaching a BCI-robot therapy protocol, using data from two pilot studies in both impaired and unimpaired people. These studies address several methodological considerations for the experimental design and system parameters for a new BCI-robot therapy protocol. In Chapter 7, the findings in the work described thus far are synthesized to inform the design and execution of a novel BCI-robot therapy. I describe the clinical study of eight people with stroke who participated in four weeks of a BCI-robot therapy experiment and present my findings on how BCI-robot training can modulate the ability to extend the fingers and may be viable as a future rehabilitation intervention. Finally, in Chapter 7, I look towards whether BCI-enhanced, robotic therapy can be made pragmatic. First, I compare a low-cost EEG headset with the clinical gold standard. Finally, I present a wearable robot for the hand. I present these low-cost devices to provide a viewpoint of this technology's eventual transfer out of the clinic and into people's homes.

CHAPTER 2: USING TARGETED NEUROPLASTICITY TO IMPROVE MOTOR RECOVERY AFTER NEURLOGICAL INJURY: A COMPUTATIONAL MODEL

2.1 ABSTRACT

People with motor deficits after stroke, spinal cord injury, or other neurologic injuries often develop abnormal patterns of neural activity that appear to limit motor recovery. New therapies that can target beneficial plasticity to critical sites could enhance recovery of more normal activity. One such therapy provides the individual with feedback that reflects the output of specific neural circuits with potential to improve motor performance. This paper describes a computational model that provides insight into the mechanisms of movement recovery and predicts optimal parameters for inducing beneficial neuroplasticity. Here we use the model to simulate the recovery of finger extension after a cortical stroke. The model employs a biologically plausible reinforcement learning algorithm in which the motor system uses feedback about simulated finger force. This guides a stochastic search for optimal activation of a network of corticospinal cells, located in two hemispheres, with a range of connection strengths to the finger extensor motor neuronal pools, and a range of intrinsic firing rate variability. When undamaged, the network lateralized cortical activation for finger extension to the contralateral hemisphere. But after a simulated stroke the network produced an abnormal pattern of cortical organization – activation in both hemispheres for unilateral movement – a result consistent with imaging data, even though this pattern produced less extension force than the remaining network was theoretically capable of. To access the latent capacity for recovery, we interdigitated normal learning (I_A) with a targeted plasticity intervention (I_B) that gave the network feedback on the summed activity of a specific, targeted population of ipsilesional cells. This intervention normalized cortical activation by re-lateralizing it, thereby improving force recovery. Its effectiveness depended on which population of cells was targeted and on the relative frequencies of I_A and I_B trials. Targeting low variability cells on 20% of trials maximized motor recovery. The model suggests that under normal reinforcement learning, cells that are more quickly optimized can block involvement of other cells that could contribute to recovery. Targeted plasticity I_B was effective at re-integrating these cells. These results provide rationale and

guidance for using targeted neuroplasticity interventions after neurologic injury, and they predict clinically testable principles for optimizing the parameters of these interventions.

2.2 INTRODUCTION

Stroke is the leading cause of disability worldwide; it affects over 700,000 new people in the US each year (Feigin et al., 2014; Lopez et al., 2006). About 80% experience motor deficits and typically undergo several months of movement rehabilitation (Gresham et al., 1995). During this period, electroencephalography (EEG) and functional magnetic resonance imaging (fMRI) reveal substantial reorganization of cortical movement-related activity (Calautti et al., 2010; Calautti et al., 2007; Cramer & Crafton, 2006; Wolpaw & Carp, 2006; C.-Y. Wu et al., 2010; Yozbatiran & Cramer, 2006). As a result, contralesional movements are typically associated with abnormally low activation of the ipsilesional cortex and abnormally high activation of contralesional cortex (Cramer et al., 1997; Fu et al., 2006; Rossiter, Boudrias, & Ward, 2014; C.-Y. Wu et al., 2010). This loss of normal hemispheric laterality correlates with decreased motor function; it may reflect a suboptimal compensatory strategy that limits motor recovery (Calautti et al., 2010; Cramer & Crafton, 2006). Therefore, abnormal movement-related cortical activation may be an important therapeutic target (Levin, Kleim, & Wolf, 2008).

Currently, however, it is not clear how interventions can restore normative biological recruitment (Cramer et al., 2011). While evidence suggests that beneficial reorganization of the sensorimotor system after stroke is dependent on the type and amount of motor training provided (Cramer et al., 2011; Kiper et al., 2016), the optimal targets and dosages for enhancing adaptive plasticity (i.e. plasticity associated with a gain in function (L. G. Cohen et al., 1997)) are unclear. Further, it is possible to elicit maladaptive plasticity (i.e. plasticity associated with a loss of function or other negative consequences) (Nudo, 2006).

Several interventions have, however, shown promise to promote adaptive plasticity, including brain stimulation and feedback-based brain imaging (Cramer et al., 2011). For example, transcranial magnetic stimulation (TMS), excites cortical neuron populations by inducing oscillatory trains of current in the cortex using extracranial magnetic coils (Plow, Carey, Nudo, & Pascual-Leone, 2009; Wagner, Valero-Cabre, & Pascual-Leone, 2007;

Webster, Celnik, & Cohen, 2006). TMS currents can be used to selectively modify brain potentials. For example, by enhancing excitability in the ipsilesional hemisphere or inhibiting the contralesional hemisphere, Fregni et al. could promote gains in motor function in people with mild to moderate movement impairment after a stroke (Fregni & Pascual-Leone, 2007). This approach has produced promising results with aphasia as well (Martin et al., 2004).

Brain imaging-based interventions to promote adaptive plasticity differ from brain stimulation in that they do not directly affect the central nervous system (CNS). Instead, they provide feedback to the patient to induce behavioral learning through operant conditioning. A protocol that bases its feedback to the patient on an electrical analog of functional activity in the CNS of that patient is known as neurofeedback, a process first attempted in 1968 (Wyrwicka & Sterman, 1968) and in humans shortly thereafter (Kamiya, 1969). Neurofeedback protocols have since been extended to induce long-term functional and structural changes in specific CNS networks in a process known as "targeted neuroplasticity" (Sitaram et al., 2016; Wolpaw et al., 1983). Such protocols have most commonly using brain-computer interface (BCI) technology. BCI proficiency has been successfully demonstrated in severely paralyzed individuals with cerebral palsy (Daly & Wolpaw, 2008), muscular dystrophy (Hashimoto, Ushiba, Kimura, Liu, & Tomita, 2010), spinal cord injury (G. Müller-Putz, Daly, & Kaiser, 2014), and stroke (Soekadar et al., 2011). This type of targeting can be achieved in real time using various imaging techniques including fMRI-based measures of localized brain activation (Christopher deCharms et al., 2005; Cox, Jesmanowicz, & Hyde, 1995), EEG (Fok et al., 2011; Ramos-Murguialday et al., 2013; Soekadar, Witkowski, Birbaumer, & Cohen, 2014), and MEG (Buch et al., 2008; Fabiani, McFarland, Wolpaw, & Pfurtscheller, 2004).

Attempts to improve motor recovery using brain-imaging-based neurofeedback training have produced mixed results. Ramos-Murguialday et al. found modest improvements in motor outcome compared to a control group in an EEG-based brain-computer interface (BCI) that triggered movement in a hand orthosis for people with chronic hand impairment after stroke (Ramos-Murguialday et al., 2013). A similar study used a magnetoencephalography (MEG)-based BCI but found no significant improvement in clinical

scales used to rate hand function (Buch et al., 2008). fMRI-based neurofeedback interventions are limited but rapidly increasing (Sulzer et al., 2013). They have, thus far, shown promising results in schizophrenia, chronic pain, dyslexia, Parkinson's disease, and depression (Cramer et al., 2011; Sulzer et al., 2013). One study targeted secondary motor areas using fMRI to decrease intracortical inhibition (Sitaram et al., 2012), which could potentially usher future gains in functional motor recovery.

Although brain imaging based neurofeedback has experienced significant growth and promising results in recent years, it has not yet reached its full potential. This is, in part, due to the complexity and cost of brain imaging techniques in clinical practice. Computational models of motor learning might therefore be useful for predicting principles of adaptive plasticity during motor rehabilitation that can be later validated in a clinical setting. However, despite a large body of computational modeling in neuroscience, only a handful of models exist that have attempted to model the mechanisms underlying sensorimotor rehabilitation. A recent review compares these models (Reinkensmeyer et al., 2016). For example, a model by Han et al. (Han et al., 2008) used a population vector framework to simulate reinforcement and error-based learning of a bilateral limb task, predicting a threshold level of motor recovery. If surpassed, spontaneous activity bootstraps future recovery, a phenomenon the authors call a "virtuous cycle". In another model of reinforcement learning, Reinkensmeyer et al. (Reinkensmeyer, Guigon, et al., 2012) employed a simplified corticospinal (CS) neural network with inherent stochastic noise to simulate finger extension force recovery after stroke. The model used a reinforcement learning algorithm to optimize CS activation patterns. The network predicted several experimental observations of motor recovery after stroke including exponential recovery, latent residual capacity, and shift of motor activity to secondary motor areas. In this paper, we expand the model of (Reinkensmeyer, Guigon, et al., 2012) to incorporate additional biologically plausible neuronal parameters and use the model to explore mechanisms of unphysiological reorganization after a simulated a stroke and the effects of targeted neuroplasticity on motor learning and cortical reorganization.

2.3 METHODS

We simulated the effects of targeted neuroplasticity in the context of learning to extend the fingers after a stroke. The mathematical model was comprised of a simulation of CS cells, located in two hemispheres, with a range of connection strengths to the finger extensor motor neuronal pools, and a range of intrinsic firing rate variability. We simulated learning finger extension in three scenarios: 1) when the network was undamaged; 2) following a unilateral (i.e. hemispheric) injury to the network, thereby simulating stroke rehabilitation, and 3) using targeted plasticity following the injury. In the targeted plasticity training condition, the simulated patient was provided direct feedback concerning the output of a targeted population of cells.

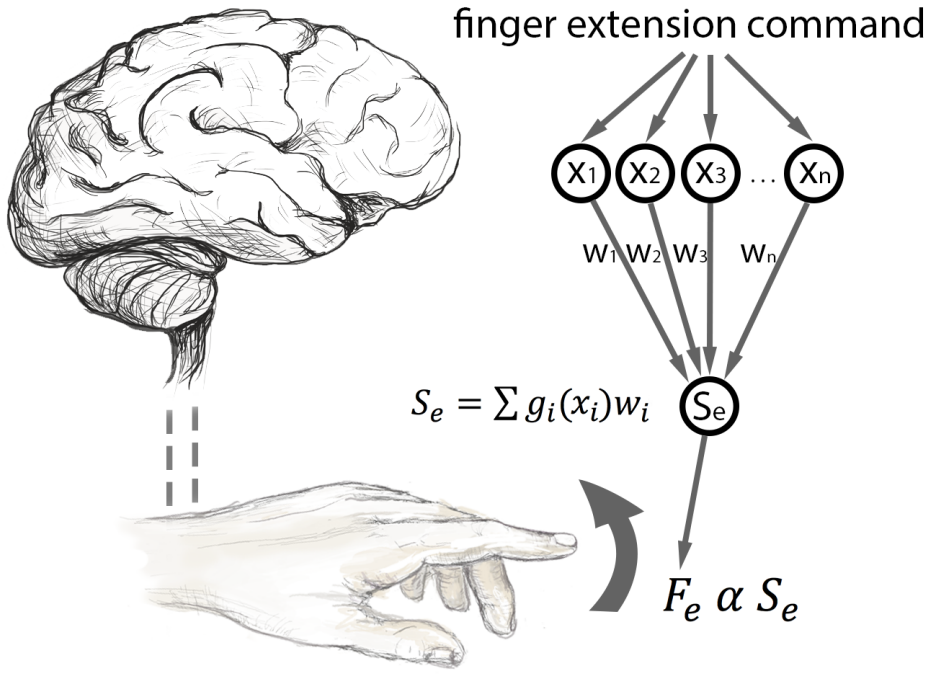

FIG. 1: ARCHITECTURE OF THE NETWORK FOR EXERTING FINGER EXTENSION FORCE. THIS TWO-LAYER FEEDFORWARD NEURAL NETWORK INCORPORATES N CORTICOSPINAL CELLS WITH ACTIVATION LEVELS X_I, GENERATED WHEN THEY ARE GIVEN A COMMAND TO MAXIMIZE FINGER EXTENSION FORCE F_E. A FINGER MOTONEURONAL POOL S_E SUMS THE WEIGHTED ACTIVATION PATTERNS. A NONLINEAR FUNCTION G_I IMPLEMENTS THE PHYSIOLOGICAL OBSERVATION THAT THE CONTRIBUTION OF ANY SINGLE CS CELL TO THE EXCITATION OF THE MOTONEURONAL POOL MUST SATURATE AT SOME FIRING RATE X_I; THAT IS, EACH CELL CAN ONLY RECRUIT A FINITE INCREMENT OF THE MOTONEURONAL POOL. THE NETWORK OPTIMIZES THE ACTIVATION PATTERN X USING REINFORCEMENT LEARNING IN SIMULATED CONSECUTIVE MOVEMENT PRACTICE TRIALS WHERE EXTENSION FORCE F_E IS THE TEACHING SIGNAL.

2.3.1 Architecture

The network was designed to simulate the behavior of CS cells in primary and secondary motor areas of both hemispheres before and after a stroke-like injury that damaged a unilateral motor area. The model incorporates a network of n CS cells that fire with activation levels (i.e. firing rates) x_i, given a command to maximize finger extension. Each CS cell is connected to a motoneuronal (MN) pool via a scalar weighting w_i. The MN pool sums the product of the cell activation x_i and weighting w_i using a saturation nonlinearity:

$$S_e = \sum g_i(x_i)w_i \quad (1)$$

where g_i sets the saturation limit of cell *i*. For simplicity, we will discuss the model with a constant saturation limit of +1 for all cells. Drawing from other distributions did not significantly affect the network dynamics discussed here. The MN pool activation level S_e is proportional to a unitless finger extension force F_e. Thus, the finger extension force generated is proportional to and determined by, the weighted, summed output of the CS network activation pattern. This model is simplified from that of (Reinkensmeyer, Guigon, et al., 2012), in that we did not simulate flexor/extensor pairs or inhibitory CS cells. Adding flexor/extensor and inhibitory connections did not alter the findings presented here or add to the findings of (Reinkensmeyer, Guigon, et al., 2012). Thus, these cell types were not included for clarity and to highlight the additions made to the model in this paper.

2.3.2 Network learning

The goal of the network is to learn the optimal activation pattern of the CS cells that results in the maximum network performance, i.e. the maximum finger extension force possible. Since the network consists only of cells that excite extensor motor neuronal pools, the optimal activation pattern is achieved when the activation of every cell is increased until the cell's saturation limit (1).

To do this, the network must iteratively adjust the activation patterns based on a single signal – the finger extension force achieved in any trial, a form of reinforcement learning. Feedback of a single signal as a method of optimizing a large network presents a

spatial credit assignment problem: if finger extension force F_e increased on the previous extension attempt, which cells are responsible for the increase? Reinforcement learning has been demonstrated to be a biologically plausible solution for solving the credit assignment problem (Anderson, Omidvar, & Dayhoff, 1997; Mazzoni, Andersen, & Jordan, 1991; Reinkensmeyer, Guigon, et al., 2012; Werfel, Xie, & Seung, 2005; Williams, 1992). Here, we implement reinforcement learning with stochastic search, using a noise process to generate a new CS network activation pattern on each movement trial, slightly perturbing the pattern from the one used in the previous movement attempt. The algorithm stores the new activation pattern if it results in increased finger extension force. Note that remembering a new activation pattern is equivalent to updating the weights of the connections from the command cell to the CS cells; we speak in terms of activations rather than weights for conceptual convenience, in the same manner as (Reinkensmeyer, Guigon, et al., 2012). Here we use the random search algorithm used in (Reinkensmeyer, Guigon, et al., 2012), a simplified form of the random search with chemotaxis algorithm first described in Anderson et al. (Anderson et al., 1997):

Given an initial activation pattern X_0 that produces a force F_0,

1. Activate CS cells with pattern $X_i=X_0+v_i$, where v_i is random noise, and measure the force F_i produced by this pattern.
2. Memorize the new pattern X_i if the force F_i it produces is greater than F_0; i.e. if $F_i>F_0$, then let $X_0=X_i$ and $F_0=F_i$.
3. Repeat.

We also tested a gradient descent stochastic search method, another biologically plausible solution to the credit assignment problem (Werfel et al., 2005). The best-first and gradient descent algorithms produced comparable results.

2.3.3 Cell parameters

CS cells in the model are described by their current activity level (i.e. its firing rate x_i), and synaptic weighting for activating the extensor MN pool (w_i). In addition, we augmented the model described in (Reinkensmeyer, Guigon, et al., 2012) to include different levels of inherent firing rate variability for each CS cell (σ_i). The network updates each cell's

activation level after a successful movement attempt, while its weighting and variability are constant throughout the simulation. The fixed weighting reflects the assumption that spared descending pathways are relatively immutable after injury, which is a simplification.

2.3.4 Synaptic weightings

The effects of both mono-synaptic and multi-synaptic CS pathways are captured in the model by a single, fixed functional connectivity from each CS cell to the simulated finger extensor MN pool (weights labeled w_i in Fig. 1). We explicitly represent both cortical hemispheres in the model, since the hemisphere ipsilateral to the moving finger is known to be able to activate the requisite MN pools through uncrossed pathways, and these pathways are thought to play a functional role after stroke (Cramer et al., 1997). We designed the distributions of the cell weightings to reflect the physiological situation. Cells from the hemisphere contralateral to the motor task are, on average, more strongly connected to the

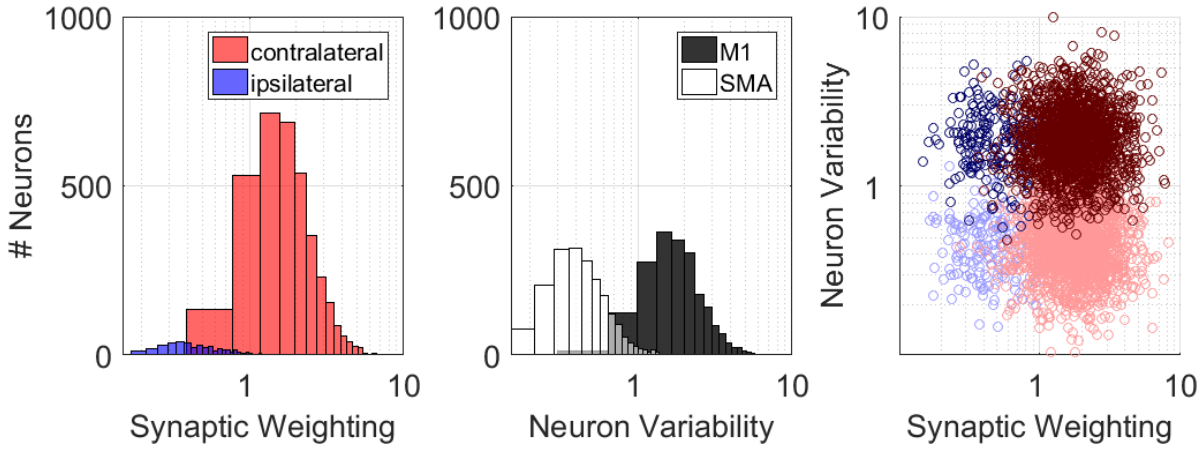

Fig. 2: Cell parameter distributions for a 10,000-cell network. Left: Synaptic weighting adheres to bimodal distributions of lognormal probability density functions whose aggregate mean is equal to one. Most cells reside in the cortex contralateral to the finger to be extended and have stronger weightings. The remaining cells reside in the ipsilateral cortex and have weaker weightings. Center: Cell variability adheres to bimodal distributions of lognormal probability density functions. Cells in primary motor areas (M1) are more task-related and exhibit more trial-to-trial variability during movement attempts. Cells in secondary motor areas (SMA) are less task-related and exhibit less trial-to-trial variability during movement attempts. Right: The resulting network has four broad types of cells -- 1: high-weighting/high-variability; 2: high-weighting/low-variability; 3: low-weighting/high-variability; 4: low-weighting/low-variability

MN pools than ipsilateral cells (Fig. 2, left). Furthermore, these contralateral cells outnumber the ipsilateral cells by a ratio of 9:1.

2.3.5 VARIABILITY

Stochastic disturbances have been shown to affect the nervous system at both the cellular level and, consequentially, the behavioral level (Faisal, Selen, & Wolpert, 2008). These disturbances drive the learning process in the simulated network via a stochastic search. The variability of a neuron's firing rate has been shown to be dependent on the neuron's activation level. Specifically, firing rate variability and mean firing rate are related by a power function, across cortical areas and behavioral conditions (Dean, 1981; Lee, Port, Kruse, & Georgopoulos, 1998). In our model, we simplify signal-dependent variability to more plainly elucidate the effects of cell variability on the network dynamics. We express the amount of trial-to-trial variability inherent in an individual CS cell's activation level by the standard deviation of a zero-mean normal distribution from which each cell's activation level is perturbed on each movement trial. Thus, a high-variability cell sees larger stochastic perturbations on average than a low-variability cell. We simplify the physiological situation in that each cell's variability remains constant.

Later, we discuss the effects of cell populations' variability on network dynamics. It is, therefore, helpful to discuss variability in terms of spatial areas of the brain similar to how we analogize synaptic weighting to laterality in the brain. Recent findings have shown that higher variability in a motor task improves motor learning (Selinger, O'Connor, Wong, & Donelan, 2015; H. G. Wu, Miyamoto, Castro, Ölveczky, & Smith, 2014). We assume that these behavioral observations are indicative of the brain areas associated with the task at hand. For example, it is well understood that primary motor cortex (M1) is active during a motor task, while secondary motor areas are less active during the same task. We therefore assume motor cortical areas more closely associated with the task have higher variability during execution of the task. For example, M1 cells have a higher variability for the finger extension task than secondary motor areas. We keep in mind that it is not likely that high- and low-variability neurons are distributed such that they are spatially exclusive (van Steveninck, Lewen, Strong, Koberle, & Bialek, 1997; Warzecha & Egelhaaf, 1999). For this reason, we

overlapped the high-variability and low-variability cells in primary and secondary motor areas, respectively. Although most high-variability cells reside in M1, there is a significant population of high-variability cells in secondary motor areas. Similarly, most low-variability cells reside in secondary motor areas while a minority of low-variability cells reside in nearby M1 (Fig. 2).

2.3.6 CELL PARAMETER DISTRIBUTIONS

Functional and structural parameters in the brain, including synaptic weightings and firing rates, are not normally distributed, but rather are strongly skewed with a heavy tail more closely approximated by lognormal distributions (Buzsáki & Mizuseki, 2014). We chose the distributions of synaptic weight, variability, and initial activation patterns based on these observations. That is, we initiated the CS activation pattern X_0 at the beginning of every simulation using a pseudorandom activation pattern sampled from a lognormal distribution. We also sampled synaptic weighting and cell variability from distributions of lognormal probability density functions. For simplicity, we will discuss the model whose weighting and activation variability were sampled from a distribution with a mean of one ($\mu=1$). Thus, the mean possible force contribution of each cell (the product of its activation and connectivity), was one ($\mu_{Fi}=1$).

2.4 SIMULATIONS

We simulated three scenarios using the model presented here: learning finger extension – 1: with the uninjured network; 2: following a unilateral injury to the network 3: using targeted plasticity training following injury. In all three scenarios, the network consisted of 10,000 CS cells. We tested initial activation patterns X_0 sampled from uniform, normal, and log-normal distributions of varying magnitudes, finding comparable results. Before the stroke and targeted plasticity simulations, the network activation pattern was kept from the final activation pattern of the uninjured network, apart from the lesioned cells whose activation and weighting were set to zero.

Since network learning is driven by movement attempts, the dosage of movement attempts affects the learning dynamics. In a recent observational study, Lang et al. found that participants with stroke completed an average of 32 functionally oriented movements per

day during upper extremity rehabilitation sessions (Lang, MacDonald, et al., 2009). However, recent rehabilitation interventions have successfully administered 150 to 250 trials per session, for up to 23 sessions (Buch et al., 2008). In the simulations presented here, the network trained for 150 trials/day for 180 days. We chose to keep dosage consistent between training scenarios for conceptual convenience and clarity of the results.

2.4.1 Scenario I: Learning with an undamaged network

Here we simulated learning in the network without simulated injury as a baseline. Finger extension force was determined using all 10,000 CS cells. The teaching signal was the finger extension force produced during subsequent movement attempts.

2.4.2 Scenario II: Recovery after injury

To simulate cell death after a stroke, we de-weighted a subpopulation of the network by permanently setting its connectivity and activation level to zero. We simulated strokes that affected randomly sampled subpopulations and several different subpopulations organized by cell parameters. Changing the location of stroke did not alter the principal findings of the model. However, the results were more pronounced with increasing stroke severity, i.e. when the more strongly connected and/or more variable network populations were damaged. For simplicity, we will present the results after a simulated stroke in the most detrimental stroke locale: high-weighting, high-variability cells. The teaching signal was the finger extension force produced from the remaining intact CS cells.

2.4.3 Scenario III: Learning with targeted feedback

Finally, we simulated learning the finger extension task during a targeted neuroplasticity intervention after a stroke-like injury. We focused on the ability for this scenario to trigger network reorganization to gain a better understanding of what dosage and brain locations could most enhance motor recovery after injury. To this end, we tested the effects of giving targeted feedback on several combinations of network subpopulations and different dosages. During targeted feedback trials, the model was only given feedback on a network subpopulation. That is, separate training signals were generated for the total network (finger extension force, I_A) and the targeted network subpopulation (targeted

intervention, I_B). During the targeted feedback trials, the reinforcement learning algorithm was only given access to the increase or decrease in net force produced by the targeted subpopulation, but the network would update all residual cells. We interspersed targeted feedback training with regular training at different ratios to determine the optimal dosage and schedule for this technique. That is, should one practice only with targeted feedback or should one intersperse normal movement trials where finger extension force is the teaching signal and, if so, what is the optimal mix of training?

2.5 RESULTS

2.5.1 SCENARIO I: LEARNING WITH AN UNDAMAGED NETWORK

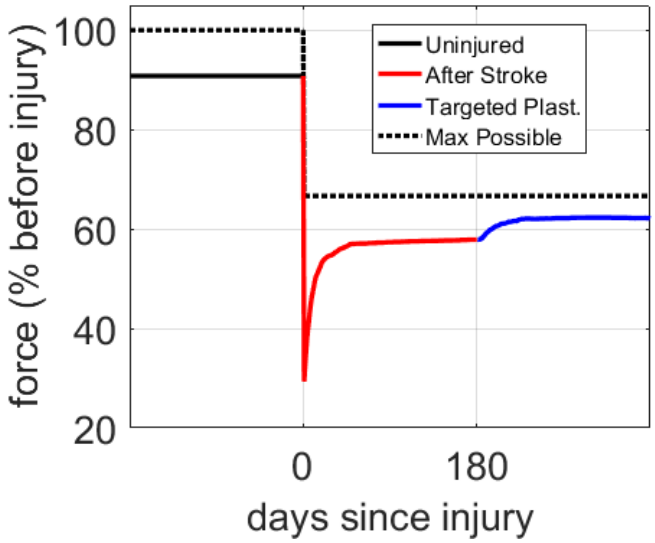

FIG. 3: FORCE PRODUCTION AS A FUNCTION OF TIME WHERE FORCE IS PRESENTED AS A PERCENTAGE OF THE MAXIMUM FORCE POSSIBLE IN THE UNINJURED NETWORK. AFTER A STROKE, FORCE PRODUCTION WAS SIGNIFICANTLY REDUCED, BUT EXHIBITED RESIDUAL CAPACITY. TARGETED PLASTICITY FACILITATED INCREASED FORCE PRODUCTION COMPARED TO NORMAL RECOVERY.

After training, the undamaged network achieved about 92% of the maximum possible finger extension force (Fig. 3). High variability cells were optimized first; that is, their activations were maximized (Fig. 4).

2.5.2 Scenario II: Recovery after injury

To simulate cell death after a stroke, we removed a subpopulation of cells from the network. This resulted in reduced force output, illustrated in Fig. 3 at day 0. Network recruitment was also suboptimal. For example, before the injury, the network favored the optimization of high-variability (M1), high-weighting (contralateral) cells, leaving low-

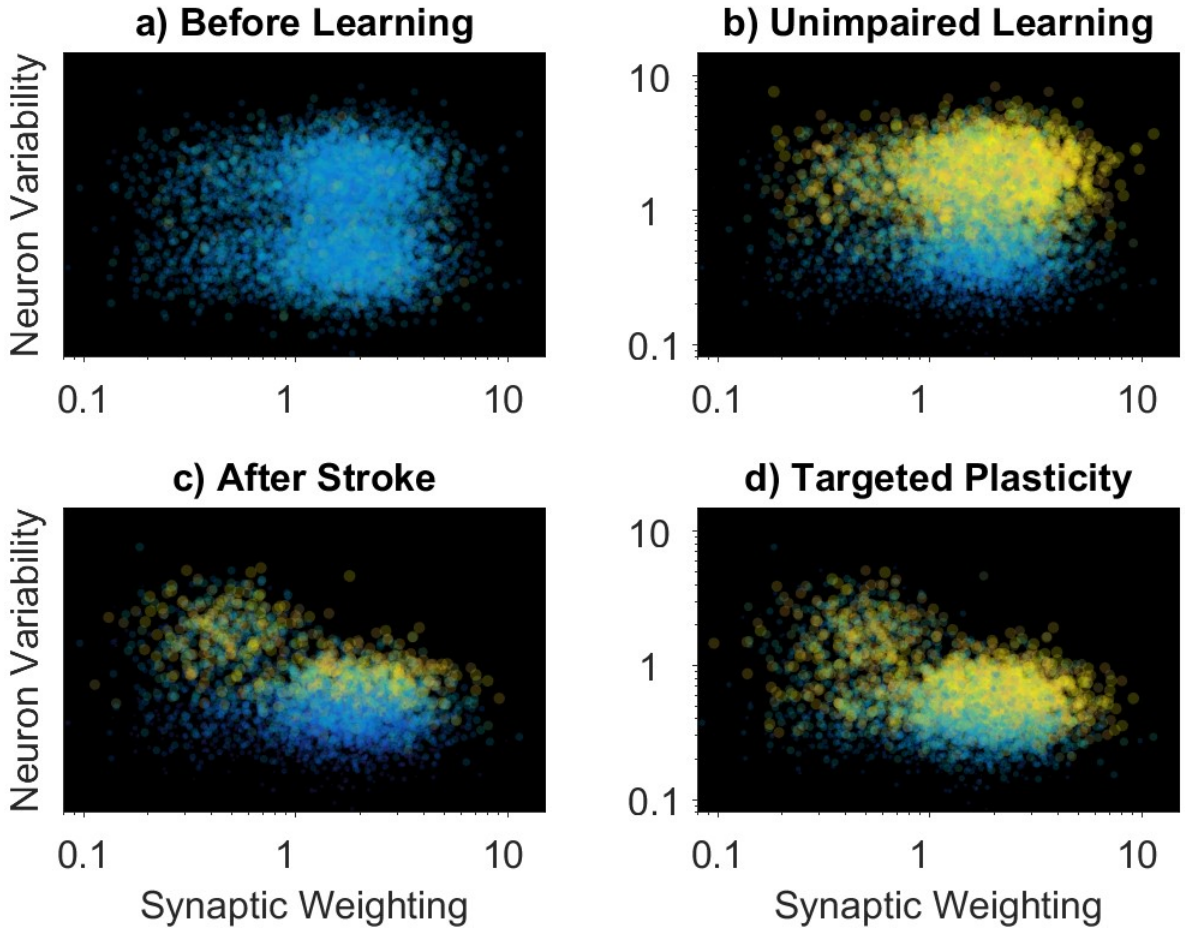

Fig. 4: Scatter plots of a 10,000-cell network's activation patterns presented in a variability/weighting parameter space after different simulations of learning. (To view results in the anatomical space, see Fig. 5) Network activation was initialized to a pseudorandom sample of activation levels, seen in A. In B, the uninjured network optimized (yellow) high-weighting/high-variability cells during learning. After a stroke, a significant portion of the high-weighting/high-variability cells were removed from the simulation, as seen by the missing cells in C. Learning after injury exhibited similar behavior to uninjured learning, favoring high-weighting/high-variability cells. Residual capacity remained because low variability cells remained unoptimized. In D, targeted plasticity was given on 20% of trials. Network recruitment was reorganized. Difficult-to-access, low-variability cells were recruited, resulting in a more evenly-dispersed activation pattern.

variability, low-weighting cells less optimized (Fig. 4b). After a simulated injury, the model again favored high-variability, high-weighting cells (Fig. 4c). However, because a significant portion of these cells was lesioned, the network recruited high-variability cells with low weighting, shifting activity towards the poorly connected contralesional hemisphere. This resulted in increased force production, but also left the network with residual capacity to generate more force (Fig. 3). Scenario III: Learning with targeted feedback

We tested the effects of giving targeted feedback on secondary motor areas (low-variability cells) to harness network plasticity to optimize previously un-optimized, but still well-connected, cells. These targeted cells represent cortical areas that have the potential to significantly improve overall network performance but are less likely to be optimized by reinforcement learning due to their relatively low variability. Given feedback on one in five trials over the same training period, the network showed a broad reorganization of cell recruitment during the motor task (Fig 4d), leading to an overall increase in finger extension force production (Fig 3).

2.5.3 Lateralization of brain activity

To visualize the predicted effect on imaged brain activity, we created a mapping of cell parameters to brain areas associated with the motor task. Specifically, we mapped -- 1: high-weighting/high-variability to contralateral M1; 2: high-weighting/low-variability to contralateral secondary motor areas; 3: weak-weighting/high-variability to ipsilateral M1; 4: weak-weighting/low-variability to ipsilateral secondary motor area. In Fig. 5, we use this mapping as a tool to visualize network reorganization across hemispheres during learning before and after a stroke or after a stroke with targeted plasticity training.

During uninjured learning, the model optimized the primary motor/high-variability cells first, which resided in the hemisphere contralateral to the finger (Fig. 5). After stroke, the model exhibited a shift in activation toward the unaffected hemisphere, i.e. toward high-variability cells with relatively low weighting. Following targeted plasticity training which targeted low-variability cells, the model re-lateralized activation, leading to improved motor recovery.

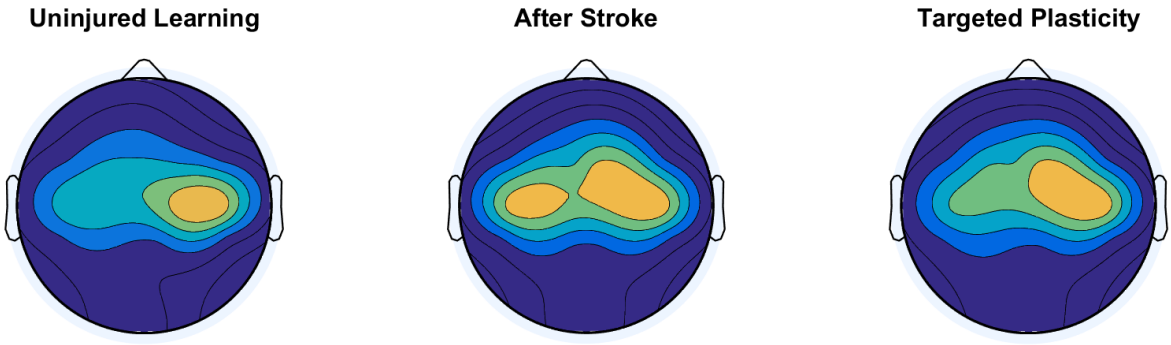

FIG. 5: VISUALIZATION OF NETWORK ORGANIZATION AT THE TERMINATION OF TRAINING IN THE THREE DIFFERENT TRAINING CONDITIONS: LEARNING IN THE UNINJURED NETWORK, LEARNING AFTER STROKE, AND LEARNING AFTER STROKE WITH TARGETED PLASTICITY. AFTER TRAINING, THE UNINJURED NETWORK FAVORS HIGH-VARIABILITY/HIGH-WEIGHTING CELLS, MAPPED AS ACTIVATION IN THE CONTRALATERAL M1 CORTICAL AREA. AFTER A STROKE, THE NETWORK CANNOT EASILY ACTIVATE LOW-VARIABILITY CELLS AND COMPENSATES BY RECRUITING HIGH-VARIABILITY/LOW-WEIGHTING CELLS IN THE IPSILATERAL (CONTRALESIONAL) CORTEX, RESULTING IN LESS-FOCAL ACTIVATION IN CONTRALATERAL (IPSILESIONAL) M1 AND BILATERAL ACTIVATION FOR A UNILATERAL TASK. BY GIVING THE NETWORK INTERDIGITATED TARGETED PLASTICITY AND REGULAR MOVEMENT ATTEMPTS, THE NETWORK REORGANIZES, RECRUITING THE HIGH-WEIGHTING BUT DIFFICULT TO ACCESS (LOW-VARIABILITY) CELLS IN CONTRALATERAL (IPSILESIONAL) SECONDARY MOTOR AREA, RESTORING LATERALITY – A MORE NORMATIVE PHYSIOLOGICAL ACTIVATION PATTERN THOUGHT TO IMPROVE RECOVERY.

2.5.4 OPTIMIZING TARGET LOCATION AND TRAINING SCHEDULE

One of the model's utilities is its ability to predict the effects of targeted feedback on different neuronal populations. First, we will define restitution as the percentage of the latent residual capacity recovered by using targeted feedback training, where zero restitution is the same force produced by the injured network and 100% restitution is the maximum force the injured network could theoretically produce. Giving feedback on bilateral secondary motor areas (low variability cells) yielded 21.3% restitution of motor function. Giving feedback on secondary motor areas in the ipsilesional cortex only (low-variability/high-connectivity cells) yielded the most recovery: 29.5% restitution. Targeting primary motor areas in the contralesional hemisphere (high-variability/low-connectivity cells) was less effective: 4.7%.

We also used the model to test the effect of varying the targeted feedback training schedule. At low dosages of targeted feedback, e.g. 1 in 1000 or 0.1% of trials, there was little to no training effect. As the ratio of targeted feedback increased above 1%, there was an

increase in restitution with a maximum occurring when targeted feedback was given on one in five or 20% of trials (Fig. 6). Restitution declined at higher dosages. For example, giving targeted feedback on one in ten trials was more effective in terms of motor recovery than giving targeted feedback on every trial. We tested the effects of dosage ratio on many different populations of cells and on many different network types, injured or uninjured. The restitution curve (Fig. 6) was robust to these changes. These results suggest that there exists an optimum dosage of targeted plasticity when interspersed with regular movement practice that is robust to changes in targeted areas.

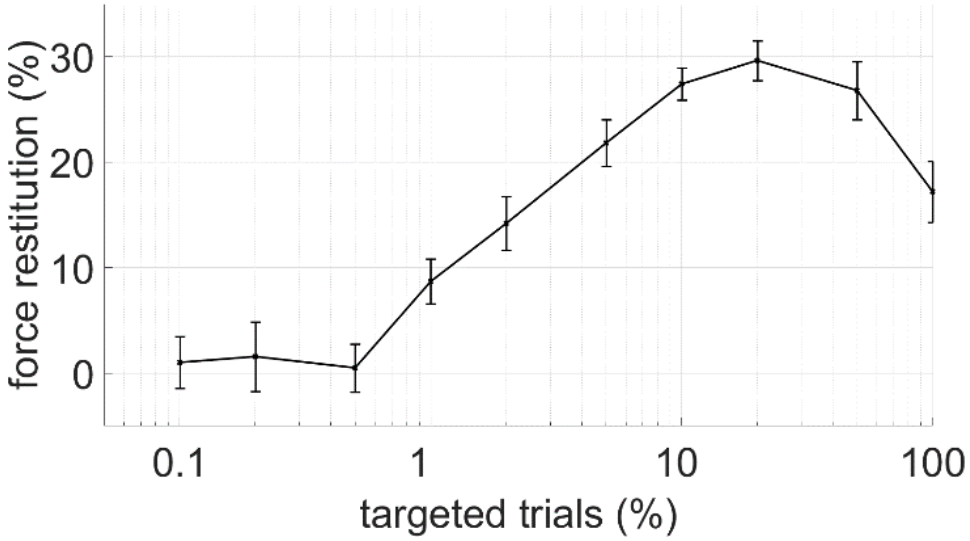

FIG. 6: FORCE RECOVERY AS A FUNCTION OF THE PERCENTAGE OF TRIALS THAT RECEIVED TARGETED FEEDBACK. ERROR BARS REPRESENT STANDARD DEVIATION WHERE THE SIMULATION WAS PERFORMED 20 TIMES FOR EACH DATA POINT. TARGETED PLASTICITY HAS LITTLE TO NO EFFECT AT DOSAGES LESS THAN 1%. RECOVERY IMPROVED WITH INCREASED DOSAGE OF TARGETED FEEDBACK, REACHING A MAXIMUM RESTITUTION WHEN 20% OF TRIALS WERE GIVEN TARGETED FEEDBACK. RECOVERY DECLINED WHEN TARGETED FEEDBACK WAS GIVEN IN EQUAL OR GREATER DOSAGE THAN REGULAR MOVEMENT PRACTICE.

2.5.5 MECHANISMS: CELL-SPECIFIC OPTIMIZATION RATES AND "BLOCKING"

To summarize, key network phenomena were: 1) hemispheric lateralization of activation following learning in the undamaged brain 2) a shift towards bilateral activation following simulated cortical stroke; 3) a residual capacity for force recovery within the context of this bilateral cortical activation pattern; and 4) re-lateralized activity and improved force recovery following targeted plasticity. What accounts for these phenomena?

Why did activity lateralize in the undamaged brain, but become bilateral after the simulated stroke? And why did targeted plasticity help remediate this situation? The answer revolves around two mechanisms: cell-specific optimization rates (by which high variability cells optimize first) and "blocking" (in which saturated cells block further optimization of less variable cells).

To elucidate these mechanisms, we used a Monte Carlo method wherein we ran the same, single time-step of the model 10,000 times; once at a time-step at the beginning of network training, and once at a time-step after the network had been trained for 180 days (100 movements per day). After training, the mean network activation improves to ~85% of its maximum. We grouped the cells into four groups: 1: fast (high variability)/strong (high weighting); 2: fast/weak; 3: slow/strong; 4: slow/weak. We calculated the probability that each group would, through their summed activity, contribute to a positive change in force, as well as the probability that the summed activity of all four groups together (i.e. the entire population) would contribute to a positive change in force. Recall, if the entire population contributes to a positive change in force, the stochastic search "captures" (i.e. remembers) the activation pattern that achieved this positive change. Further, we calculated the mean change in activation (δX), across cells in each group, which would be expected should a positive change be captured. Finally, we calculated the mean contribution to a change in force (δF).

Which populations does the network optimize first? Before training, none of the cells were optimized (Fig 7b), and thus they increased or decreased their activity with equal probability on each trial (Fig. 7f). High-variability cells change by a relatively large amount on each movement attempt. Higher weighting to MN pools also increases the mean contribution in force. Thus, fast/strong cells optimize quickly (Fig 7e, before training), but eventually saturate (nonlinearity g described in (1)) after training (Fig 7b). At this point, they cannot contribute positively to force or it is extremely unlikely (Fig 7e, after training). The network then favors the optimization of fast/weak cells (Fig. 7d, after training).

Why are the fast/weak cells optimized before the slow/strong cells that have more potential to contribute to network performance? The answer lies in the network's

teaching signal: force. Because the network is only provided feedback on force, it optimizes network populations by their force contribution, not their activation change. This is apparent in the mean change in force (δF) for captured trials, where fast/weak and slow/strong networks are contributing to changes in force equally after training (Fig 7e, after training). Despite equal force contributions, the high variability fast/weak cells are optimizing more quickly than slow/strong cells due to their weak weightings (Fig. 7d).

Why did the network learn at increasingly slow rates, failing to optimize some cells? During training, the motor system learns based on its training signal: finger extension force. The probability that a cell can produce a change in activation that contributes to a positive change in force production is not equal for all cells once training starts. Saturated cells cannot contribute positively to force production. Strongly-connected and more-variable cells (fast/strong) optimize more quickly and thus, on average, saturate first. For the model to capture a new CS activation pattern, yet-to-be optimized cells must not only produce their own net positive effect on the model, but must also overcome any negative effect of the more-variable cells that are, on average, contributing negative forces (Fig. 7e). As more cells saturate, the chance of achieving a positive net change for all cells decreases (Fig. 7, right). Thus, the less-variable cells are effectively "blocked". This phenomenon, underpinned by the nonlinear saturation function, g, describes the latent residual capacity observed in the model (Fig. 3).

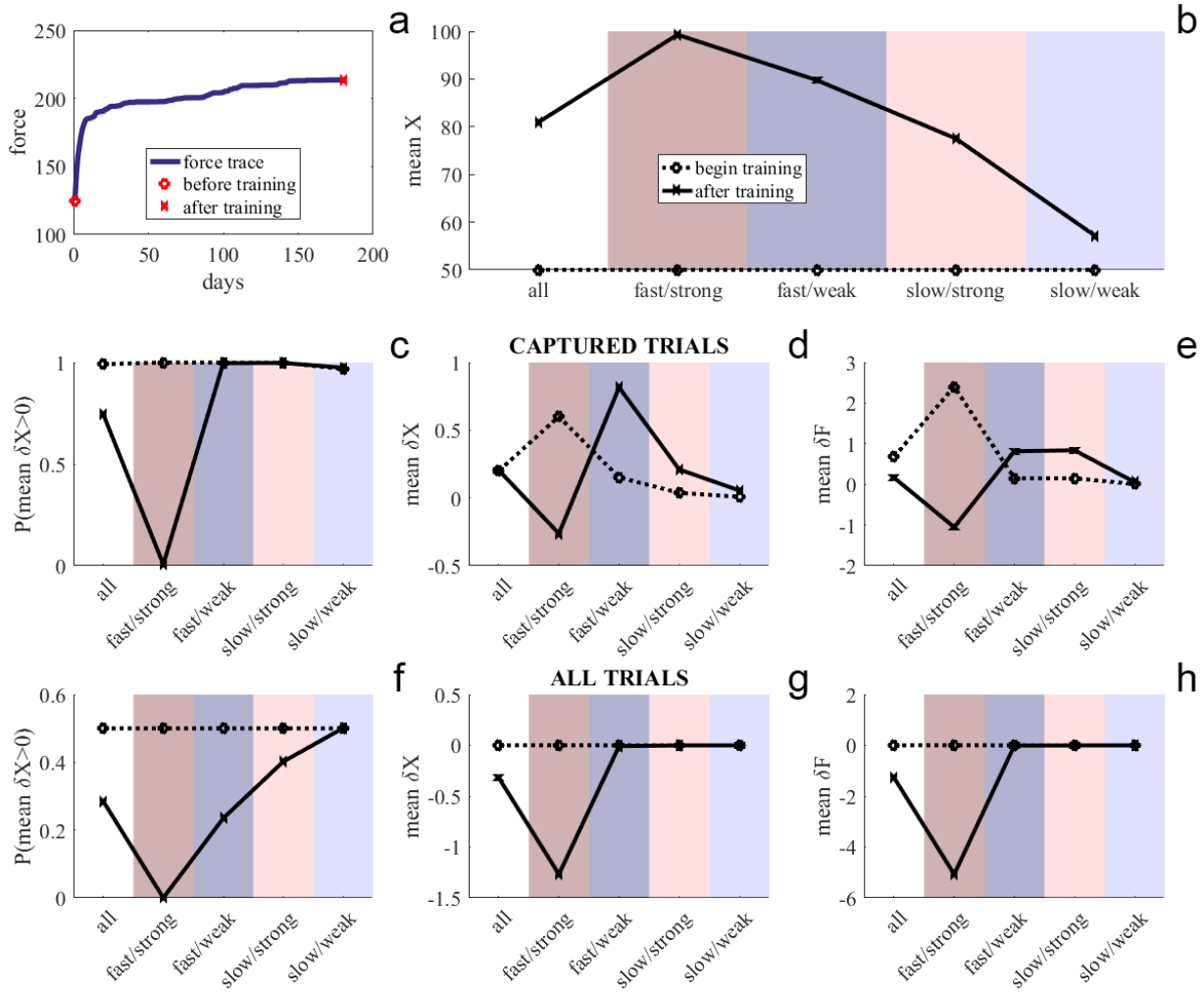

FIG. 7 NETWORK DYNAMICS CALCULATED AT TWO TIME STEPS, BEFORE AND AFTER A PERIOD OF TRAINING, USING A MONTE-CARLO SIMULATION. A: FORCE GENERATION OVER TRAINING PERIOD OF 180 DAYS (100 MOVEMENT ATTEMPTS/DAY). B: MEAN ACTIVATION LEVEL FOR EACH CELL POPULATION, BEFORE AND AFTER TRAINING. C: PROBABILITY THAT A CELL POPULATION'S MEAN CHANGE IN ACTIVATION WAS POSITIVE ON A CAPTURED TRIAL. D: MEAN CHANGE IN A CELL POPULATION'S ACTIVATION LEVEL, BEFORE AND AFTER TRAINING, FOR CAPTURED TRIALS. THIS IS EFFECTIVELY THE RATE OF OPTIMIZATION. E: A CELL POPULATION'S MEAN CONTRIBUTION TO THE FORCE CHANGE ON A GIVEN CAPTURED TRIAL, BEFORE AND AFTER TRAINING. THIS DESCRIBES WHICH POPULATION THE MODEL IS CURRENTLY OPTIMIZING. F: PROBABILITY THAT A CELL POPULATION'S MEAN CHANGE IN ACTIVATION WAS POSITIVE ON ANY GIVEN TRIAL. G: MEAN CHANGE IN A CELL POPULATION'S ACTIVATION LEVEL, BEFORE AND AFTER TRAINING, FOR ALL TRIALS. H: A CELL POPULATION'S MEAN CONTRIBUTION TO THE FORCE CHANGE ON ALL TRIALS, BEFORE AND AFTER TRAINING.

2.6 DISCUSSION

The model supports the premise that targeted plasticity can enhance motor recovery. The key results were:

- The network favored optimization of high-variability (M1) and high-weighting (contralateral) cells.
- Before injury, the network recruited high–variability cells, resulting in hemispheric lateralization of activity for the finger extension movement.
- After injury, the network recruited high-variability cells, even those with low weighting, i.e. contralesional hemisphere.
- Blocking leaves residual capacity for motor recovery.
- Targeted plasticity allowed the network to recruit previously difficult-to-access, low-variability cells, resulting in increased finger extension force.
- Optimal cell types to target are those with low variability, and highly connected cells, i.e. cells with potential to contribute to motor function that resist optimization due to blocking.
- There exists an optimum dosage of targeted plasticity when interspersed with regular movement practice – about 20%.

We first discuss the computational mechanisms explaining these results, and then directions for future research.

2.6.1 OPTIMIZATION PREFERENCES AND RESIDUAL CAPACITY

During training, the motor system learns by adjusting the output of CS motor cells using stochastic search based on knowledge of the overall motor performance, i.e. finger extension force. Strongly-connected and more-variable (fast) cells optimize more quickly, and thus, on average, saturate first. As more fast/strong cells saturate, they effectively "block" other cells, and the network loses out on their potential contribution. This results in latent residual capacity for network performance that is difficult for the network to access.

2.6.2 Network organization after injury

During uninjured learning, i.e. without simulated injury, the model optimizes high-variability (M1) cells first. Thus, learning a left-hand task would trigger learning in right hemisphere motor areas (Fig. 5), consistent with normative fMRI and EEG evidence where sensorimotor activation preceding and during a motor task is seen in primary motor areas associated with the task and contralateral to the limb involved (Grefkes & Fink, 2011; Kim et al., 1993; Pfurtscheller & Lopes da Silva, 1999).

When the motor cortical areas associated with hand movements are affected by an infarct (high variability, high weighting), cell death reduces their contributions to motor tasks, resulting in reduced motor performance (Fig. 3). As a result, the model exhibited a profound reorganization of network recruitment after stroke, a phenomenon well evidenced in clinical data (Grefkes & Fink, 2011; Yozbatiran & Cramer, 2006; Zemke, Heagerty, Lee, & Cramer, 2003). Specifically, the model exhibited a shift toward the unaffected hemisphere (Fig. 5), i.e. toward low-weighting, high-variability cells (Fig. 4), a result reflected in clinical fMRI studies of motor network reorganization after injury, wherein people with stroke often activate motor regions in the unaffected hemisphere during unilateral movements of the affected limb (Cramer et al., 1997; Grefkes & Fink, 2011; C.-Y. Wu et al., 2010). The network exhibited limited motor performance, mirroring clinical findings that have associated bilateral recruitment of motor areas during unilateral motor tasks with poor performance (Nelles et al., 1999). Indeed, previous studies have demonstrated functional improvement in people with stroke after they reduced activation in the unaffected hemisphere (Dong, Dobkin, Cen, Wu, & Winstein, 2006; Miyai et al., 2003).

2.6.3 Normal practice and targeted neuroplasticity

Recent findings have shown that higher variability in a motor task elicits improved motor learning (Selinger et al., 2015; H. G. Wu et al., 2014). However, primary motor areas (that typically exhibit high variability) may be damaged after a neurologic injury such as stroke. The model shows that, given regular movement practice, the brain will favor recruitment in the fastest learning areas of the network that will produce some recovery (Fig. 5, After Stroke), further evidenced in clinical data (Cramer et al., 1997). These activation

patterns are likely suboptimal, and will, therefore, limit recovery (Calautti et al., 2010; Cramer & Crafton, 2006). However, there exist network populations that have potential to improve motor recovery, but are difficult to access with regular motor practice. Given targeted plasticity feedback, the model exhibited a shift towards more normative brain patterns (Fig. 5, targeted plasticity), leading to improved motor recovery (Fig. 3).

The model suggests that the optimal cell types to target are those with low variability, i.e. cells that are less likely to already be optimized, and high weighting, suggesting that training the ipsilesional cortex (contralateral to movement) with robust structural connectivity to the MN pools associated with the task is important. Clinical studies of targeted feedback and cortical activation after neurologic injury also suggest that targeting brain areas that are normative to the motor task, i.e. with high connectivity, is more beneficial to motor recovery (Calautti et al., 2010; Cramer & Crafton, 2006).

2.6.4 Clinical applications

These results present a rationale for targeted feedback training to guide restitution of more normal recruitment in the affected hemisphere. The model predicts that, given a modest dose of targeted feedback motor practice, the network can recover significant amounts of residual force compared to traditional motor practice. This result is consistent with clinical evidence that has shown appropriate targeted feedback therapy can induce widespread adaptive plasticity leading to network reorganization associated with increased motor function (Ramos-Murguialday et al., 2013; Thompson, Pomerantz, & Wolpaw, 2013; Thompson & Wolpaw, 2015). Here, we discuss real-world interventions with the potential to facilitate targeted feedback training.

Real-time neuroimaging has been suggested as a tool to provide targeted feedback with the intention of improving recovery after neurologic injury (Cramer et al., 2011). This approach most commonly involves fMRI or EEG-based brain-computer interfaces (BCI) that are capable of imaging neural activation in real time. In one operant conditioning paradigm, the system rewards activation of pre-selected brain states by giving feedback directly to the participant and asking them to modify that brain state (Buch et al., 2008; Christopher deCharms, 2008; Ramos-Murguialday et al., 2013). This BCI approach has the effect of

temporarily amplifying cell networks that are not yet optimized, allowing those cells to train uninhibited by the more variable, highly trained cells. For example, Ramos et al. rewarded mu rhythm desynchronization in the ipsilesional motor cortex during intended movement in people with severe hemiparesis after stroke by providing robotically assisted hand grasping movement. In this study, the method of feedback, i.e. teaching signal, was both visual and proprioceptive in nature. BCI participants exhibited modest improvements in motor recovery compared to a sham-control group (Ramos-Murguialday et al., 2013). A similar study by Buch et al. rewarded mu-rhythm modulation in a magnetoencephalography-based BCI and reported no significant improvement in clinical scales used to rate hand function (Buch et al., 2008). These examples emphasize that, although BCI-based rehabilitation shows promise for improving motor recovery after stroke, identifying brain states that have the potential to improve motor recovery is a significant roadblock to optimizing BCI therapies. The model predicted specific principles of neural circuits that would most benefit motor recovery, given targeted feedback. Specifically, rewarding normative biological brain states in motor areas previously unassociated with the task, but still within the ipsilesional hemisphere may be more likely to enhance motor recovery.

Another principle predicted by the model is that, as the dose of targeted feedback training increases, overall motor recovery increases up to a maximum when targeted feedback is given on one in five or 20% of total movement attempts. Although there is a growing body of literature regarding the effects of targeted neuroplasticity, there have been, to our knowledge, no studies on the dose necessary to optimize motor recovery. This is a clinical hypothesis immediately testable in both human and animal models of motor recovery during targeted plasticity training. In one of the first successful targeted feedback applications, feedback was provided on 100% of movement trials while training the spinal stretch reflex (Wolpaw et al., 1983). A more recent study of targeted plasticity training as an intervention in people with stroke also provided feedback on 100% of trials (Buch et al., 2008). Our model suggests that the results of these interventions, and those like it, could be further improved with the principles on optimizing targeted plasticity training identified here.

2.6.5 Identifying a feedback modality

Reinforcement learning requires a method of feedback for evaluation. In the example scenario of learning finger movement after a simulated stroke, we assumed that the amount of finger extension force was available to the CS cell network of the simulated patient. However, diminished afferent sensation after stroke may make the amount of force difficult to interpret or completely opaque to the patient in severe cases. Many real-world applications of BCI use other unimodal or multimodal methods of feedback. The output of the system can be used for control of several external devices that provide varying types of feedback including orthoses (Buch et al., 2008; King et al., 2011; S. Norman et al., 2016; Ramos-Murguialday et al., 2013), on-screen cursors (Fabiani et al., 2004; McFarland, Sarnacki, & Wolpaw, 2015), or direct electrical stimulation of muscles (King et al., 2015). These feedback methods provide varying levels and types of sensation including visual, auditory, proprioceptive, and haptic stimuli. It is not yet clear which method or a combination of methods is optimal in each scenario, although they are likely task and subject specific. The modality of feedback is one possible future extension not considered in the model presented here.

2.6.6 Model generalizations and utility

Computational models of motor learning can simulate real-world scenarios of learning, especially after simulated neurologic injuries such as stroke (Reinkensmeyer et al., 2016). Although we discussed the model in terms of finger extension after a stroke, it is generalizable to many behaviors and CNS circuits. For example, with little to no modification, the CS cells could activate foot or leg MN pools to simulate ankle extension. The model may also be useful for entirely different CNS functions, including spinal circuits (Wolpaw & Tennissen, 2001). These are just a few examples of possible model applications that could lead to clinically testable hypotheses of motor learning in the CNS.

2.7 CONCLUSION

In this paper, we used a computational model to study finger extension after a simulated stroke to elucidate principles of motor performance before and after a stroke and after a stroke with targeted plasticity training. The model predicted latent residual capacity

for additional motor recovery after a stroke followed by a dose of normal movement practice. This residual capacity is difficult for reinforcement learning to access without extrinsic assistance because the optimization of low-variability cells that may have significant capacity to improve overall network performance becomes increasingly unlikely as the network optimizes high-variability cells. This result suggests that brain networks possess the capacity to generate significant improvements that current rehabilitation is not yet capable of revealing. Thus, the network exhibits utility in predicting how to exploit this residual capacity through targeted neuroplasticity interventions. After a simulated stroke that affected finger extension, the network produced abnormal cortical reorganization, including bilateral activation for unilateral movement, a result consistent with imaging data. In doing so, the network produced less force than it was theoretically capable of, indicating residual capacity for recovery. We then subjected the model to normal movement practice interdigitated with targeted plasticity training wherein feedback was given on the summed activity of a targeted population of ipsilesional cells. This training restored more normal cortical activation, i.e. unilateral activation in the ipsilesional hemisphere for a unilateral motor task, improving force recovery. The effectiveness of this therapy depended on the parameters of the cells targeted and the frequency with which targeted training was given. Targeting ipsilesional secondary motor areas on 20% of trials restored normative biological recruitment to the ipsilateral hemisphere and optimized force recovery. These results provide a rationale for using targeted neuroplasticity interventions after a neurologic injury and predict generalizable principles for optimizing the parameters of these interventions.

2.8 APPENDIX

2.8.1 CHARACTERIZING THE LEARNING CURVE WITH RESIDUAL CAPACITY

A key property of the model is the "residual capacity" of the model's force production after injury. That is, simulations exhibited learning curves of force production that did not reach their full potential, even through extensive motor practice, but which appeared to approach an asymptote (see Fig. 3), a result consistent with clinical evidence of force recovery after injury (Ada, Dorsch, & Canning, 2006; Barreca, Wolf, Fasoli, & Bohannon, 2003; French et al., 2007; Kwakkel et al., 2007; Page, Gater, & Bach-y-Rita, 2004; Rijntjes,

2006; Stinear et al., 2007; van der Lee et al., 2001). In fact, the force profile does continue to increase, similar to a power curve (Newell & Rosenbloom, 1981), but at an increasingly slow rate. A power curve never saturates. We simulated "100 years" of motor practice (150 trials/day). The network recovers ever-smaller amounts of force at high amounts of practice. Given infinite time, it approaches an asymptote due to the nonlinear maximum firing rate function g, described in Eq. 1. Thus, the learning curves described in Fig. 3 do not obey a power curve at large time scales. Furthermore, a single exponential function cannot accurately describe both 1) the initially fast learning of the network, and 2) its latent residual capacity at even modest simulation time lengths. Force production over time appears to be the sum of fast and slow exponential curves. This "double exponential" learning curve can be defined as:

$$f = \alpha(1 - e^{\frac{-t}{\tau_{slow}}}) + (1 - \alpha)(1 - e^{\frac{-t}{\tau_{fast}}}) \quad (2)$$

Where τ represents the time constant of each curve, α is a proportionality constant, and the compound curve sums to 1 as $t \to \infty$. This equation, a "mixed exponential" learning curve first shown in human motor learning literature (Newell & Rosenbloom, 1981), sufficiently describes learning in the model presented here and in (Reinkensmeyer, Guigon, et al., 2012), including the compound curvature and latent residual capacity phenomenon.

CHAPTER 3: HOW DO STRENGTH AND COORDINATION RECOVERY INTERACT AFTER STROKE? A COMPUTATIONAL MODEL FOR INFORMING ROBOTIC TRAINING

Note: This chapter has been published as:

Norman, Sumner L., Joan Lobo-Prat, and David J. Reinkensmeyer. "How do strength and coordination recovery interact after stroke? A computational model for informing robotic training." Rehabilitation Robotics (ICORR), 2017 International Conference on. IEEE, 2017.

3.1 ABSTRACT

Robotic devices can train strength, coordination, or a combination of both. If a robotic device focuses on coordination, what happens to strength recovery, and vice versa? Understanding this interaction could help optimize robotic training. We developed a computational neurorehabilitation model to gain insight into the interaction between strength and coordination recovery after stroke. In the model, the motor system recovers by optimizing the activity of residual corticospinal cells (focally connected, excitatory and inhibitory) and reticulospinal cells (diffusely connected and excitatory) to achieve a motor task. To do this, the model employs a reinforcement learning algorithm that uses stochastic search based on a reward signal produced by task execution. We simulated two tasks that require strength and coordination: a finger movement task and a bilateral wheelchair propulsion task. We varied the reward signal to value strength versus coordination, determined by a weighting factor. The model predicted a nonlinear relationship between strength and coordination recovery consistent with clinical data obtained for each task. The model also predicted that stroke can cause a competition between strength and coordination recovery, due to a scarcity of focal and inhibitory cells. These results provide a rationale for implementing robotic movement therapy that can adaptively alter the combination of force and coordination training to target desired components of motor recovery.

3.2 INTRODUCTION

Stroke is the leading cause of disability worldwide, affecting over 700,000 people in the US each year (Feigin et al., 2014; Lopez et al., 2006). It is estimated that 80% of survivors experience a motor deficit for which they typically undergo months of rehabilitation (Gresham et al., 1995). During this period, people experience substantial reorganization of

cortical movement-related activity that drives motor recovery (Cramer & Crafton, 2006; C.-Y. Wu et al., 2010).

Many robotic devices have been developed to serve as therapeutic aids in the rehabilitation process of stroke survivors (Maciejasz, Eschweiler, Gerlach-Hahn, Jansen-Troy, & Leonhardt, 2014). Robot-assisted therapy is considered to meet or improve motor outcomes compared to conventional therapy (Kwakkel et al., 2007; Janne M Veerbeek, Langbroek-Amersfoort, van Wegen, Meskers, & Kwakkel, 2016), making possible a larger number of movement repetitions while being less labor intensive for therapists. Furthermore, robotic devices can provide quantitative data for systematic evaluation of patients' progress.

Immediately after a stroke that has injured motor areas of the brain, strength and coordination are both impaired (Kamper & Rymer, 2001; Lang & Schieber, 2003). Therefore, motor training after stroke must be comprised of these two complementary aspects (Xu et al., 2016). Robotic devices can train strength, coordination, or some combination of both. For example, resistive training (Stein et al., 2004) and viscous force field training (Baur, Klamroth-Marganska, Giorgetti, Fichmann, & Riener, 2016; Stienen et al., 2007) are strategies that primarily reward force gains. On the other hand, mirrored assisted movement therapy, in which the paretic limb attempts to mimic movements of the non-paretic limb (Lewis & Perreault, 2009), and weight-supported, targeted reaching are training strategies that primarily reward coordination gains.

A key type of coordination relevant to hand function is individuation, the ability to mobilize one finger while inhibiting movement of another. Several robotic devices have been developed for retraining hand strength and finger individuation (e.g. (Ingemanson et al., 2015; Taheri et al., 2012)), but the relationship between recovery of the two is unclear. Recently, using an isometric force measuring apparatus, Xu et al. tracked the finger strength and individuation of 54 patients with hemiparesis for one year after their stroke (Xu et al., 2016). They found that recovery of strength and finger individuation were highly correlated for the patients whose strength recovery was less than 60% of the non-paretic hand. After this point, individuation nearly fully recovered, and further improvements in strength were not met with further improvements in individuation, resulting in a non-linear relationship

between them (Fig. 4). They suggested that this non-linearity is evidence that recovery of strength and individuation are, in part, mediated by different corticospinal tract (CST) and non-CST processes, respectively.

Coordination of the two arms is also important to stroke recovery. Studies with wrist accelerometry indicate that a large fraction of daily movements is bimanual (Bailey, Klaesner, & Lang, 2015). Several robotic devices have been developed to retrain bimanual coordination and strength after stroke, including a novel lever drive wheelchair (LARA) recently developed in our laboratory (Brendan W Smith, Zondervan, Lord, Chan, & Reinkensmeyer, 2014). Bimanual coordination, such as that required to drive LARA, requires the ability to move the arms in specific patterns, independently of each other. We have just begun collecting data on how people with an acute stroke learn to drive LARA, but for our first participant we found that coordination (measured by wheelchair steering error) improved quickly to a maximum across several training sessions, while strength (measured indirectly by wheelchair speed) improved more slowly and continuously (Fig. 5).

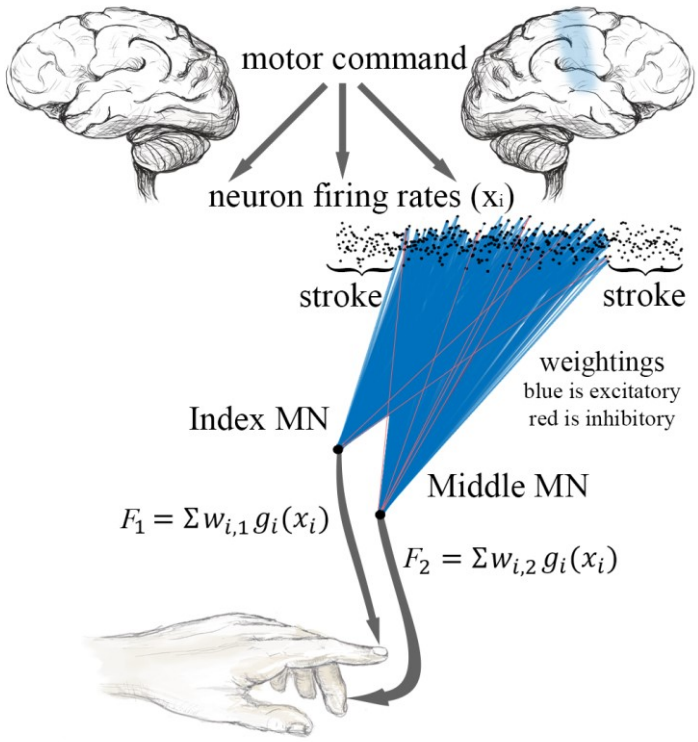

FIGURE 1: MODEL ARCHITECTURE FOR SIMULATING FORCE PRODUCTION BY THE INDEX AND MIDDLE FINGERS OF THE LEFT HAND. A TWO-LAYER FEEDFORWARD NEURAL NETWORK INCORPORATES 400 CORTICOSPINAL & RETICULOSPINAL CELLS WITH FIRING RATES x_I PROJECTING TO FINGER MOTONEURONAL POOLS VIA WEIGHTINGS $w_{I,1}$ AND $w_{I,2}$. THE POOLS SUM THE WEIGHTED ACTIVATION PATTERNS TO PRODUCE FORCES F_{INDEX} AND F_{MIDDLE}. g_I IS A NONLINEAR FUNCTION WITH A SATURATION, SO THE FIRING RATE x_I CONTRIBUTES AT MOST AN INCREMENTAL AMOUNT TO FORCE PRODUCTION.

Computational neurorehabilitation is an emerging area that uses mathematical models of learning and plasticity to understand movement recovery after neurologic injury (Reinkensmeyer et al., 2016). One such model studied force recovery after stroke by employing a neural network to simulate corticospinal (CS) recruitment (Reinkensmeyer, Guigon, et al., 2012). Learning was based on a reinforcement learning algorithm that used inherent stochastic noise and the reward signal of force production to optimize CS activation patterns. The network predicted several clinical observations of force recovery after stroke including a latent residual capacity for force production in the injured network, and a shift of motor activity to secondary motor areas. In this paper, we expand the model of (Reinkensmeyer, Guigon, et al., 2012) to simulate the coordination of MN pools innervating two fingers or two arms, thus allowing us to study the recovery of strength and coordination.

We first test the competency of the model to replicate the non-linear strength/coordination recovery relationship observed with finger movement recovery and LARA training after acute stroke, then use the model to study how training that prefers strength or coordination affects recovery of the other.

3.3 METHODS

We developed two computational neurorehabilitation models to simulate recovery of a finger task (requiring strength and individuation) and learning to drive a bilaterally propelled wheelchair (requiring strength and bimanual coordination) after stroke. Both models are comprised of a two-layer neural network (Figs. 1 and 2). For both models, the goal of the network is to approach the optimal activation pattern of motor cells that results in a maximum network performance, i.e. force and/or individuation/coordination. To this end, the network must iteratively improve its activation pattern based on feedback to the network about its performance. This presents a spatial credit assignment problem: If network performance improves, which cell or cells were responsible? Reinforcement learning has been suggested as a biologically plausible solution to the credit assignment problem and is effective as a learning method in this type of neural network (Anderson et al., 1997; Mazzoni et al., 1991; Reinkensmeyer, Guigon, et al., 2012). In this model, we implement reinforcement learning with stochastic search, which uses a stochastic noise process to generate new activation patterns, an algorithm used previously in (Reinkensmeyer, Guigon, et al., 2012), which is a simplification of the random search with chemotaxis algorithm described in (Anderson et al., 1997):

Given an initial activation pattern X_0 that produces a performance resulting in a reward signal R_0, then on each subsequent movement attempt i,

1. Activate CS cells with pattern $X_i=X_0+v_i$, where v_i is stochastic noise.
2. Measure R_i produced by this pattern.
3. If the resulting performance improves, i.e. $R_i>R_0$, then let $X_0=X_i$ and $R_0=R_i$.
4. Repeat.

3.3.1 FINGER MOVEMENT TASK

For the finger task, we arranged the motor cells in a single hemisphere that projects to two flexor MN pools: one for the index finger, and one for the middle finger. To reflect the physiological situation, CS motor cells make up the bulk of focal cells, i.e. cells that project to one finger only, and are comprised of ~0.8% inhibitory neurons (Witham, Fisher, Edgley, & Baker, 2016). Reticulospinal (RS) motor cells are more diffusely innervated, i.e. connected to both fingers, and do not contain inhibitory neurons (Riddle, Edgley, & Baker, 2009). Generally speaking, CS cells facilitate individual finger movement by virtue of their focal connections and inhibitory cell make-up. RS cells are always connected to the motor neurons of both fingers; thus, each cell's firing rate contributes more to the networks overall force output, e.g. power grip. Network weightings reflect monosynaptic connections and the combined effect of polysynaptic projections to MN pools, and their static nature is a simplification. Excitatory neurons are positively weighted; inhibitory neurons are negatively weighted.

We simulated the finger force production task using a network of 400 cells with pseudorandom weightings from a unit-mean, unit-variance normal distribution. Focal cells (i.e. CS cells) comprised 40% of the network; 60% of cells projected to both fingers (some CS and all RS cells). The firing rates, x_i, are multiplied by their respective weighting, w_i, to the MN pools and summed using:

$$F_1 = \sum w_{i,1} g_i(x_i) \quad (1)$$

$$F_2 = \sum w_{i,2} g_i(x_i) \quad (2)$$

where g represents a nonlinear saturation function that ensures individual cells' contribution to the force output is limited. The result of this sum, F, is proportional to the force produced by the respective finger.

We defined the finger task as trying to move one finger with as much force as possible while inhibiting movement in the other finger. In other words, the model would ideally increase F_1 while maximizing the individuation index (3), i.e. minimize F_2. We chose this task because it is analogous to the finger individuation tasks described in (Xu et al., 2016).

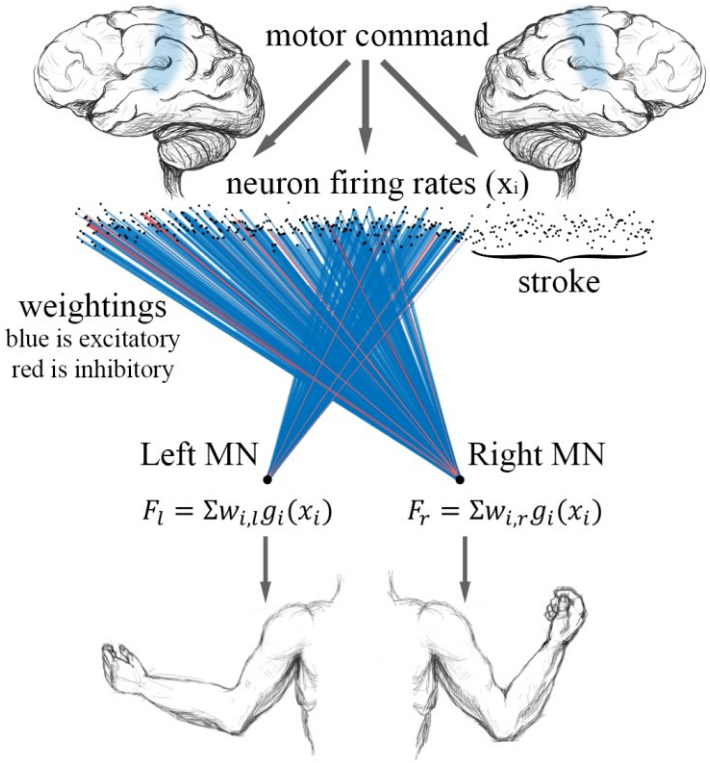

FIGURE 2: MODEL ARCHITECTURE FOR SIMULATING FORCE BY THE TWO ARMS TO PROPEL A LEVER DRIVE WHEELCHAIR. A TWO-LAYER FEEDFORWARD NEURAL NETWORK INCORPORATES 400 CORTICOSPINAL & RETICULOSPINAL NEURONS WITH FIRING RATES X_I. CELLS PROJECT TO ARM MOTONEURONAL POOLS VIA WEIGHTINGS $W_{I,L}$ AND $W_{I,R}$. LEFT AND RIGHT MN POOLS SUM THE WEIGHTED ACTIVATION PATTERNS TO PRODUCE FORCES F_L AND F_R. G_I SATURATES FIRING RATES OF X_I.

$$I = \frac{F_1 - F_2}{F_1 + F_2} \tag{3}$$

The network is rewarded for achieving movements with greater force and better individuation. We defined a reward function that weights these factors using α, with F normalized by the maximum possible F the network can produce. A weighting $\alpha=0$ indicates that the patient only values being able to individuate their finger movements, and $\alpha=1$

indicates that the patient only values generating force. Their weighted sum results in the reward signal, R:

$$R = \alpha F + (1 - \alpha)|I| \quad (4)$$

3.3.2 Bilateral wheelchair task

In another application of the model, we arranged the cells in bilateral hemispheres. Two MN pools were used: one for the left arm, and one for the right, where 90% of connections are projected to the contralateral MN pool and 10% to the ipsilateral MN pool in line with human anatomy (Tanji, Okano, & Sato, 1988). In the case of a simulated unilateral stroke, we de-weighted a portion of the right hemisphere, simulating the death of these cells that control the left arm.

We evaluated this model by simulating a bilateral wheelchair driving task where the arms must coordinate, working together to drive the wheelchair forward by generating as much symmetric force as possible. Ideally, the network would increase F_l and F_r while coordinating the arms, which means driving the individuation index towards zero to produce equal forces, e.g. drive in a straight line. Here, F_l and F_r can be understood as the peak force produced by each arm on each push of the levers of the chair. The network was given

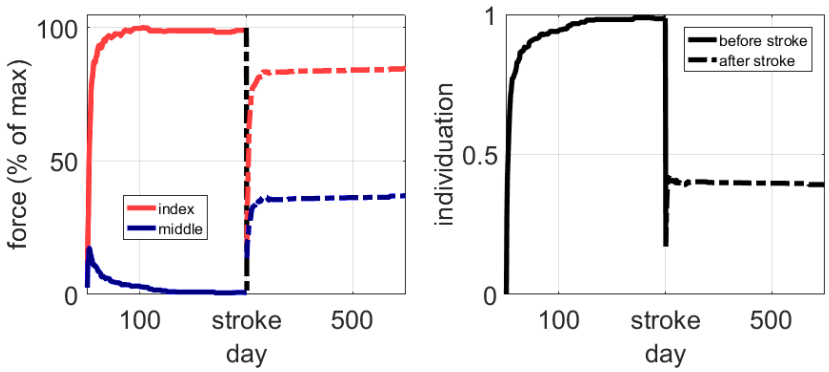

Figure 3: Simulated force production and individuation index as a function of time before and after a unilateral stroke affecting the index and middle fingers of the left hand. Using a reward function that equally valued force and individuation, the uninjured network increased index finger force while inhibiting the middle finger. After the stroke, the network increased index finger force production, but did not inhibit middle finger force production, sacrificing individuation for index finger strength recovery.

feedback on the summed force from the arms (5) and coordination (6) using a reward function (7) slightly modified from the one presented in (4) for the finger task. For this reward function, $\alpha=1$ still indicates that the patient only values force (assessed by speed of the wheelchair) but $\alpha=0$ indicates that the patient only values coordination in the sense of individuation=0 (i.e. driving straight in the wheelchair).

$$F = F_l + F_r \tag{5}$$

$$I = \frac{F_l - F_r}{F_l + F_r} \tag{6}$$

$$R = \alpha F + (1 - \alpha)(1 - |I|) \tag{7}$$

3.4 RESULTS

We simulated the process of learning force and individuation in a finger movement task and a bilateral wheelchair propulsion task after a simulated stroke. We first show that the model predicts the nonlinear relationship between strength and coordination recovery observed in recent clinical data for these tasks. We then use the model to determine how training that prefers strength or coordination affects recovery of the other aspect of motor control.

3.4.1 Finger Task

For the finger task, we first trained the uninjured network with 200 movement attempts per day for 300 days. We then imparted a stroke, eliminating 50% of CS cells projecting to both finger MN pools. The network was given a dose of movement attempts to simulate acute movement therapy, followed by typical at-home movement, in the same manner as (Reinkensmeyer, Guigon, et al., 2012) and in keeping with clinical observations of paretic limb-use after stroke (Lang, MacDonald, et al., 2009). Fig. 3 shows the response of the model given an equal weighting between force and individuation training (α=0.5). Key results are that 1) force in the targeted finger (index finger) maximized in the uninjured network but only recovered to 81% of its pre-injury force, and 2) the network learned to inhibit the middle finger to maximize individuation before the injury but did not inhibit it as effectively after injury, resulting in a decreased individuation index. In fact, the force produced by the middle finger increased, because this helped the network use the diffusely innervated cells (i.e. the cells that excited the MN pools of both fingers) to increase the force of the index finger. Thus, valuing strength recovery diminished individuation recovery.

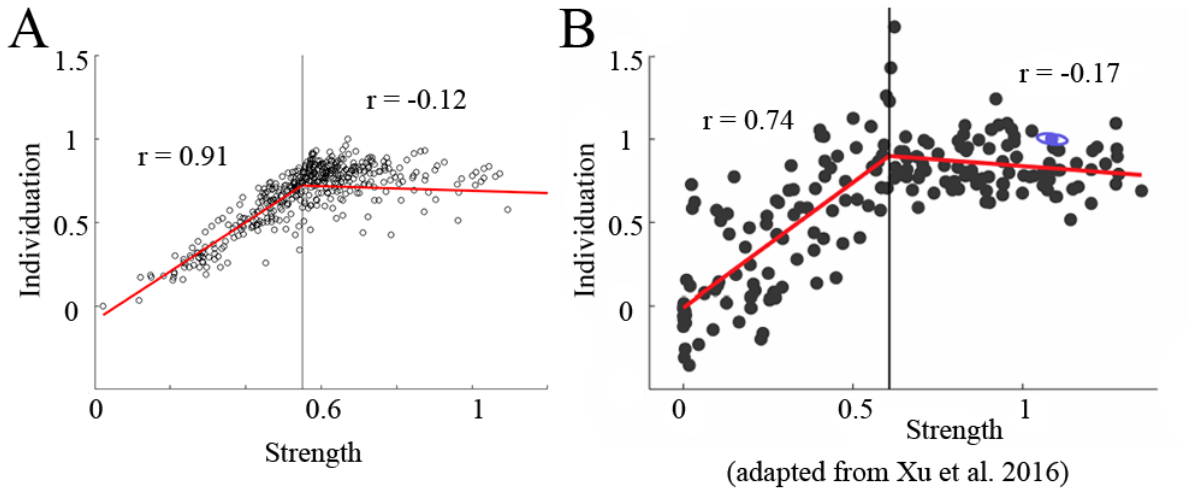

Figure 4: The non-linear relationship between force and individuation. A: simulated results. B: results adapted from Xu et al. (Xu et al., 2016). Both plots show the results of 54 people (simulated in A and actual in B) with varying degrees of stroke learning a finger individuation task over 52 weeks of training. Force and individuation co-varied linearly until individuation saturated, at which point further increases in force were no longer met with increases in individuation. Each point represents one of the 54 people at one of four time points during recovery.

In Fig. 4, we plot strength versus individuation in order to compare to clinical data from (Xu et al., 2016). We ran the simulation 54 times at varying levels of stroke for 52 weeks of movement practice of 1000 movements per week to replicate (Xu et al., 2016), which evaluated 54 subjects over 52 weeks. The progression of strength and individuation in the network varied non-linearly (Fig. 4A), a result consistent with (Xu et al., 2016) (Fig. 4B).

3.4.2 Bilateral wheelchair task

For the bilateral wheelchair task, we trained a network initialized to a pseudorandom activation pattern sampled from a unit-mean, unit-variance normal distribution for 300 runs "in the wheelchair" with $\alpha=0.7$. We did not pre-train the network, as learning to use a lever drive wheelchair is presumably a novel task people have not encountered before a stroke. Force improved in both arms simultaneously. Coordination between the arms was measured

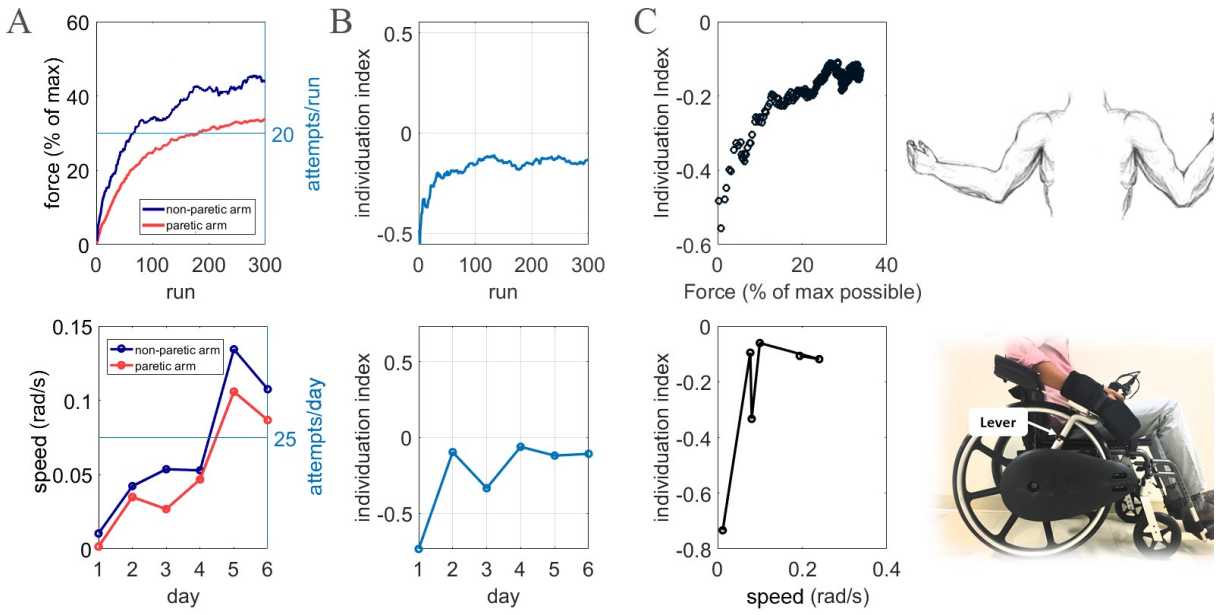

Figure 5: Comparison of a simulation (top row) and empirical (bottom row) data from a person with sub-acute stroke learning to drive a novel lever drive wheelchair that rewards coordinated, bilateral strength, i.e. increasing force and making individuation index = 0. Column A: Force/speed production in the impaired arm and unimpaired arm. The non-paretic arm matches the paretic arm to maintain synchrony. Column B: Individuation index (Equation 4). Initially, the non-paretic arm overpowers the paretic arm, resulting in a negative individuation index. The network improves coordination until it saturates near zero. Column C: Force and individuation improve together, in a non-linear fashion.

using the individuation index *I*, and the reward function rewarded *I=0* so that the arms pushed in synchrony.

Over six daily 20-minute training sessions, an individual with sub-acute stroke learned to use LARA, a novel lever drive wheelchair (Fig. 5). Forward driving using LARA is a bimanual skill that requires pushing the levers with both arms in a coordinated way. In each session, the participant was asked to drive in a straight line for two minutes. The angular velocity of the levers and wheelchair speed were recorded. Here, we compare the force generation of the model to the wheel speed of the chair, which we assume to be proportional. The subject provided informed consent to participate in this experiment, which was approved by the U.C. Irvine Institutional Review Board. We found that over the six training sessions, the participant increased wheelchair speed and lever pumping coordination. Their force and coordination improved in a similar non-linear fashion as the simulation (Fig. 5).

3.4.3 Interaction between strength and coordination training

These results show that the model is competent to replicate the non-linear relationship between strength and coordination recovery. But how does the model behavior depend on α, the weighting constant in the reward function that determines how to relatively reward strength and coordination? We simulated the finger movement task with $0 \leq \alpha \leq 1$ for a simulated 52 weeks (1000 movement per week), with and without a stroke that eliminated 50% of CS cells. As shown in Fig. 6, for the uninjured network, training with a wide range of α (i.e. all but $\alpha=0$ or $\alpha=1$) resulted in full strength *and* individuation. Thus, when uninjured, if the network was rewarded to some degree for both strength and coordination, it eventually fully maximized both. In contrast, for the stroke-damaged network, training with any $\alpha > 0.5$ resulted in mostly strength recovery and with any $\alpha < 0.5$ resulted in mostly individuation recovery. Therefore, stroke caused a tradeoff between strength and coordination recovery that didn't exist before injury.

3.5 DISCUSSION

We developed a computational neurorehabilitation model to gain insight into the interaction between strength and coordination recovery after a stroke. The model was

competent to replicate the nonlinear relationship between strength and coordination observed in clinical recovery data for a finger force production task and a bilateral wheelchair propulsion task. The model also suggested that stroke can cause a tradeoff between strength and coordination recovery, a tradeoff that doesn't exist for an uninjured network. We now briefly discuss the mechanisms that support these observations, then highlight implications for robotic therapy.

3.5.1 Neural resource scarcity causes a strength/individuation recovery tradeoff

What resources does the motor system need to achieve both strength *and* individuation? If there are enough focal cells to maximally activate the motor neuronal pools associated with the task, the motor system can learn to activate those cells through

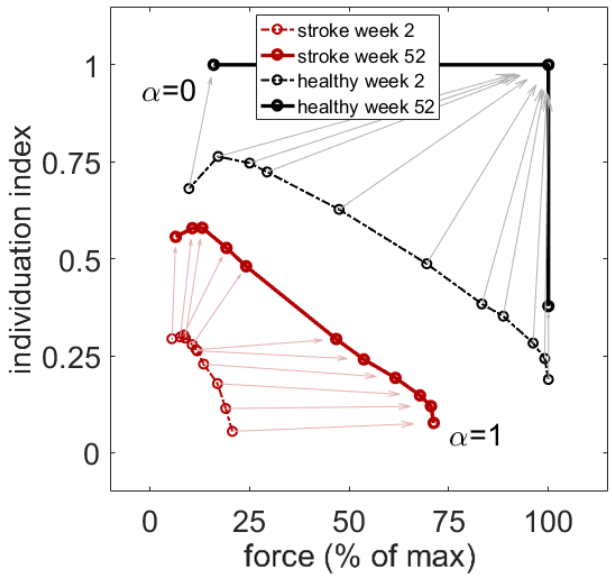

Figure 6: The strength and individuation recovery relationship as α varies. *α=1* only values strength; *α=0* only values individuation. The curves are shown at simulated week 2 (dotted) and week 52 (solid). We include results from the uninjured network (black) and from a network with a stroke that destroyed 50% of the CS cells. From the upper left to lower right, the α increases from 0 to 1. Arrows connect points with the same α. Note the convergent dynamics before stroke. All but extreme α result in full individuation and strength. Compare the divergent dynamics after stroke, where favoring strength results in almost exclusive strength recovery, and favoring individuation results in almost exclusive individuation recovery.

reinforcement learning and achieve maximum strength *and* individuation. However, if there aren't enough focal cells, e.g. after cell death, the motor system faces a tradeoff: If it recruits diffusely connected cells that increase strength, individuation suffers. One solution is to mitigate the unwanted effects of the diffusely connected cells by recruiting surviving CS inhibitory cells. But the number of these cells is limited, especially after injury (Witham et al., 2016). On the other hand, to maximize individuation recovery, the motor system can choose to activate only focal CS cells, and only as many diffusely connected cells as whose unwanted effects can be inhibited. But, in this case, strength recovery is limited. Thus, the model predicts that resource scarcity, i.e. limited focal and inhibitory cells after a stroke, causes a strength/individuation tradeoff. These dynamics are consistent with the proposal that strength and individuation recovery are mediated by different CST/non-CST processes (Xu et al., 2016), and shed light on how those processes might interact.

3.5.2 A SPECIFIC EXAMPLE OF THE TRADEOFF

Consider the specific example in which simulating cell death after a stroke reduced both strength and individuation in the finger movement task (Fig. 3), a result consistent with the clinical literature (Kamper & Rymer, 2001; Lang & Schieber, 2003). Although the network recovered much of its strength through rehabilitation (81%), it did not learn to inhibit the middle finger, causing a reduced level of individuation after the injury (*I=0.4*). Why did the network fail to learn to inhibit movement in the middle finger, even though the reward function contained a term for rewarding individuation? As outlined above, the answer lies in the network anatomy. Before the injury, a significant minority (40%) of CS pathways were focal, i.e. connected from one CS cell to one MN finger pool. After the injury, roughly half of these focal neurons were destroyed, so the network learned to recruit more diffusely-connected RS cells that were connected to both fingers (Witham et al., 2016), in order to generate forces. In minor strokes, the residual CS network can activate enough inhibitory neurons to inhibit any middle finger movement induced by activation of cells connected to both fingers. However, after a more severe stroke, there were not enough inhibitory CS cells to inhibit the middle finger movement, resulting in reduced individuation. Thus, the greater reliance on more diffusely innervating cells, coupled with the scarcity of focal CS inhibitory cells, limited individuation recovery.

3.5.3 EXPLAINING THE NON-LINEAR RELATIONSHIP

This observation can also explain the non-linear relationship between force and individuation recovery observed by Xu et al. (Xu et al., 2016) and replicated here. Individuation and strength recovery can proceed in tandem until all focal cells are recruited, then, proceed further by recruiting the diffuse cells, until all inhibitory cells are recruited. Accessing these complex patterns becomes increasingly difficult for a stochastic search. Thus, strength and individuation cannot be further improved with standard doses of movement practice. Thus, a nonlinearity arises when the motor system runs out of resources for individuation.

3.5.4 RECOVERY IN THE WHEELCHAIR TASK

In the wheelchair task, strength and coordination recovered together. Recall that, for this task, coordination was defined as both arms working together in symmetry – exactly what the bilaterally connected cells enable. Thus, their recruitment contributes to both strength and coordination, allowing full recovery of both without a competition/tradeoff between them as is the case in the finger tapping individuation task.

At first glance, it may appear as though the non-paretic arm was unable to generate forces as large as pre-injury (Fig. 5A). The reason for this is straightforward. Again, the simulation required force and coordination of the arms in synchrony, implemented as a reward function (7) that rewarded $I=0$, i.e. bilateral symmetry. Although the non-paretic arm was capable of much higher forces than the paretic arm, it sacrificed those forces to avoid a penalty in the coordination term of the reward signal (7), thereby improving coordination before optimizing force. In this case, since bilateral, symmetric coordination was being rewarded, which can be implemented with bilaterally connected cells, strength and coordination recovery proceeded quickly together, until coordination reached a maximum.

3.5.5 IMPLICATIONS FOR ROBOTIC THERAPY

If limited neural resources after stroke cause competition between strength and coordination recovery, what are the implications for robotic therapy? One might predict that devices will excel at training strength but not coordination, or coordination but not strength, because of the tradeoff and depending on which factor they reward more. However, there

are some values of α, within a narrow range, that can cause both coordination and strength improvements, depending on the amount of network damage. Robotic movement therapy devices can, in theory, precisely value strength or coordination training. Perhaps they can be an elegant aid for maximizing functional recovery, by measuring ongoing recovery of strength and coordination, then adaptively mitigating the effects of under-training one of them.

CHAPTER 4: MOVEMENT ANTICIPATION AND EEG: IMPLICATIONS FOR BCI-CONTINGENT ROBOT THERAPY

Note: This chapter has been published as:

Norman, Sumner L., et al. "Movement Anticipation and EEG: Implications for BCI-Contingent Robot Therapy." IEEE Transactions on Neural Systems and Rehabilitation Engineering 24.8 (2016): 911-919.

4.1 ABSTRACT

Brain-computer interfacing is a technology that has the potential to improve patient engagement in robot-assisted rehabilitation therapy. For example, movement intention reduces mu (8-13 Hz) oscillation amplitude over the sensorimotor cortex, a phenomenon referred to as event-related desynchronization (ERD). In an ERD-contingent assistance paradigm, initial BCI-enhanced robotic therapy studies have used ERD to provide robotic assistance for movement. Here we investigated how ERD changed as a function of audio-visual stimuli, overt movement from the participant, and robotic assistance. Twelve unimpaired subjects played a computer game designed for rehabilitation therapy with their fingers using the FINGER robotic exoskeleton. In the game, the participant and robot matched movement timing to audio-visual stimuli in the form of notes approaching a target on the screen set to the consistent beat of popular music. The audio-visual stimulation of the game alone did not cause ERD, before or after training. In contrast, overt movement by the subject caused ERD, whether or not the robot assisted the finger movement. Notably, ERD was also present when the subjects remained passive and the robot moved their fingers to play the game. This ERD occurred in anticipation of the passive finger movement with similar onset timing as for the overt movement conditions. These results demonstrate that ERD can be contingent on expectation of robotic assistance; that is, the brain generates an anticipatory ERD in expectation of a robot-imposed but predictable movement. This is a caveat that should be considered in designing BCIs for enhancing patient effort in robotically-assisted therapy.

4.2 INTRODUCTION

Robotic devices, such as powered exoskeletons, have demonstrated utility for rehabilitation therapy of the upper extremity for individuals with stroke and other

neurologic impairments (Klein et al., 2008; Reinkensmeyer, Wolbrecht, et al., 2012; Sanchez Jr et al., 2005). In the most commonly used paradigm, the robotic therapy device physically assists the patient in completing repetitive desired movements that are pre-specified by a computer game that provides audio-visual cues (Reinkensmeyer, Wolbrecht, et al., 2012; Taheri et al., 2012). Physical assistance is thought to enhance proprioceptive input, which may aid neural reorganization (Reinkensmeyer et al., 2004). In past studies, robotic therapy has been shown to match or better the results obtainable with conventional rehabilitation movement therapy (Kahn et al., 2006; P. S. Lum, Burgar, Shor, Majmundar, & Van der Loos, 2002; Reinkensmeyer, Wolbrecht, et al., 2012).

Research suggests that an important factor for ensuring the effectiveness of robotic therapy is active effort by the patient (Hidler et al., 2009; Hornby et al., 2005; Hornby, Reinkensmeyer, & Chen, 2010; Hu et al., 2009; Kaelin-Lang et al., 2005; Lotze et al., 2003). A key study showed that repetitive robotic movement of the upper extremity with a passive stroke patient has little therapeutic effect compared to robotic therapy in which the patient and robot work together (Hu et al., 2009). Another study found no improvements in clinical movement scales following continuous passive range of motion therapy of the stroke-impaired arm (Volpe et al., 2005). It has also been shown that physically assisting in movement with a robot can trigger slacking by the motor system, which is an automatic and subconscious reduction in patient effort (Israel et al., 2006; Reinkensmeyer et al., 2004; Reinkensmeyer, Wolbrecht, et al., 2012; Wolbrecht et al., 2008). Thus it is important when designing robotic therapy systems to develop methods that encourage patient engagement and effort during the therapy and prevent slacking, since robotic assistance may in some cases innately encourage slacking.

Electroencephalography (EEG) based Brain Computer Interface (BCI) systems have been proposed for the purpose of enhancing robot-assisted rehabilitation training (Buch et al., 2008; Formaggio et al., 2013; Fu et al., 2006; Ramos-Murguialday et al., 2013). It is yet unclear how best to harness the strengths of these systems together, but one rationale focuses on promoting patient engagement (Hu et al., 2009; Reinkensmeyer et al., 2004). A BCI system could be used to detect movement intention, and the robotic therapy system could be programmed to provide assistance contingent on the sensed movement intention.

For this purpose, mu and beta frequency bands (8-12, and 13-35 Hz) have been suggested for identifying brain states associated with movement intention (Alegre et al., 2002; Buch et al., 2008; Cassim et al., 2001; Formaggio et al., 2014; Formaggio et al., 2013; Fu et al., 2006; G. R. Müller-Putz et al., 2007; Nakayashiki, Saeki, Takata, Hayashi, & Kondo, 2014; Pfurtscheller & Aranibar, 1977; Pfurtscheller & Lopes da Silva, 1999; Ramos-Murguialday et al., 2013). Mu and beta sensorimotor rhythm (SMR) oscillatory amplitude is known to attenuate during preparation for an overt movement or motor imagery, a phenomenon referred to as event related desynchronization (ERD) (Pfurtscheller & Lopes da Silva, 1999).

ERD has been used successfully as a control signal for BCI applications, including, recently, robot-assisted therapy (Buch et al., 2008; Fabiani et al., 2004; Fok et al., 2011; Ramos-Murguialday et al., 2012; Ramos-Murguialday et al., 2013; Yuan & He, 2014). However, use of ERD as a contingent control signal for robotic therapy has not been shown to decisively improve motor outcomes for robotic therapy after stroke. One study that employed a BCI-contingent orthosis movement paradigm found no significant improvement in clinical scales used to rate hand function after the study (Buch et al., 2008). Another, larger study found modest improvements in motor outcome measures compared to a sham control group who received random imposed (passive) movements (Ramos-Murguialday et al., 2013).

It is possible that ERD is not tied to movement intention alone, but may instead be the result of sensory feedback associated with movement, whether active or passive. Indeed, previous research has suggested that ERD occurs during passive movements driven by a robotic orthosis or an experimenter, similar to when the subject performs overt movement or motor imagery (Alegre et al., 2002; Cassim et al., 2001; Formaggio et al., 2014; Formaggio et al., 2013; G. R. Müller-Putz et al., 2007; Ramos-Murguialday et al., 2013). For example, Alegre et al. (Alegre et al., 2002) studied beta band desynchronization in six healthy volunteers during passive wrist extensions performed with the help of a pulley system at random intervals. The passive movements were found to induce ERD after the movement onset. The authors concluded that proprioceptive inputs induce ERD similar to that observed during voluntary movements. Another study analyzed beta ERD during passive and attempted foot movements in unimpaired subjects and subjects with paraplegia after spinal

cord injury (SCI) (G. R. Müller-Putz et al., 2007). Passive motions were controlled using a custom foot release mechanism at eight second intervals. A significant ERD was found to occur ~500ms before movement onset in the unimpaired participants. Thus, in this case, ERD was found to anticipate predictable passive movement of the foot. These findings suggest that ERD is not solely related to the intention to move, but is also influenced by proprioceptive input and/or the expectation of imposed movement. Therefore, these findings have implications for the use of ERD as a control signal for detecting patient motor engagement during robot-assisted therapy. If the user's expectation and preparation for somatosensation as a result of predictable, passive motion is sufficient cause to trigger an ERD, the user might no longer need to actively engage in overt movement to cause the ERD trigger signal and the contingent imposed robotic movement.

The purpose of this study was to determine the effect of passive movement and subject effort on sensorimotor ERD within the context of a robot-assisted therapy paradigm we previously developed for retraining finger rehabilitation and individuation after stroke (Taheri et al., 2012). Robotic assistance and motor activity were treated as binary categorical design factors in a 2^2 factorial experiment, resulting in four primary conditions: A) active subject/passive robot, B) active subject/active robot, C) passive subject/passive robot, and D) passive subject/active robot (see Table I). Audio-visual stimulation without subject or robot movement was also tested to identify any changes in ERD that may be elicited by the robotic-therapy computer gaming paradigm itself.

TABLE I
FACTOR COMBINATIONS CORRESPONDING
TO THE FOUR EXPERIMENTAL CONDITIONS

		ROBOT	
		passive	*active*
PARTICIPANT	*active*	A	B
	passive	C	D

4.3 METHODS

4.3.1 EXPERIMENTAL SETUP

The Finger INdividuating Grasp Exercise Robot or "FINGER", described at length in (Taheri et al., 2012), was used as the robotic therapy device in this study (See Fig. 1). This robot facilitates the naturalistic grasping patterns of the index and middle fingers together or individuated. Robot assistance used a position feedback controller to follow a minimum-jerk trajectory which began 500ms before the note reached the target. The robot spent 500ms providing flexion assistance, followed by 500ms of extension assistance. Finger movements were mapped to corresponding cues on a screen in front of the participant and set to popular music in the form of a custom video game similar to Guitar Hero©. The gaming environment and user interface software were tailored specifically for this study. We previously found a therapeutic benefit to playing a similar version of the game after stroke (N. Friedman et al., 2014).

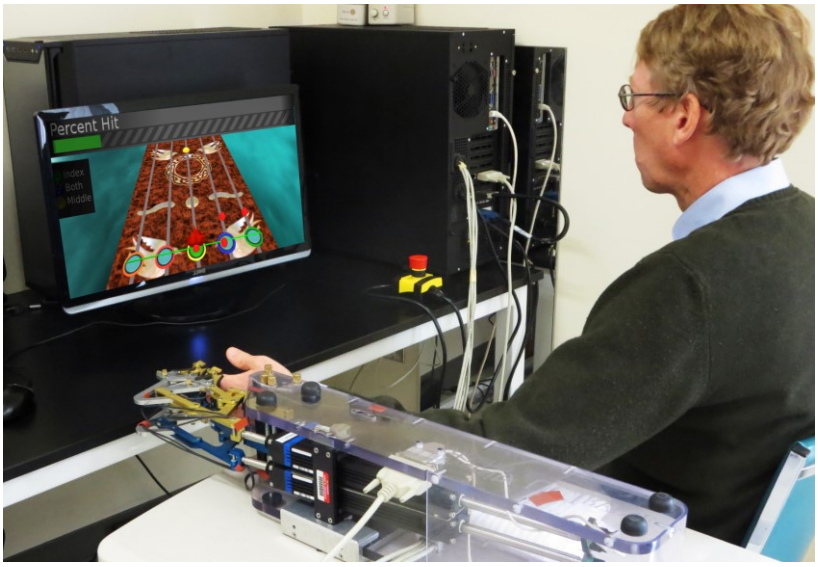

FIG. 1 EXPERIMENTAL SETUP. A USER IS SHOWN USING THE ROBOT TO PLAY THE GAME USED IN THIS STUDY. THE FINGER INDIVIDUATING GRASP EXERCISE ROBOT (FINGER) APPEARS IN THE FOREGROUND. FINGER MAKES USE OF TWO STACKED, SINGLE-DEGREE-OF-FREEDOM EIGHT-BAR MECHANISMS DESIGNED TO ASSIST THE USER IN NATURALISTIC GRASPING TRAJECTORIES FOR EACH, OR BOTH OF THE INDEX AND MIDDLE FINGERS. FINGER IS BACKDRIVEABLE. ROBOTIC FEEDBACK GAINS, WHICH DETERMINE THE ROBOTIC FORCES, WERE HELD CONSTANT FOR ACTIVE ROBOT CONDITIONS. FINGER DID NOT PROVIDE ANY ASSISTANCE DURING THE PASSIVE ROBOT CASES.

In the game, a note appears on screen for two seconds. The note moves down, reaching a target near the bottom of the screen. Notes were timed to reach the target with the beat of the music ("Blackbird" by The Beatles, 94 bpm, 62 notes). Notes were selected to occur at a maximum frequency of every four beats, which resulted in a minimum inter-note period of 2.55 seconds. Maximum note spacing was every eight beats (5.11 seconds).

During active portions of the experiment, the participant attempted to match the speed and timing of the note to complete the flexion portion of the grasping trajectory just as the note reaches the target. An on-screen marker represented the position of the robot. If the participant attained the desired amount of flexion and accurately matched the timing of the note, the game considered this a "hit" and provided visual feedback in the form of a fire graphic on the target and a progress bar counter increase (See Fig. 2). In some experimental conditions, we used the robot to assist in completing the movement with the correct finger at the correct time. More details of the assistive control algorithm can be found in (Taheri et

FIG. 2 THE GAMING ENVIRONMENT USED IN THIS EXPERIMENT. NOTES STREAMED DOWN THE SCREEN IN SYNCHRONY WITH POPULAR MUSIC. THE USER TRIED TO MATCH A FINGER FLEXION TO THE TIMING OF THE NOTE CROSSING THE TARGET AT THE BOTTOM OF THE SCREEN. FIRE APPEARED WHEN A NOTE WAS HIT, AND A SCORE BAR AT THE TOP OF THE SCREEN GAVE VISUAL PERFORMANCE FEEDBACK. GREEN NOTES INDICATED A DESIRED INDEX FINGER MOVEMENT, YELLOW NOTES A MIDDLE FINGER MOVEMENT, AND BLUE NOTES INDICATED THAT BOTH FINGERS SHOULD GRASP TOGETHER. ORANGE AND RED NOTES WERE NOT USED. RED SPHERES ABOVE THE THREE VIRTUAL "STRINGS" ON THE RIGHT WERE MAPPED TO ACTUAL ROBOT FINGER POSITIONS IN REAL TIME, AND WERE INTENDED TO BE MATCHED TO NOTE TIMING ON SCREEN. IN THIS SCREENSHOT, THE USER HAD JUST EXECUTED A HIT WITH THE YELLOW NOTE/MIDDLE FINGER. A SECOND NOTE HAS JUST APPEARED ON SCREEN, AND WILL REACH THE TARGET 2 SECONDS LATER.

al., 2012), but essentially the movements followed a minimum-jerk trajectory calculated to guide the subject using a position feedback controller. The minimum-jerk trajectory had a duration of 500ms for flexion assistance, and a second minimum-jerk trajectory of duration 500ms was used for extension assistance, with no pause in between.

EEG data was collected using 256 electrodes, sampled at 1 kHz using the EGI Geodesic EEG System 400. Impedance values were kept below 100 kOhm. Raw EEG data was exported for offline analysis in Matlab. Marker timing data was captured from the gaming environment. Robot position, velocity, and controller gains were also sampled and recorded at 1 kHz.

4.3.2 PARTICIPANTS

Twelve unimpaired participants took part in this study (6 male; 6 female). All participants provided written informed consent and the study was approved by the Institutional Review Board of UC Irvine. A prerequisite for study inclusion was naivety to the experiment and gaming environment. All participants were considered unimpaired, and had no history of neurologic injury. In a study of EEG during shoulder-elbow movements, both unimpaired and stroke survivors were found to exhibit significantly greater ERD intensity while using their non-dominant arm vs. their dominant arm (Fu et al., 2006). To maximize the ERD signal, all participants used their non-dominant hand in the robot. All participants were right handed, and thus used their non-dominant left hand.

4.3.3 EXPERIMENTAL DESIGN

We used a two factor, two level (2^2) factorial design (Table I). The two factors were robot assistance (on or off), and overt motor activity (on or off). We will use the term "overt" to refer to a willed, voluntary, finger movement by the subject. In the factorial part of the experiment, each subject experienced each of the four conditions, labeled in Table I, A through D. We also tested the effect of audio-visual stimulation alone before and after the four conditions. This condition was the same as that used in the factorial block (Table I, C).

The subjects' fingers were first fastened to the robot as they sat comfortably in front of the screen. The gaming environment was loaded and the test song played while the

participant watched. Participants were instructed to remain as still as possible during this audio-visual only condition. The robot did not provide any assistance. At the conclusion of the experiment, the participant was then asked to complete this same task again.

After the initial audio-visual only session, the participants were allowed to familiarize themselves with the robot and gaming environment during a short training session. Robot assistance was included during the training period, but limited to small forces that could not successfully complete the movement without the overt movement of the subject. Subjects were instructed to actively participate in the motor task to the best of their ability. All participants trained on the same song ("Gold on the Ceiling" by The Black Keys, 104 notes) until both the participant and experimenter felt comfortable in the participant's ability to understand the gaming environment and perform to an acceptable level. All participants exceeded an 80% note "hit" rate in the gaming environment during the training period. All participants gained proficiency within three test songs, and most within two.

The factorial part of the experimental session was divided into four runs consisting of one run per each of the four experimental conditions, for each participant. Inter-participant session order was randomized using a Williams Design Latin Square to minimize first order carryover effects. Factor combinations were explained to the participant by the test proctor using standardized scripts. Participants were allowed to ask clarification questions regarding their role during the current factor combinations, but were not privy to why the combination was being tested. During all combinations, participants completed one song, consisting of 62 notes (trials) each. The song, "Blackbird" by The Beatles, was the same for all participants and all conditions.

4.3.4 Data analysis

Raw EEG data were recorded using the EGI Geodesic EEG System 400 with 256 electrodes at 1 kHz. Data were exported for offline analysis in Matlab (7.10.0, MathWorks, Inc., Natick, MA). The continuous EEG signal was detrended and low pass filtered at 50Hz. A surface LaPlacian filter was then applied to reduce effects of volume conduction. Eighteenth-order Legendre polynomials were used with a smoothing factor of $1x10^{-6}$. The data were

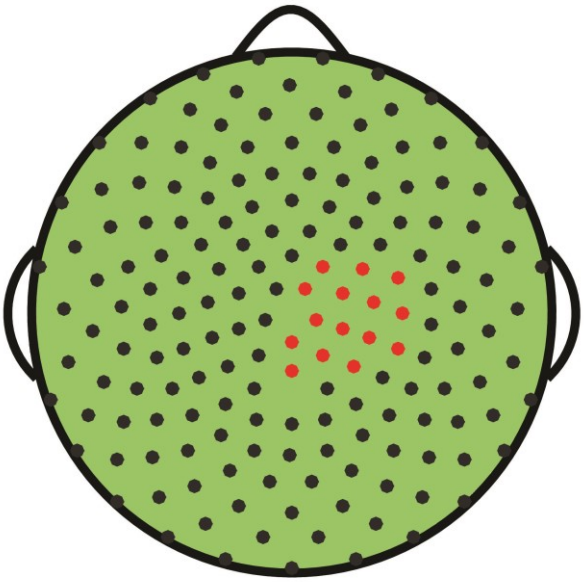

FIG. 3. TOPOGRAPHICAL SELECTION OF CHANNELS FOR INCLUSION IN PROCESSING. PARTICIPANTS USED THEIR LEFT (NON-DOMINANT) HAND IN THE MOVEMENT TASK. CHANNEL SELECTION INCLUDED THE CONTRALATERAL SENSORIMOTOR CORTEX SURROUNDING *C4*, AS WELL AS CENTRAL AREAS NEAR *CZ* AND *CPZ*.

then manually screened for artifacts such as eye blinks or muscle activity in the neck or face. Trial-channel combinations exhibiting artifact were marked for removal from later analysis.

For time-frequency decomposition, a Morlet wavelet transformation was applied. Wavelet transformations used 5 cycles at the lowest frequency of 5Hz and increased to 12 cycles at the highest frequency of 40 Hz. Wavelet analysis was applied at 1Hz steps resulting in 36 distinct frequencies. Wavelet transformation was performed on the continuous EEG data to eliminate the possibility of edge effects. Trials were then segmented into 3000ms epochs surrounding the note-target time, where the epoch start time was 1500ms prior to the note reaching the target. Trial-channel combinations marked for removal during data screening were removed at this point.

Power within a frequency bin was calculated as the magnitude of the complex coefficient result of the wavelet transformation:

$$P_f(t) = |\,\mathbf{\Psi}_f(t) \otimes S(t)| \quad (1)$$

where P_f is the power at a given frequency, f, Ψ is the Morlet wavelet, and S is the EEG signal. All are functions of time, t. The symbol | | represents the complex norm, and $\otimes$ represents the complex convolution. Power was then normalized using the decibel normalization method outlined in (M. X. Cohen, 2014), and described by:

$$dB_{tf} = 10\ log_{10} \frac{activity_{tf}}{\overline{baseline}_f} \quad (2)$$

where $\overline{baseline}_f$ is the scalar mean power taken across the baseline time period, defined as the initial 250ms of each note (trial). In the same equation, t and f are time and frequency points, respectively. The baseline period began 500ms after the note initially appeared on screen. The baseline period ended approximately 800ms before movement, and 1250ms before the note reached the target (end of flexion).

In previous studies that explored the effects of active and passive movements on ERD, maximum modulation of sensorimotor rhythm appeared in electrodes overlying the right and left motor cortices, locations *C4* and *C3*, respectively (Alegre et al., 2002; Formaggio et al., 2013; Yuan, Perdoni, & He, 2010). During overt hand movement as well as motor imagery and passive movements, SMR modulation appeared primarily in contralateral M1, although bilateral modulation was also seen in some cases. Channel selection for this experiment was based on consideration of these previous studies' results (i.e. over *C4*). We then verified the topography of SMR modulation of the participants in this study. In an intermediate analysis, topographical location of ERD maxima confirmed SMR modulation in contralateral motor cortex near *C4* as well as lesser activity in several subjects near *CPz*. A combination of electrodes overlying *C4* and *CPz* that exhibited time-locked motor behavior was selected for analysis (see Fig. 3).

A 2x2 ANOVA was conducted on the maximum pre-movement decibel normalized desynchronization value (in dB) and max post-movement offset decibel normalized synchronization value (in dB), with a significance level set to $p < 0.05$. Robot assistance and

overt movement (i.e. active movement by the subject) were treated as binary categorical design factors.

4.4 RESULTS

None of the 12 subjects exhibited ERD during the audio-visual only condition presented at the beginning and end of the experiment (see Fig. 6). Consistent with this, no ERD was seen in the audio-visual only condition in the factorial part of the experiment (passive subject/passive robot).

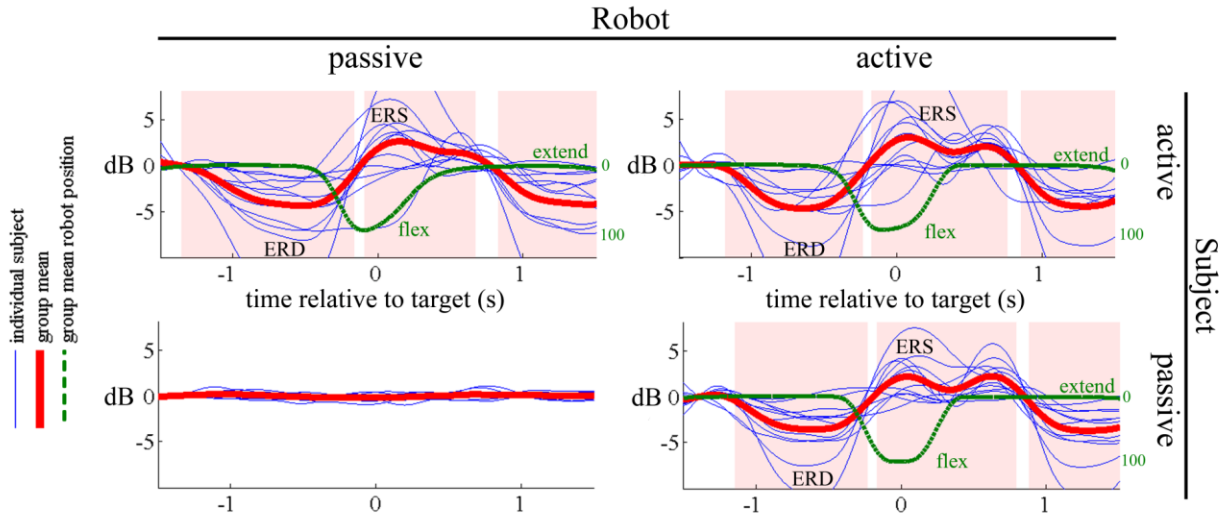

FIG. 4. MEAN MU BAND (8-13 HZ) POWER ACROSS SUBJECTS. TIME = 0 CORRESPONDS TO THE MOMENT WHEN THE MOVING NOTE CROSSED THE TARGET LOCATION. THIN BLUE TRACES REPRESENT INDIVIDUAL PARTICIPANT MEANS. THICK RED TRACE REPRESENTS GROUP-LEVEL MEAN. RED SHADING INDICATES AMPLITUDE SIGNIFICANCE (T-TEST) FOR EACH CONDITION COMPARED TO THE AUDIO-VISUAL ONLY (PASSIVE SUBJECT/PASSIVE ROBOT) CONDITION. SIGNIFICANT ERD AND ERS WERE SEEN IN ALL THREE CONDITIONS IN WHICH A MOVEMENT OCCURRED. ERD PRECEDED MOVEMENT IN ALL CASES. PEAK ERS VALUES OCCURRED JUST AFTER FINGER FLEXION. GREEN TRACES SHOW MEAN ROBOT TRAJECTORY, WITH FLEXION BEING DEFINED DOWNWARD. SCALE REFERS TO PERCENT RANGE OF MOTION. DISCRETE FLEX/EXTEND PORTIONS OF THE GRASPING TRAJECTORY, WITH A NO-MOVEMENT INTERVAL AT THE TARGET TIME (T=0), IS ILLUSTRATED BY THE PASSIVE SUBJECT/ACTIVE ROBOT CONDITION (MOVEMENT DURATION 937MS). A SMOOTH GRASPING MOVEMENT CONSISTING OF A FLEXION FOLLOWED IMMEDIATELY BY AN EXTENSION WITH NO PAUSE BETWEEN IS SEEN IN THE ACTIVE SUBJECT/PASSIVE ROBOT CONDITION (DURATION 1637MS). ROBOT ASSISTANCE AIDED A SHORTER EXTENSION PERIOD IN THE ACTIVE SUBJECT/ACTIVE ROBOT CONDITION (DURATION 1253MS). THERE WAS NO MOVEMENT IN THE PASSIVE SUBJECT/PASSIVE ROBOT CONDITION.

In contrast, ERD was observed in the three conditions that involved physical movement of the fingers, including the condition in which the subject remained passive and the robot moved the subjects' fingers (see Fig. 4). In all, 10 out of 12 subjects exhibited ERD during active subject/passive robot movements. 11 out of 12 exhibited ERD during active subject/active robot movements. 10 out of 12 exhibited ERD during the passive subject/active robot movements. All 12 subjects exhibited ERD within at least one of the physical movement conditions. There was also evidence of event-related synchronization (ERS) in these three conditions, as seen by a rebound in power occurring at the end of the initial finger flexion, approximately 200ms after movement offset.

The timing of the ERD and ERS were similar in the three experimental conditions in which they occurred (Fig. 4, Table II) with some minor differences. ERD began approximately 600-900ms before the start of movement in all three conditions, including when the subject remained passive but the robot moved. ERD in the active subject/passive robot condition preceded that of the remaining two movement conditions. Secondary ERS was seen following the finger extension period in Fig. 4 in the active robot conditions. These secondary ERS signals were not statistically significant from the active subject/passive robot condition. However, the mean secondary ERS value was largest in the passive subject/active robot condition (2.19 dB), followed by the active subject/active robot condition (1.96 dB). No

TABLE II
ERD/ERS TIMING

	ERD		ERS	
Condition	start	end	start	end
A) motor only (active)	-854	333	405	1169
B) robot+motor (active)	-682	263	323	1258
C) audio-visual only	none	none	none	none
D) robot only (passive)	-642	266	333	1287

TIME PERIODS IN WHICH EVENT RELATED DESYNCHRONIZATION AND SYNCHRONIZATION ACHIEVED STATISTICAL SIGNIFICANCE RELATIVE TO BASELINE, VIA POINTWISE T-TEST ($P < 0.05$) ARE GIVEN IN MILLISECONDS RELATIVE TO MEAN MOVEMENT ONSET.

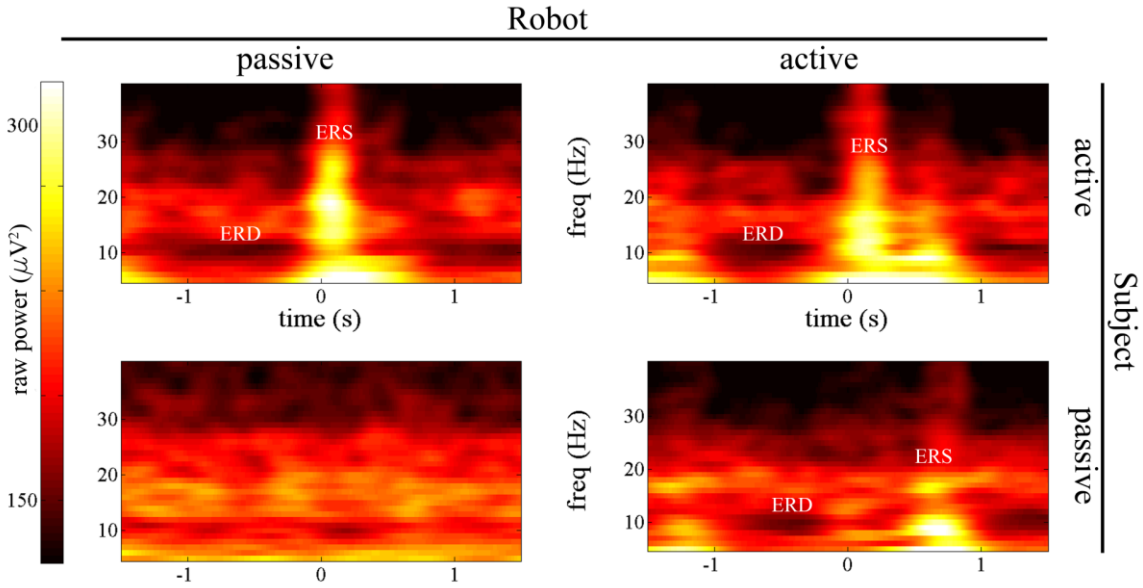

FIG. 5. TIME-FREQUENCY POWER MAPS DURING THE FOUR CONDITIONS FOR AN EXAMPLE SUBJECT. TIME = 0 CORRESPONDS TO THE MOMENT WHEN THE MOVING NOTE CROSSED THE TARGET LOCATION. THIS SUBJECT SHOWED MU BAND (8-12 HZ) ERD AND BETA BAND (13-30 HZ) ERS IN THE THREE MOVEMENT CASES. MU ERD ALWAYS PRECEDED MOVEMENT. BETA ERS FOLLOWED THE COMPLETION OF FINGER FLEXION, OCCURRING AT T=0 IN THE SUBJECT ACTIVE CONDITIONS. A SECOND, SMALLER ERS WAS SEEN IN THE ROBOT ACTIVE CONDITIONS. ERS APPEARED ONLY AFTER FINGER EXTENSION IN THE PASSIVE SUBJECT/ACTIVE ROBOT CONDITION.

secondary local maxima were seen in the active subject/passive robot condition. ERS was also seen to last longest in the active robot conditions, likely due to the secondary ERS feature. In these conditions, ERS extends to approximately 1000ms after finger-extension was complete.

Robotic assistance increased ERD magnitude for the pre-movement onset ERD, but it only approached significance (ANOVA, p = 0.07). It also increased the magnitude of the post-

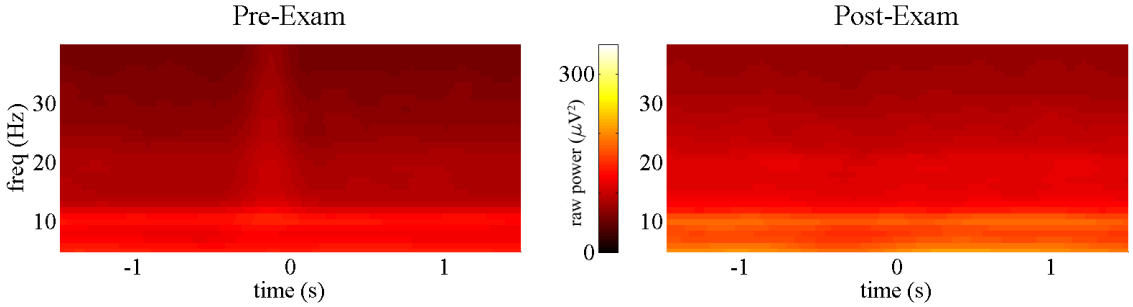

FIG. 6. GROUP-LEVEL MEAN POWER AMPLITUDE TIME-FREQUENCY MAP IN THE AUDIO-VISUAL ONLY CONDITION. RESULTS ARE SHOWN AT PRE-EXAM AND POST-EXAM TESTS. NO SIGNIFICANT POWER MODULATION WAS RECORDED IN EITHER TEST. TIME = 0 CORRESPONDS TO THE MOMENT WHEN THE MOVING NOTE CROSSED THE TARGET LOCATION.

movement ERS, but again it only approached significance ($p = 0.06$). Overt movement did not significantly alter ERD amplitude ($p = 0.66$) or ERS amplitude ($p = 0.88$). Interaction effects between robotic assistance and overt movement were not significant for ERD ($p = 0.59$) or ERS ($p = 0.99$). A comparison of each time point revealed no significant differences in the passive subject/active robot condition compared to the active subject conditions as well (t-test, $p > 0.05$). The maximum across-subject ERD value seen in the passive subject/active robot condition was found to reach 3.68 (+/- 2.96) dB. The maximum across-subject ERD value seen in the active subject/passive robot condition was larger at 4.35 (+/- 3.71) dB, but the difference was not significant (t-test, $p = 0.63$).

A total of 9 out of 12 subjects showed ERD primarily within the mu band (8-13 Hz). The remaining exhibited primarily beta-focused desynchronization (13-30 Hz). Two of these subjects exhibited ERD from 17-22 Hz, and the remaining subject showed ERD from 12-18 Hz. An example of broadband power amplitude can be seen for one subject in Fig. 5. Again, no significant modulation was seen in the passive subject/passive robot, audio-visual stimulation only condition. Mu-rhythm specific ERD was seen prior to movement onset with a peak at approximately -500ms and 10 Hz. This subject also exhibited prominent beta rebound at the end of finger flexion. These were especially noticeable in the active subject/active robot condition where beta ERS can be seen after flexion at approximately 12-28 Hz.

4.5 DISCUSSION

In a robotic neurorehabilitation setting, the patient is often given the task of combinations of overt movement, robotic assistance, and external audio-visual stimuli associated with a computer game. The effects of these stimuli and interaction with one-another on ERD have not yet been well defined. The aims of this study were to identify the effects of these factors on ERD using a prototypical robotic therapy paradigm. ERD was found to precede movement during all three movement conditions, and notably even in the passive subject/active robot condition. No significant power modulation was seen in the audio-visual only condition before or after the factorial conditions were completed. ERS was identified during post-movement periods, with a tendency toward a secondary ERS in the

robotically assisted conditions. Next we discuss the effects of robotic assistance on ERD and ERS. We will highlight the implications of these effects with regard to patient engagement in therapy and future BCI-robot therapy paradigms.

4.5.1 Effects of robot assistance on ERD

This study identified pre-movement ERD during passively imposed movement, suggesting that ERD during passive movement is not tied solely to proprioceptive feedback, but is likely the result of preparation for the impending somatosensory input the movement will produce. In many past studies, ERD has been found to follow imposed movement onset, and has been attributed to proprioceptive feedback (Alegre et al., 2002; Cassim et al., 2001; Ramos-Murguialday et al., 2012). During self-paced movements however, ERD has been observed to precede movement onset (Derambure, Defebvre, Bourriez, Cassim, & Guieu, 1999; Pfurtscheller & Lopes da Silva, 1999; Pfurtscheller, Stancak Jr, & Edlinger, 1997; Stančák Jr, Feige, Lücking, & Kristeva-Feige, 2000). Pre-movement ERD has also been observed previously before cued predictable movements (Nakayashiki et al., 2014; Pfurtscheller & Aranibar, 1977), including passive movements imposed on the subject (Formaggio et al., 2014; G. R. Müller-Putz et al., 2007). This study built on these findings, showing that ERD appeared in advance of a predictable imposed movement from a robotic orthosis when the subject was instructed to remain passive. Because proprioceptive feedback is not yet affected by the imposed movement during the pre-movement interval, these findings suggest there is a cortical preparation of the somatosensory system in advance of an imposed movement. The existence of ERD before movement onset, comparable to that found preceding overt movement, suggests that ERD can become contingent on the expectation of robotically-imposed movement. That is, ERD is not uniquely tied to active movement but can reflect preparation for movement, whether active or passive.

ERD preceding both active and passive movements may be explained by two physiological mechanisms: the efference copy and anticipatory attention. Unlike studies that used random movement intervals (Alegre et al., 2002; Cassim et al., 2001), participants in the present experiment were aware of the existence and timing of oncoming notes.

Participants had sufficient time to prepare for the movement, whether active or imposed by the robot. Past studies have found that the brain predicts oncoming sensory information related to an intended movement so that the system can learn and adapt to changes (S.-J. Blakemore, Wolpert, & Frith, 2000; Kawato, 1999; Wolpert, Ghahramani, & Jordan, 1995). When a command is sent to the motor system to generate movement, an internal copy of the command is created to predict sensory consequences of the movement. This phenomenon is referred to as an efference copy. The efference copy is collated with sensory inputs produced by the movement, allowing a comparison of the expected movement (forward model) and the actual movement. In one study, subjects performed a self-paced finger-tapping task that alternated hands (Bai, Mari, Vorbach, & Hallett, 2005). ERD was observed to occur up to two seconds before movement over the contralateral hemisphere during dominant hand movements, and bilaterally during non-dominant hand movements. The authors suggest that while ERD of the contralateral sensorimotor cortex is an excitatory process, ERD of the ipsilateral hemisphere may be the result of an efference copy reflecting inhibition of movement. During the passive subject/active robot condition of the current experiment, participants expected movement but suppressed overt intention of that movement. Although the descending motor command was inhibited, the internal network requires the efference copy to predict the somatosensation of the imposed movement (S. J. Blakemore, Goodbody, & Wolpert, 1998). Therefore, in the current experiment, ERD preceding movement may be the EEG correlate of the efference copy sent in preparation for predictable imposed movement. Others have suggested that contralateral beta ERD may be a corollary of anticipatory attention to a future motor stimulus (Pfurtscheller, Krausz, & Neuper, 2001). It may be the case that ERD measured here is the result of maintained attention to the oncoming note stimulus. Examination of the effects of predictable and unpredictable cueing would be necessary to further explore the roles of the efference copy and movement inhibition on the magnitude and temporal features of ERD.

4.5.2 Implications for patient engagement in BCI-robot therapy

Although ERD has been shown to be a reliable control signal for BCI applications, the use of BCI-contingency in robot therapy has not yet been proven superior to traditional or robotic therapy. One important rationale for using BCIs in robotic therapy is ensuring the

active engagement of the patient in the movement task (Hu et al., 2009; Reinkensmeyer et al., 2004). This study shows that ERD can be contingent on the expectation of passive, imposed robotic movement. Therefore, in a predictable task therapy environment, the use of ERD as an orthosis control signal does not necessarily require the patient's active motor engagement in the task, but simply the expectation of robotic movement. These findings suggest that ERD is not only an indicator of motor intention, but may also be an indicator of preparation for somatosensation. Producing anticipatory ERD in expectation of an upcoming passive movement could, in theory, allow the patient to slack, which, as described previously, is, a subconscious and involuntary phenomenon wherein the patient allows the robotic environment to supersede their effort in overt movement during the task (Wolbrecht et al., 2008). As such, ERD may be suboptimal as a signal to ensure patient motor engagement in BCI-contingent robot therapy.

Despite the possibility of reduced patient motor engagement in a BCI-contingent robot therapy paradigm, the patient must also exhibit some amount of expectation for the sensory feedback of the passive movement in order to create an anticipatory ERD as seen in this study. An important question is whether sensory engagement alone, without overt movement intention, is enough to aid motor outcome after therapy. A recent paper found modest improvements in a BCI-contingent robotic therapy group versus a sham control group who received randomized robotic movements not contingent on the BCI (Ramos-Murguialday et al., 2013). The sham control group was not able to predict the movement, and therefore unable to train ERD. These findings may indicate that the generation of ERD, even if it is generated in preparation for sensory stimuli only, may be beneficial to motor outcome.

4.5.3 Absence of effects of audio-visual stimuli

Power modulation did not appear in any of the audio-visual only condition exams. The final audio-visual only condition is of particular interest, as it occurred after repetitive conditioning of motor activity to the audio-visual stimuli. The gaming environment in this study utilized very engaging visual and aural cueing matched to overt movement and haptic feedback. Popular music with a consistent beat was chosen for maximum influence on the

participant; and indeed the gaming paradigm used here is similar to the third most popular video game in history. By repeatedly matching hundreds of individuated finger movements to the audio-visual cues on screen, the participant was placed in a scenario that one might expect would lead to classical conditioning. However, the lack of activity in the final audio-visual condition suggests an insusceptibility of EEG power modulation to conditioning based on audio-visual cueing or gaming environments commonly seen in robot therapy. This finding also rules out the possibility that the gaming environment affected ERD in the remaining conditions. This is an important null result for ERD-based BCIs relying on aural and/or visual cues, as it suggests that the cueing environment alone is unlikely to falsely trigger a BCI contingent robot; rather the imposed movement by the robot plays a key role. An anticipatory ERD is only generated if the user associates an audio-visual cue as indicating an upcoming movement, whether active or passive.

4.5.4 Effects of robotic assistance on synchronization after movement

Event related synchronization or "rebound" occurred following finger flexion offset in all three movement conditions. These findings agree with Pfurtscheller et al., who characterized the temporal traits of ERS, finding that a burst of beta power appeared within a one second interval following movement offset (Pfurtscheller et al., 1997). Post movement beta ERS has since been shown to follow voluntary hand movements (Müller et al., 2003; Neuper & Pfurtscheller, 2001; Pfurtscheller, Zalaudek, & Neuper, 1998; Stančák Jr et al., 2000), as well as passive movements (Cassim et al., 2001; Müller et al., 2003). ERS following movement matches previous findings, with the exception of a second, smaller synchronization that was more prominent in the robot active conditions.

The presence of a secondary synchronization in the two active robot conditions may be a result of the discrete flexion/extension forces applied by the robot. Secondary synchronizations seen in the active robot conditions were not statistically significant from the active subject/passive robot case. However, the group-level mean ERS was larger in the active robot conditions and ERS significance periods ended later. The mean secondary synchronization was greatest in the passive subject/active robot condition, followed by the active subject/active robot condition. ERD and ERS in relation to kinematic and kinetic hand

movements were recently characterized by use of a 3x4 factorial design experiment in which the subjects repeated hand grasping movements at different speeds and forces (Nakayashiki et al., 2014). The authors found that although grasping force did not affect the magnitude or time course of ERD/ERS, repeating grasping motions caused repeated up-modulation of the signal power. This supports our findings, because in the present experiment the robot assistance for flexion and extension were separated by approximately a ~200ms interval in which no movement occurred, thereby creating two distinct motions (flexion, pause, extension), and therefore two distinct synchronization features. In contrast, in the active subject/passive robot condition the finger extension occurred immediately after the finger flexion without a pause, and therefore did not show a secondary ERS.

4.5.5 Limitations and future research

In this experiment, we studied unimpaired subjects. Exclusion of the confounding influence of brain lesions on EEG activity allowed us to gain insight into the normative interaction between robotic assistance and brain activity. However, one study found that peak ERD during attempted shoulder-elbow movements was smaller in individuals with a stroke compared to unimpaired subjects (Fu et al., 2006). Although this study did not test passive movements, there is a possibility that ERD preceding passive movements may be diminished in people with neurologic impairment. A future aim of this research is the replication the experiment utilizing participants with a stroke.

This study used a factorial combination of overt movement and robot assistance, rather than online BCI contingent control of the robot to study the potential effects of robotic therapy on event related EEG features. The observation that the pre-movement ERD was contingent on the robotic assistance has implications for using contingent-BCI to improve patient engagement. However, it will be important to verify the results presented here in an online BCI-contingent robot therapy paradigm in future work.

Fine motor tasks such as finger individuation are important for daily function. Furthermore, it has been suggested that isolated, individualized movement deficit also affects impairment in gross movements, such as elbow extension (Zackowski, Dromerick, Sahrmann, Thach, & Bastian, 2004). A recent study employed an EEG based BCI in decoding

individuated finger movements, and achieved accuracy significantly above chance level (Liao, Xiao, Gonzalez, & Ding, 2014). It may therefore be possible to decode EEG-based signals in real time for the online BCI-contingent control of individual fingers in the FINGER robotic orthosis, which may improve therapeutic outcome.

A logical progression of this work would be the identification of an event-related brain state robust to the effects of robot-contingent triggering. Functional connectivity has been shown to vary between active and passive movements during motor tasks (Formaggio et al., 2014), and therefore may be useful as an indicator for active motor engagement in the context of BCI-robot therapy. A second approach might forego a-priori feature selection altogether, using machine learning algorithms to decode movement intention. Past studies have used similar approaches to classify resting state versus active or imagined movements (Blankertz, Dornhege, Krauledat, Müller, & Curio, 2007; Fabiani et al., 2004). To our knowledge, no such approach has been applied to the classification of passive versus active movements. Such an approach may be able to isolate the spatio-spectral EEG features associated with active motor engagement in the task. This would circumvent the robot-contingency observed in ERD preceding passive movements. If patients are indeed slacking in the current BCI-contingent robotic therapy paradigms, a passive/active classification BCI paradigm might encourage patient motor engagement in the task, improving motor outcomes after therapy.

4.6 ACKNOWLEDGMENT

We would like to thank Dr. Jonathan R. Wolpaw and Dr. Dennis McFarland of the National Center for Adaptive Neurotechnologies (www.neurotechcenter.org) (NIBIB/NIH Biomedical Technology Resource Center P41EB018783) at the Wadsworth Center of the New York State Department of Health in Albany, N.Y who were essential in the initiation of this research and supported us throughout the study.

This work was supported in part by R01 (NIH-R01HD062744-01) from the National Center for Medical Rehabilitation Research, part of the Eunice Kennedy Shriver National Institute of Child Health and Human Development, and in part by the National Center for Research Resources and the National Center for Advancing Translational Sciences, National

Institutes of Health, through Grant UL1 TR000153. The content is solely the responsibility of the authors and does not necessarily represent the official views of the NIH.

CHAPTER 5: DETECTING ACTIVE MOVEMENT IN A ROBOT-ASSISTED PROTOCOL

5.1 INTRODUCTION

After neurologic trauma, such as a stroke, robot-assisted movement therapy has been shown to match or better the results obtainable with conventional rehabilitation (Kahn et al., 2006; P. S. Lum et al., 2002; Reinkensmeyer, Wolbrecht, et al., 2012).. However, robotic assistance can cause "slacking" in the patient, an automatic and subconscious reduction in effort (Israel et al., 2006; Reinkensmeyer et al., 2004; Reinkensmeyer, Wolbrecht, et al., 2012; Brendan Wesley Smith, 2017; Wolbrecht et al., 2008). In recent years, brain-computer interface (BCI) research has aimed to use signals acquired from electrodes on the patient's scalp to detect brain states associated with movement intention, and reward the patient by triggering robotic assistance (Ramos-Murguialday et al., 2013). However, in a recent study, we found that passive, robotically imposed movements alone can produce brain states that are typically associated with actual movement from the participant (S. Norman et al., 2016). This phenomenon has the potential to cause false positive movement of the robot, allowing the patient to slack, even in a BCI-contingent robot-assisted environment. Using data driven techniques, here we identify brain states that can discriminate active versus passive movements in 12 unimpaired participants in a robot-assisted environment with the goal to inform the BCI methodology and experimental design of BCI-robot therapy.

5.2 METHODS

Here, we used the dataset available from (S. L. Norman et al., 2016) where twelve unimpaired subjects played a computer game designed for rehabilitation therapy with their fingers using the FINGER robotic exoskeleton (Taheri et al., 2014). In the game, the participant and robot matched movement timing to audio-visual stimuli in the form of notes approaching a target on the screen set to the consistent beat of popular music. We used a two factor, two level factorial design where the factors were robot assistance (on or off) and overt motor activity by the subject (active or passive) resulting in 4 experimental conditions. Participants completed a total of 62 trials in each condition. In this study, we compare brain activity from two conditions: 1) the robot was actively moving the fingers but the participant

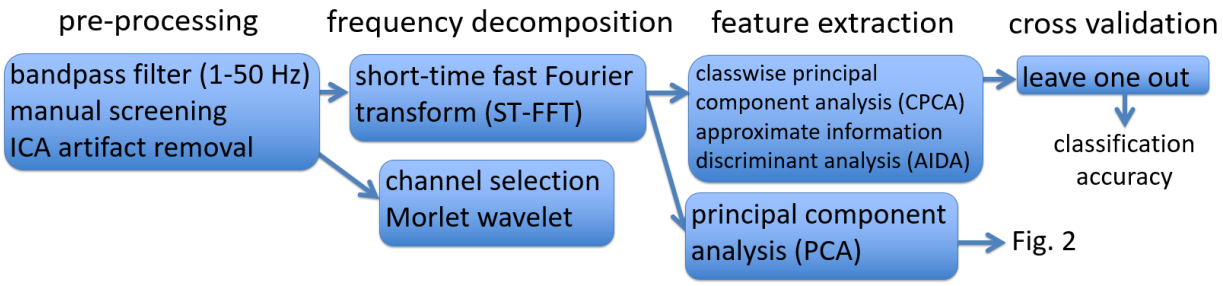

FIG. 1. DATA PROCESSING METHODS OUTLINE

was instructed to remain passive; and 2) the robot was actively moving the fingers and the participant was instructed to actively play the musical computer game. Raw EEG data were recorded using the EGI Geodesic EEG System 400 with 256 electrodes at 1 kHz. The continuous EEG signals were detrended and low pass filtered at 50Hz. A surface LaPlacian filter was then applied to reduce effects of volume conduction. For the results presented in (S. L. Norman et al., 2016), we applied a Morlet wavelet transformation for time-frequency decomposition. Here, we use a short-time fast Fourier transform (ST-FFT) to ease the computational cost of time-frequency decomposition associated with high density EEG arrays, i.e. 256 channels sampled at 1 kHz. Trials were segmented into 3000ms epochs surrounding the note-target time, where the epoch start time was 1500ms prior to the note reaching the target. Power was normalized using the decibel normalization method outlined in (M. X. Cohen, 2014), and used in Chapter 4 (S. L. Norman et al., 2016).

To discern the primary differences between passive and active movements, we treated robot assistance and overt movement (i.e. active movement by the subject) as binary categorical design factors in two approaches. First, we applied across-subject principal component analysis to discern the spatiotemporal patterns that described the most variance in the dataset for each condition, e.g. passive vs. active. We use this as a data exploration technique to identify common differences in people's brains, between the active and passive conditions, that might inform future experiment task design. We then used Information Discriminant Analysis (IDA), a feature extraction technique, to test the feasibility of classifying active vs. passive movements in real time (Nenadic, 2007). Due to the high dimensional nature of the data, i.e. considering temporal dynamics, spatial patterns, spectral bands, etc., we used the solution described by Das & Nenadic, which was specifically

designed to extract features from high dimensional data (Das & Nenadic, 2009). That is, we applied classwise principal component analysis (CPCA) and the Approximated Information Discriminant Analysis (AIDA) techniques described in (Das & Nenadic, 2008, 2009). Here, we treated passive and active movements as categorical variables. We treated trials as replicates in a training set within subjects. We performed this analysis for each subject, independently. We used a leave-one-out technique to cross-validate these results, and averaged the accuracy across subjects.

5.3 RESULTS

Principal component analysis revealed that, after the movement onset of a subject-passive, robot-imposed, movement, 57% of the variance in the sensorimotor rhythm occurred in the primary and secondary motor areas contralateral to the movement. On average, a large desynchronization was seen immediately following movement onset, e.g. *t=0* (Fig. 2, left). In contrast, the primary source of variance during subject-active, robot-active movements occurred in the prefrontal cortex. A large desynchronization occurred preceding movement and immediately rebounded after movement onset.

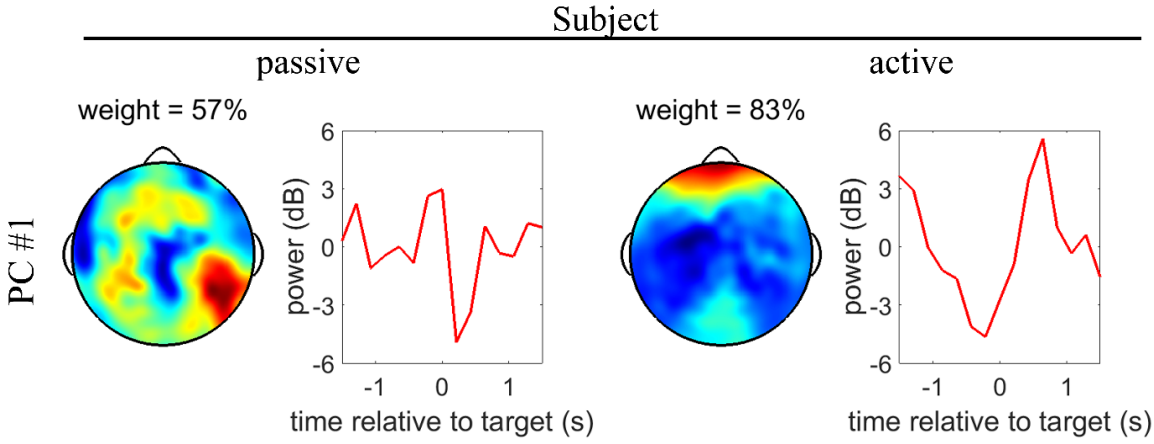

FIG. 2 FIRST PRINCIPAL COMPONENT DURING PASSIVE, ROBOT-IMPOSED MOVEMENTS (LEFT) AND DURING PURPOSEFUL, ACTIVE MOVEMENTS (RIGHT) TOPOGRAPHICAL WEIGHTINGS ARE SHOWN IN AN ACROSS-SUBJECTS ANALYSIS. DESYNCHRONIZATION IMMEDIATELY POST-MOVEMENT-ONSET IN SENSORIMOTOR AREAS DESCRIBE 57% OF THE VARIANCE DURING PASSIVE MOVEMENTS. PRE-MOVEMENT DESYNCHRONIZATION IN PREFRONTAL AREAS DESCRIBE 83% OF THE VARIANCE DURING ACTIVE MOVEMENTS

We were also successful in identifying brain states that can discriminate active movement intention and are robust to the influences of the robotic environment. Using the

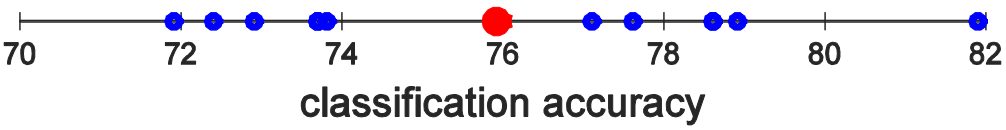

FIG. 3 CLASSIFICATION ACCURACY OF 12 PARTICIPANTS. ACCURACY RANGED FROM 72% TO 82% WITH A MEAN ACCURACY OF 75.9%.

discriminant techniques described above, we were able to discriminate passive and active movements in an average of 75.9% of trials, across participants. Accuracies in 12 subjects ranged from 62% to 82% (Fig. 3).

5.4 DISCUSSION

Using the classification techniques described here, our BCI predicted patient engagement in the task with a 75.9% accuracy on an individual trial basis. Although these results were encouraging, these were under ideal conditions and in unimpaired participants. Due to the confounding nature of stroke on neuroimaging and its underlying brain mechanisms, these accuracies might worsen in people with stroke. For these reasons, we did not pursue this method of classification for an online application.

During the passive movement condition, the topography and resulting temporal signal of the first principal component showed a reduction in sensorimotor rhythm amplitude, commonly referred to as an event-related desynchronization (ERD) (Pfurtscheller & Lopes da Silva, 1999). ERD is most commonly observed in volitional movements but, in recent years, increased attention has been given to ERD in passive movements and its potential role in rehabilitation (Formaggio et al., 2013; S. L. Norman et al., 2016; Tacchino et al., 2016). The primary physiological finding of this exploratory study was the variance in signal in the prefrontal cortex preceding movement when the participant was subsequently engaged in the motor task. This finding lends insight into the normative neurophysiological progression of planning for an intended movement. Indeed, the involvement of prefrontal networks in decision making has been observed before. Frith et al. found that, for willed acts in which the participant had to make a deliberate choice, blood flow in the dorsolateral prefrontal cortex was increased (Frith, Friston, Liddle, & Frackowiak, 1991). The prefrontal variance observed in this short study was likely associated with the motor matching task associated with the musical computer game, which required a

deliberate choice preceding the finger movement. Thus, designing robotic therapy games to require choice, then monitoring pre-frontal activity, may be a simple way of encouraging and providing feedback on engagement during rehabilitation training.

CHAPTER 6: TOWARDS A CLINICAL APPLICATION OF BCI-ROBOT MOVEMENT THERAPY

Note: Portions of this chapter have been published as:

Norman, S.L., McFarland, D.J., Sarnacki, W.A., Wolpaw, J.R., Wolbrecht, E.T., Reinkensmeyer, D.J. (2016, May). Sensorimotor Rhythms During Preparation for Robot-Assisted Movement, BCI Meeting.

McFarland, D.J., Norman, S.L., Sarnacki, W.A., Wolbrecht, E.T., Reinkensmeyer, D.J., Wolpaw, J.R. (2016, November). BCI-Based Sensorimotor Rhythm Training Can Affect Individuated Finger Movements, Neuroscience 2016.

6.1 INTRODUCTION

Brain-computer interface (BCI) technology can restore communication and control to people who are severely paralyzed. BCI technology might also be able to enhance rehabilitation of motor function (Daly & Wolpaw, 2008). Previous research has shown that training sensorimotor rhythm (SMR) activity can modulate reaction times in a BCI (Boulay, Sarnacki, Wolpaw, & McFarland, 2011) and in motor performance, in a joystick-based cursor movement task (McFarland et al., 2015), in people without impairment. A main goal of this dissertation is to develop and test BCI-robot protocols for modulating motor performance in people with a stroke in the context of developing a potential therapeutic intervention. Toward this end, in this chapter, we aim to answer several key preliminary questions for people with and without impairment to inform the experimental design and methodology of a pilot clinical study of BCI-Robot therapy for retraining finger movement in people with stroke. Specifically, we aim to answer the following questions: **1)** In adults without motor impairment, can training pre-movement SMR activity in the EEG over contralateral sensorimotor cortex affect the performance of individuated finger movements? **2)** Can a previous developed methodology to discriminate movement using pre-movement EEG features (McFarland et al., 2015) also predict finger movement in people with stroke? **3)** In people with chronic motor impairment after stroke, can we detect with comparable robustness from pre-movement EEG whether the person intends to flex or extend the finger?

6.2 SENSORIMOTOR RHYTHM TRAINING MODULATES INDIVIDUATED FINGER MOVEMENTS

The primary goal of this pilot study was to answer the question: In adults without motor impairment, can controlling pre-movement SMR activity in the EEG over contralateral sensorimotor cortex affect the performance of individuated finger movements? In addition to this question, we investigated several methodological choices surrounding a finger-individuated BCI-robot protocol including the effects of cued vs. uncued movement, bipolar vs. Laplacian channels, and active vs. passive movements.

6.2.1 METHODS

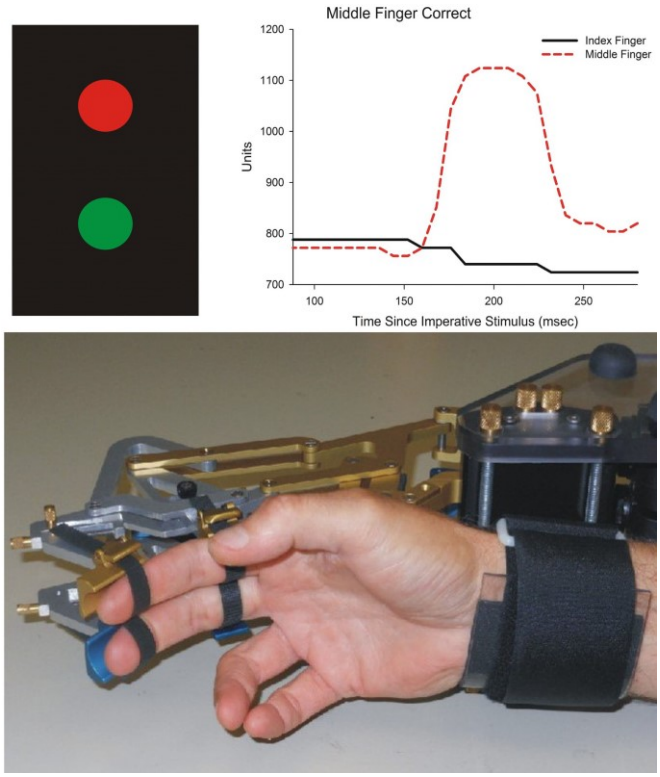

FIG. 1. IN THE UPPER LEFT PANEL, THE RED CIRCLE ON TOP INDICATES THAT THE INDEX FINGER SHOULD REMAIN EXTENDED WHILE THE GREEN CIRCLE BELOW INDICATES THAT THE MIDDLE FINGER SHOULD BE FLEXED. THE RESPONSE WAVEFORMS ARE SHOWN IN THE UPPER RIGHT PANEL. THE RESPONSE FEATURES ANALYZED WERE LATENCY TO START, LATENCY AND AMPLITUDE OF MAXIMUM ACCELERATION, AND LATENCY AND AMPLITUDE OF PEAK RESPONSE.

Six (N=6) unimpaired volunteers, aged 25 to 53, took part in this study. In Phase 1, each subject performed a go-nogo task in which flexion of the index finger and/or middle finger was cued by visual stimuli on a video screen (Fig. 1) and assisted by the robot. Robot assistance was provided by the Finger Individuating Grasp Exercise Robot (FINGER) (Taheri et al., 2012). FINGER can assist flexion/extension of the index and middle fingers along a naturalistic grasping/release trajectory. Robot data were sampled at 1000Hz and sub-sampled/recorded at 64Hz. On the "Go" trials, the robot only assisted the user after they reached a finger extension force threshold, requiring the participant to initiate each trial of their own volition. Assistance forces were based on a position (PD) controller that corrected user movement towards a minimum-jerk trajectory that would complete a full movement in 0.5 s. Thus, if the user lagged the trajectory, the robot would assist them. However, if the user exceeded the trajectory, the robot would slow them down.

We compared two pre-response cuing conditions on separate days: 1) a warning stimulus that did not inform about which fingers would be requested to be flexed (Fig. 2, UnCued) and 2) a pre-trial cuing of the to-be-flexed fingers (Fig. 2, PreCued). We also tested two movement types: flexion and extension. Thus, there were four experimental conditions including the mixtures of cued/uncued and flexion/extension movements. EEG activity for the pre-movement period was analyzed to identify SMR features, i.e. amplitudes in specific mu (9-13 Hz) or beta (18-27 Hz) frequency bands at locations over the sensorimotor cortex, which best predicted movement versus no movement. We did this for each of the four experimental conditions. In Phase 2, the participant was trained to increase or decrease this SMR feature. In Phase 3, the subject was cued to either increase or decrease this SMR feature prior to finger movement, and the impact of pre-movement SMR amplitude on movement performance was assessed (Fig. 3).

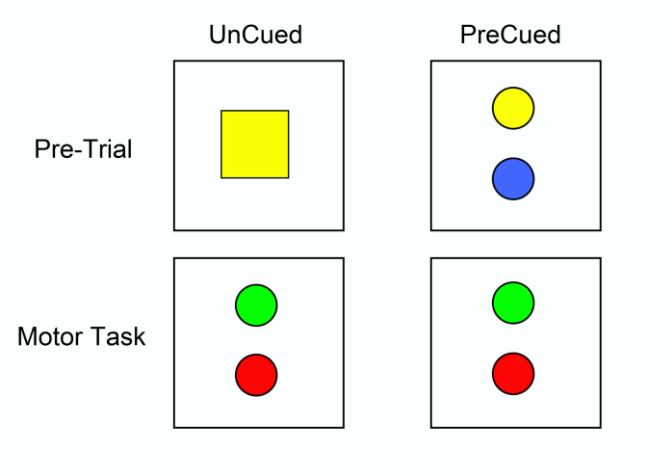

FIG. 2. THE LEFT PANEL ILLUSTRATES THE CONDITION WHERE THE TO-BE-FLEXED FINGERS ARE NOT IDENTIFIED DURING THE PRE-TRIAL PERIOD. THE RIGHT PANEL ILLUSTRATES THE CONDITION WHERE THE TO-BE-FLEXED FINGERS ARE IDENTIFIED DURING THE PRE-TRIAL PERIOD. IN THE PRECUED CONDITION, YELLOW ON TOP INDICATES THAT THE INDEX FINGER WILL SUBSEQUENTLY BE FLEXED AND BLUE ON THE BOTTOM INDICATES THAT THE MIDDLE FINGER WILL REMAIN EXTENDED.

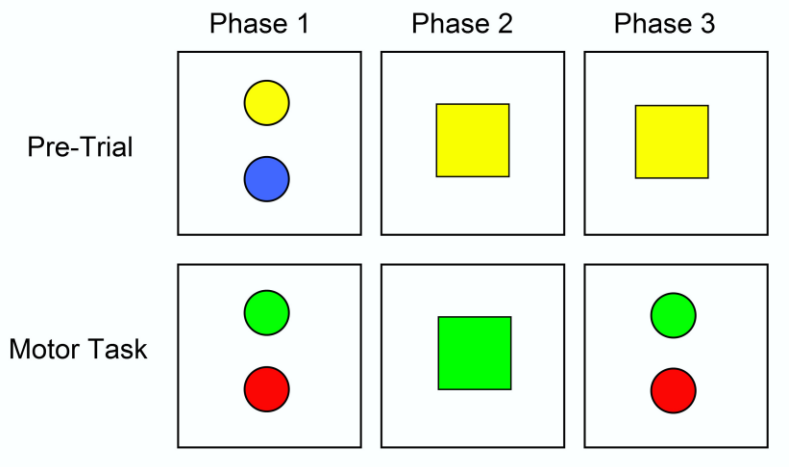

FIG. 3. THREE PHASE DESIGN. THE LEFT PANEL SHOWS THE CUED TASK THAT WAS USED TO IDENTIFY SMR FEATURES FOR TRAINING (4 SESSIONS). THE MIDDLE PANEL SHOWS THE TRAINING PHASE (10 SESSIONS). SUBJECTS LEARNED TO REDUCE SMR FEATURES WITH YELLOW TARGETS AND INCREASE SMR FEATURES WITH BLUE TARGETS. WITH SUCCESS, TARGETS TURNED GREEN. THE RIGHT PANEL SHOWS PHASE 3 STIMULI (5 SESSIONS). SUBJECTS GENERATED APPROPRIATE SMR CONDITIONS TO INITIATE MOTOR TASKS.

6.2.2 RESULTS

We tested several regression models: elastic net with l_1 and l_2 regularization, and Ordinary Least Squares. Phase 1 predictive models were successful across all participants in

that they could predict go vs. nogo during the training period using any of the model types. That is, the response parameters (uncued and cued go/nogo for all finger combinations) were correlated with 24 EEG features using ordinary and l_1 penalized canonical correlation models (Witten, Tibshirani, & Hastie, 2009). The l_1 penalty produced sparse solutions, and was thus thrown out. We generated these models on training data from the first day of data. In general, the comparisons' generalization to test data, taken on the second day, was poor.

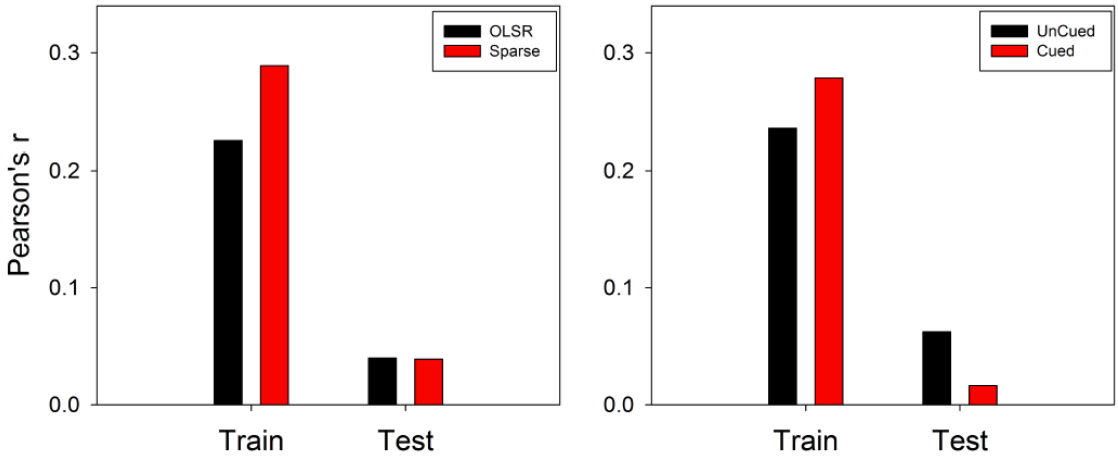

FIG. 4. PHASE 1 PREDICTION OF RESPONSE PARAMETERS FOR PRE-TRIAL CUED AND UNCUED CONDITIONS. THE LEFT PANEL COMPARES THE SPARSE AND ORDINARY MODELS WHEN USED FOR PARAMETER ESTIMATION AND MODEL VALIDATION (MODEL X USE INTERACTION, F=28.48, P<0.0001). THE RIGHT PANEL COMPARES THE CUED AND UNCUED CONDITIONS (CUE X USE INTERACTION, F=5.30, P<0.0468). IN THESE COMPARISONS, GENERALIZATION TO TEST DATA WAS GENERALLY POOR.

We also tested two types of EEG montage transforms: Laplacian transform (McFarland, McCane, David, & Wolpaw, 1997) and bipolar derivations involving channels *C3* and either *AFz*, *FCz*, *CPz*, or *POz*. We then correlated cued movement or rest with 24 EEG features using the OLSR and elastic net penalties (Zou & Hastie, 2005). Bipolar derivations consistently outperformed the Laplacian transformation (Fig. 5).

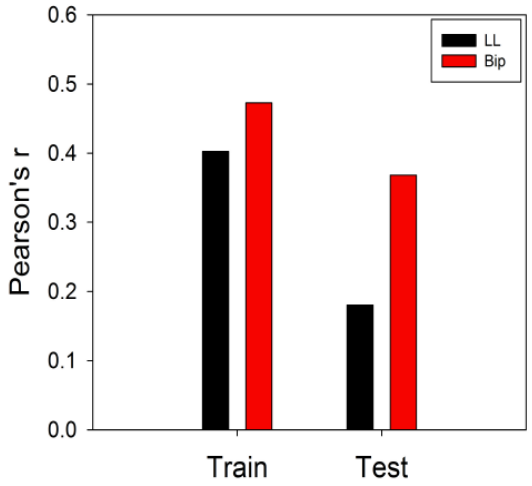

FIG. 5. PHASE 1 PREDICTION OF STIMULUS CONDITIONS FOR THE PRE-TRIAL CUED TASK. THIS FIGURE COMPARES THE RESULTS OF EEG FEATURES DERIVED WITH EITHER A LARGE LAPLACIAN (LL) TRANSFORM OR BIPOLAR DERIVATIONS (BIP). CORRELATIONS AND GENERALIZATION TO TEST DATA WAS BETTER FOR BIPOLAR DERIVATIONS.

Finally, we tested the ability of the model types to predict active vs. passive movements. That is, volitional/active movements by the participant in the robot vs. passive, robot-imposed movements of the fingers. Models based on passive movement data generalized better than active movement models (Fig. 6). In addition, all the penalized models generalized better than OLSR.

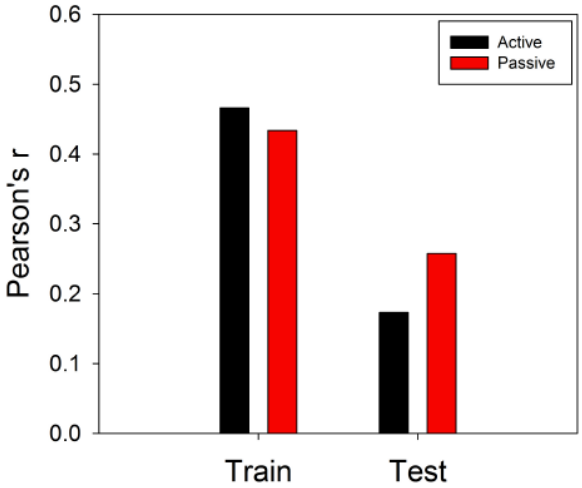

FIG. 6. PHASE 1 PREDICTION OF STIMULUS CONDITIONS FOR THE PRE-TRIAL CUED ACTIVE AND PASSIVE MOVEMENTS. A COMPARISON OF ACTIVE AND PASSIVE MOVEMENT CONDITIONS REVEALED THAT MODELS BASED ON PASSIVE MOVEMENT DATA GENERALIZED BETTER THAN ACTIVE MOVEMENT MODELS.

After phase 2 training, all participants generated significantly higher SMR amplitudes on the blue target trials and smaller SMR amplitudes on the yellow trials. Here, we present a topographical map of r^2 values describing what areas of the brain, for each participant, correlated with the yellow vs. blue response parameter. Participants, A, B, C, and F used their right hands; participants D and E used their left hands. Participants A, B, E, and F showed lateralized activation contralateral to the limb being moved in primary sensorimotor cortex, although participant F did show some bilateral activation. Participants C and D exhibited more central activation patterns. The amplitude spectra reveal that most participants were modulating in the mu or beta band, or both. For example, participant D showed a clear separation of the spectra for go vs. nogo trials at approximately 20 Hz. Participants C and F exhibited small amounts of low-frequency modulation.

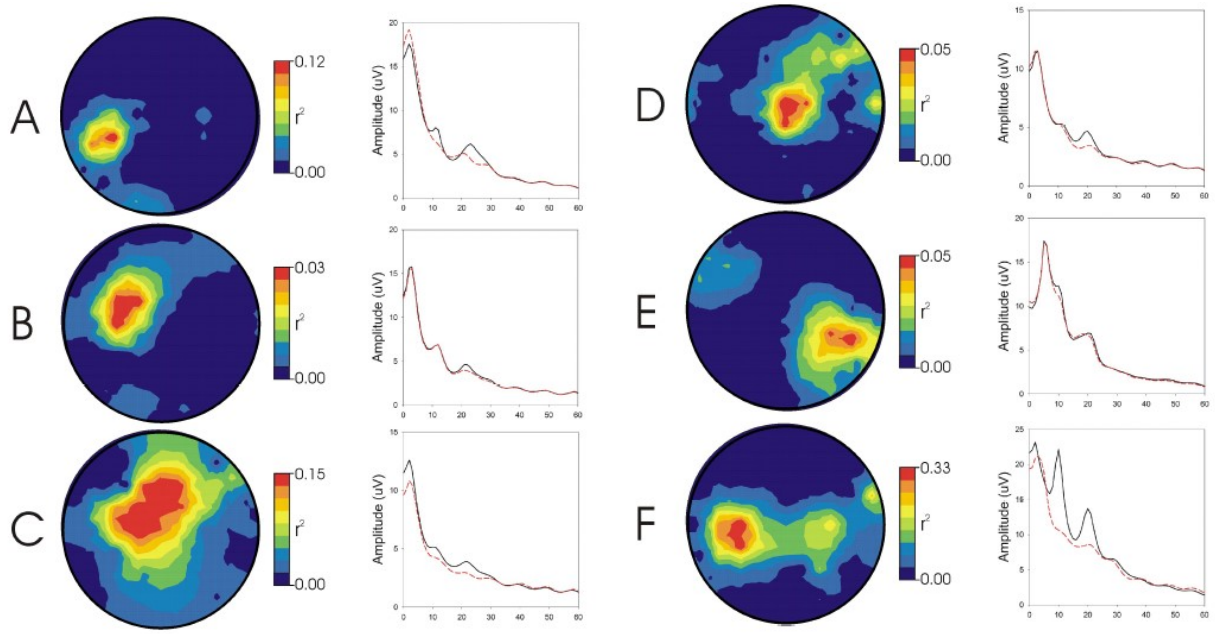

FIG. 7. R^2 TOPOGRAPHIES AND VOLTAGE SPECTRA FOR EACH INDIVIDUAL SUBJECT ON THE LAST SESSION OF PHASE 2 BCI TRAINING.

Finally, we examined the effects of voluntary pre-movement SMR modulation on subsequent motor performance. In Table 1, we present the movement measure mean values across all responses for each participant. A few key results are that four of six participants significantly altered their response latency, maximum response latency, and maximum acceleration

latency by modulating pre-movement SMR and four participants, including three of the aforementioned, significantly altered their maximum acceleration amplitude.

TABLE 1: PHASE 3 FINGER MOVEMENT PERFORMANCE ON TRIALS WITH BLUE (SMR INCREASE) AND YELLOW (SMR DECREASE) CUES FOR INDIVIDUAL SUBJECTS. LATENCIES ARE IN MSEC AND AMPLITUDES ARE IN PERCENTAGE OF MAXIMUM POSSIBLE. SIGNIFICANCE LEVELS ARE DENOTED BY: *P<0.05, **P<0.01, ***P<0.001, +P<0.0001.

Table 1: Phase 3 Movement Performance

Subject	SMR	SMR feature	Latency (ms)	Max Amplitude	Time to M.A. (ms)
A	Increase	4.27	827	61.2	981
	Decrease	4.18+	767	63.8	921
B	Increase	2.52	497	69.2	763
	Decrease	2.02+	459**	69.9	633+
C	Increase	1.96	627	82.6	855
	Decrease	1.31+	521+	82.4	718+
D	Increase	3.32	484	88.7	805
	Decrease	1.95+	475	89.6	803
E	Increase	5.57	821	50.6	988
	Decrease	3.35+	978**	44.5**	1103*
F	Increase	7.43	622	57.5	897
	Decrease	4.04+	556	57.2	832++

Although many subjects exhibited significantly altered movement performance as the result of successfully modulating pre-movement SMR, the effect on movement was not consistent across subjects or indeed, across responses, i.e. which finger moved (Fig. 8). For example, Participants B and D, both subjects' latency was shorter when they moved two fingers after successfully decreasing their pre-movement SMR compared to when they moved two fingers after increasing their pre-movement SMR. In both subjects, latency was longer with two finger movements than one finger movements. In contrast to two finger movements, when these participants moved one finger after successfully decreasing pre-movement SMR, the reduction in latency was less in subject B and even reversed in subject D. Thus, in these subjects, SMR effects varied with response requirements.

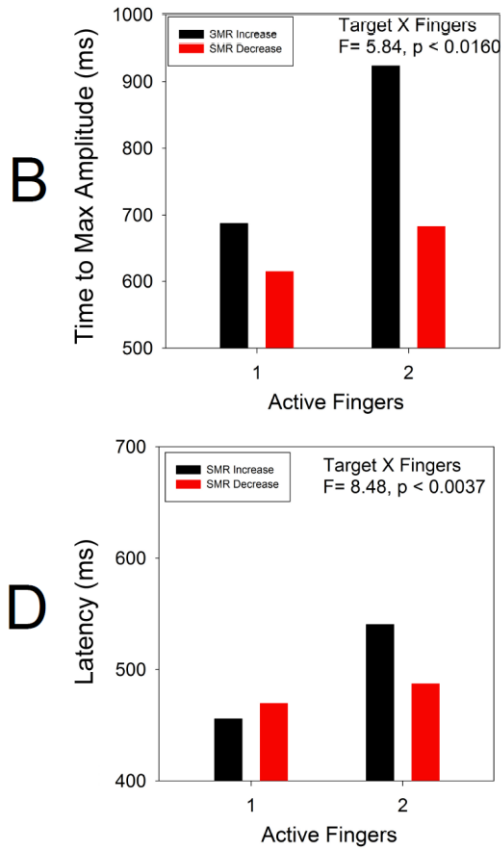

FIG. 8. PHASE 3 MOTOR PERFORMANCE FOR SUBJECTS B (UPPER PANEL) AND D (LOWER PANEL) AS A FUNCTION OF NUMBER OF ACTIVE FINGERS (ONE OR BOTH). IN BOTH SUBJECTS, LATENCY IS LONGER WITH TWO FINGER MOVEMENT AND DECREASES WHEN SMR IS VOLUNTARILY DECREASED. WITH SINGLE FINGER MOVEMENTS, THIS EFFECT IS LESS (SUBJECT B) OR REVERSED (SUBJECT D). THUS, SMR EFFECTS CAN VARY WITH RESPONSE REQUIREMENTS.

6.2.3 DISCUSSION

Previous research has shown that controlling pre-movement sensorimotor rhythm (SMR) activity can modulate reaction time in mental tasks (Boulay et al., 2011) and motor tasks such as a joystick-based cursor movement task (McFarland et al., 2015). Here, we found that, in adults without motor impairment, controlling pre-movement SMR activity in the EEG over contralateral sensorimotor cortex can modulate the performance of subsequent movement performance in a finger movement task. This provides a rationale for using this finger movement test in a BCI-robot protocol in people with stroke.

In addition to this primary finding, we also found several secondary findings. First, we found that cued and uncued movements had comparable correlations to the response

value (Fig. 4), indicating feasibility in a BCI methodology designed around either approach. Thus, in Chapter 7, we describe a BCI-robot therapy protocol for people with stroke designed around both cued and uncued movements. Next, we found that Bipolar channels performed better than Laplacian channels (Fig. 5). Thus, in the following work we discard Laplacian channel analysis in favor of Bipolar channels. We also found that the models continued to perform, and in-fact performed better in the test data set, for passive movements compared to active movements (Fig. 6). Again, this highlights the sensory nature of the sensorimotor cortex, especially in a robot-assisted movement environment, and is confirmatory of my previous results described in (S. L. Norman et al., 2016). Next, we describe a second pilot experiment that explores several other questions pertaining to BCI-robot training, but now in a study of people with chronic movement disability after a stroke.

6.3 PREDICTING FINGER MOVEMENT IN PEOPLE WITH CHRONIC STROKE

The primary goal of this pilot study was to answer the question: Can our existing methodology to discriminate movement using EEG, so-far tested only in unimpaired people, also predict movement in people with stroke? We also aim to explore whether finger flexion, or finger extension, stand to experience greater effect from SMR training in people with stroke.

6.3.1 METHODS

We recruited five (N=5) individuals with paresis of the left hand resulting from chronic stroke, all male, aged 27-73 (mean 56 +/- SD 17.9), Fugl-Meyer Assessment (FMA) at baseline 47.8+/-8.4, Box & Blocks Test (BBT) at baseline 23.4 +/-10.7. Participants performed a go-nogo finger movement task using the FINGER robot-assisted movement system (Taheri et al., 2014). Visual stimuli cued movement conditions for index, middle, or both fingers. Participants used their impaired hand to complete finger individuated extension and finger individuated flexion tasks to discern any differences in motor performance and EEG signals between the two. Robot assistance was provided only after the subject initiated movement, detected by FINGER when the user exceeded a force threshold against the robot. No assistance was provided for incorrect movements. Participants completed two sessions with at-least 24 hours between them. Each session consisted of six two-minute runs of approximately 18 trials per run.

Visual cues were given on the screen to cue the participants' movement. At the beginning of each trial, two dots, arranged vertically on a monitor in front of the participants, presented different colors. The top dot represented the imperative stimuli for the index finger, while the bottom finger represented the imperative stimuli for the middle finger. During a pre-movement period, the dots would present as either yellow or blue. Yellow dots indicated that the corresponding finger would subsequently be cued to move while blue dots indicated that the corresponding finger would not be cued to move. The pre-movement stimulus appeared on the screen for an average of 1.5 sec, but was randomized to avoid predictive movements by the participant. After the pre-movement stimuli were presented, the movement cue was given. At this point, yellow circles turned green for 'go' and blue

circles turned red for 'no-go' for the corresponding fingers. The participant would attempt to move the finger(s) that was given a 'go' cue, as quickly and as far as possible. Participants were assisted by the Finger Individuating Grasp Exercise Robot (FINGER) (Taheri et al., 2012). Robot data were sampled at 1000Hz and sub-sampled/recorded at 64Hz. On the "Go" trials, the robot only assisted the user after they reached a finger extension force threshold, requiring the participant to initiate each trial of their own volition. The size of the circles on screen would grow with the position change of a correctly-moved finger. At the completion of movement, defined as 90% of the maximum range of the robot, the large green circle would turn white to indicate a successful trial. An example of a successful index finger flexion trial can be seen in Fig. 9.

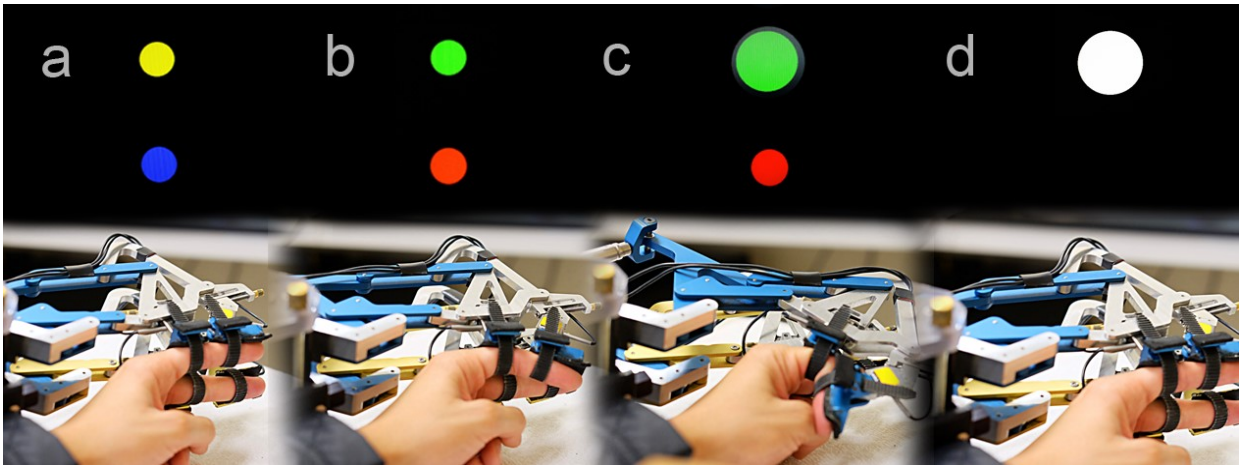

FIG. 9. TIME PROGRESSION OF AN INDEX FINGER FLEXION 'GO' TRIAL. TOP: VISUAL CUES GIVEN TO THE PARTICIPANT. BOTTOM: THE CORRESPONDING RESPONSE OF A PARTICIPANT USING FINGER. AN EXAMPLE MOVEMENT PROGRESSION CAN BE SEEN STARTING WITH A, AN INDEX MOVEMENT PREPARATION CUE (YELLOW DOT), AND B, THE 'GO' CUE (GREEN DOT) AND THE CORRECT MOVEMENT RESPONSE (INDEX FINGER FLEXION). IN C, THE PARTICIPANT'S CORRECT RESPONSE HAS ELICITED ROBOT ASSISTANCE FOR THE REMAINDER OF THE MOVEMENT. VISUAL FEEDBACK IS GIVEN IN THAT THE GREEN CIRCLE GROWS WITH FINGER POSITION. IN D, THE CUE TURNS WHITE INDICATING A PROPERLY EXECUTED MOVEMENT BEYOND A TARGET DISTANCE. AFTER THIS, THE PARTICIPANT WAS GIVEN VISUAL FEEDBACK ON THE LATENCY FROM GO CUE TO FINGER MOVEMENT INITIATION, WHICH THEY WERE INSTRUCTED TO MINIMIZE, AND THE ROBOT RETURNED THE PARTICIPANT'S FINGER BACK TO THE STARTING POSITION.

EEG was recorded using 16 electrodes embedded in a cap (ElectroCap, Inc.) according to the modified 10-20 system referenced to the mastoid and re-referenced, in software, to a common average transform (McFarland et al., 1997). Spectral analysis was performed using the 16th order autoregressive algorithm described in (McFarland & Wolpaw, 2008).

Amplitudes for six 3-Hz spectral bands from 6-24 Hz were computed for 400-ms sliding windows updated every 50 ms. The response parameters (go vs. nogo for all finger combinations) were correlated with 24 EEG features (amplitudes for each spectral band & location) using ordinary least square regression (OLSR) and canonical correlation (Elastic Net) with l_1 penalties models (Witten et al., 2009). We used the glmnet package from R (J. Friedman, Hastie, & Tibshirani, 2010). Data from session 1 was used as the training set. We validated the model using data from session 2, on a different day.

6.3.2 Results

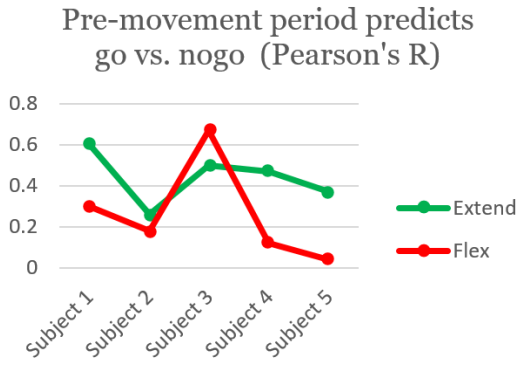

Fig. 10. Pearson's R Values for the best predictor model by subject. Pre-movement period SMR features predict go vs. nogo. Flexion and Extension movements results are given.

For the finger extension task, the OLSR modeling of pre-movement SMR features on the training set (first day) successfully predicted go/nogo cues in all five participants ($p<0.05$) on the test data (second day). The elastic net model successfully predicted go/nogo cues in 4/5 participants. For the finger flexion task, the OLSR model successfully predicted go/nogo cues in just 1/5 participants, and the elastic net model successfully predicted go/nogo cues in just 2/5 participants. We outline these results by each participant and motor task (flex/extend) in Table 2. Overall, models of pre-movement SMR predicted go vs. nogo with better accuracy for finger individuated extension movements compared with flexion movements in four out of five subjects (Fig. 10).

TABLE 2: PEARSON'S R VALUES. PRE-MOVEMENT SMR FEATURES PREDICT GO VS. NOGO (TARGET COLOR). ELASTIC NET AND ORDINARY LEAST SQUARES REGRESSION (OLSR) RESULTS FOR BOTH FLEXION AND EXTENSION MOVEMENTS. *P<0.05. **P<0.01.

Subject	Model	Extend	Flex
1	**Elastic Net**	.55**	.30**
1	**OLSR**	.60**	0.18
2	**Elastic Net**	NA	NA
2	**OLSR**	.26*	0.18
3	**Elastic Net**	.50**	.67**
3	**OLSR**	.37**	.42**
4	**Elastic Net**	.36**	NA
4	**OLSR**	.47**	0.12
5	**Elastic Net**	.34**	NA
5	**OLSR**	.37**	0.04

Pre-movement features showed varying results across participants (Fig. 11). The strongest pre-movement and intra-movement correlations for participant 1 were in the 18 Hz band and located above contralateral motor cortex. Participants 2 and 4 had little spatial or spectral variation in pre-movement correlations but showed significant correlations at 18 Hz and 12 Hz, respectively, during the intra-movement period. Participants 3 and 5 showed broad spatial and spectral patterns correlating to the go/nogo condition. In general, intra-movement features were more robust, showing predictive power in all five participants. We present the correlation topographies for each participant and frequency band in Fig. 11 for comparison to the pre-movement period topographies. However, because these features are of little utility in an SMR training BCI protocol, we did not investigate these signals any further.

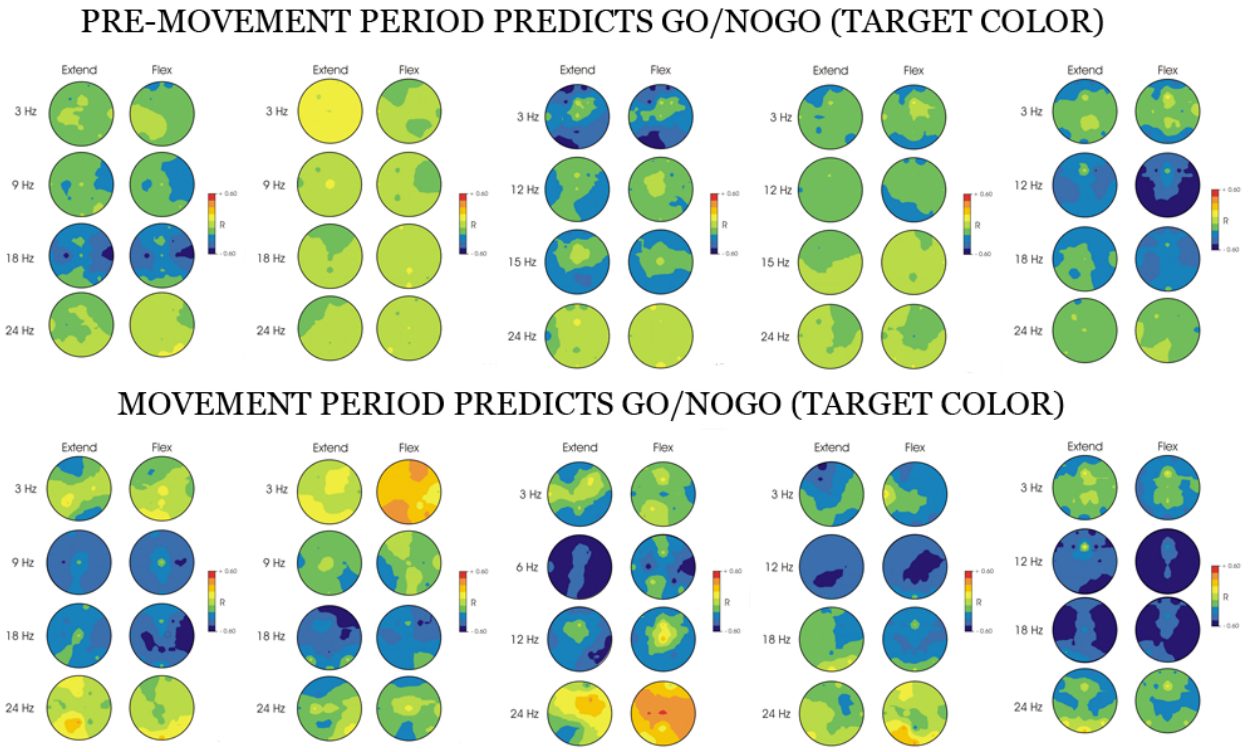

FIG. 11. TOPOGRAPHICAL MAPS OF PEARSON'S R VALUES FOR PREDICTING WHETHER THE PARTICIPANT IS PREPARING TO RESPOND OR WITHHOLD A RESPONSE (I.E. TARGET COLOR GREEN VS. RED) BASED ON SMR PRECEDING MOVEMENT ONSET (SEE FIG 9A). EACH GROUPING OF TWO COLUMNS REPRESENTS DATA FROM EACH SUBJECT.

6.3.3 DISCUSSION

These results show that we could predict the willing intent to move the finger in a person with stroke using an SMR-based BCI protocol over the course of multiple session. Our previous work (McFarland et al., 2015) in unimpaired people suggests that operant conditioning of SMR features during movement preparation can improve subsequent motor performance. The present results provide a potential basis for conditioning such activity in people with motor deficit after stroke to beneficially modify neural circuits important to finger movement.

A secondary finding is that EEG features predicting finger extension generalized to a second session with better accuracy than features predicting finger flexion. Finger extension deficit is a major contributor to movement disability in the hand for people with chronic stroke (Lang, DeJong, & Beebe, 2009), and, conveniently, the current results show that an ensuing finger extension movement is more robust to detection with pre-movement EEG

features than finger flexion. Thus, in Chapter 7, we describe a BCI-robot therapy protocol for people with stroke designed to train finger extension rather than finger flexion.

By focusing on the movement preparation period, this work is exploring a new way in which BCI technology might contribute to rehabilitation after stroke or in other chronic movement disorders. BCI-based shaping of pre-movement SMR activity together with robot-assisted movement could potentially enhance rehabilitation and augment recovery of hand function.

CHAPTER 7: LEARNING TO CONTROL PRE-MOVEMENT SENSORIMOTOR RHYTHM CAN IMPROVE FINGER EXTENSION AFTER STROKE

7.1 ABSTRACT

Brain-computer interface (BCI) technology, combined with robot assistance, is attracting increasing interest as a possible tool for enhancing rehabilitation therapy of motor function after stroke, yet the optimal way to apply this technology is unknown. Here, we studied the immediate and therapeutic effects of learning to control pre-movement sensorimotor rhythm (SMR) using a BCI on subsequent finger extension ability of people with moderate to severe hand impairment after chronic stroke. Eight participants (mean Box and Blocks Test (BBT) score = 14 compared to a normal score of 70) completed four weeks of an EEG-based training protocol during which they practiced finger extension with assistance from the FINGER robotic exoskeleton. During the first week (Phase 1) we identified individualized SMR features in the pre-movement EEG that correlated with the intent to try to extend the finger. Next, for two weeks (Phase 2), the participants learned to increase or decrease their selected SMR features given visual feedback, without moving the fingers. Finally, in the fourth week (Phase 3), participants were cued to increase or decrease their SMR feature immediately prior to attempting to extend the fingers. Six of eight participants achieved reliable control of the BCI in Phase 2, but spectral analysis indicated the possibility of non-EEG control by two of these six. In Phase 3, the four participants with brain-based control of the BCI initiated finger extension faster after decreasing compared to increasing pre-movement SMR amplitude, consistent with previous findings with unimpaired people. We also show, for the first time, that these participants extended the fingers more forcefully after decreasing pre-movement SMR amplitude. Across the course of training, participants' hand function, measured by the BBT showed modest improvement (4.3 +/- 4.5). BBT score at screening predicted the final change in BBT score (R^2=0.63, p=0.019), and the strength of this effect was significantly improved by limiting the model to the participants with BCI control (R^2=0.99, p=0.005). That is, participants with higher baseline finger function had significantly better motor outcome following the BCI-based training, and those that achieved brain-based control benefit most. These results show that learning to control pre-movement SMR can modulate finger extension ability, and suggest

possible therapeutic carry-over from the BCI training process, meriting further investigation in a rehabilitation context.

7.2 INTRODUCTION

Stroke is the leading cause of disability worldwide (Feigin et al., 2014; Lopez et al., 2006), affecting over 700,000 people in the US each year (Broderick et al., 1998). It is estimated that about 80% of people with acute stroke experience motor deficits (Gresham et al., 1995). After injury, people with stroke typically undergo several months of movement rehabilitation with the goal of improving functional movements.

Robotic devices, such as powered exoskeletons, have been suggested to assist rehabilitation therapy for people with stroke and other neurologic impairments (Reinkensmeyer et al., 2004). Robotic assistance has been shown to enhance afferent feedback, which may aid neural reorganization (Hornby et al., 2010). Past literature has shown the efficacy of robot-assisted therapy to equal or better the results of conventional rehabilitation techniques (Hidler et al., 2009; Volpe et al., 2005). Robot-assisted therapy is not without its flaws, however. For example, maintaining active effort by the patient is vital to motor recovery (Hu et al., 2009; Lotze et al., 2003; Reinkensmeyer et al., 2004). Unfortunately, patient engagement is not guaranteed in a robot-assisted environment due to a phenomenon called “slacking”, a subconscious and automatic reduction in effort by the patient (Reinkensmeyer, Wolbrecht, et al., 2012; Wolbrecht et al., 2008). Furthermore, control strategies such as force amplification and gravity cancellation are not sufficient for patients with severe paralysis. Brain-computer interface (BCI) technology has been proposed as one potential solution to augment robot-assisted therapy for the purpose of restoring motor function after neurologic injury (Daly & Wolpaw, 2008). Toward this end, we explore the possibility that BCI training could enhance the efficacy of robot-assisted movement training for people with stroke.

BCI has also been suggested to leverage neuroplasticity to improve motor outcome after neurologic injury. Since its inception in the 1940’s, activity dependent plasticity, i.e. “Hebbian” plasticity, has been expanded to apply to representational plasticity documented after subjects endured manipulations of inputs from the peripheral nervous system

(Buonomano & Merzenich, 1998). In 1991, Taub's study in macaque monkeys demonstrated cortical reorganization after undergoing peripheral nerve limb deafferentation over a decade earlier (KAAS, TAUB, & MISHKIN, 1991). Sensorimotor rhythm (SMR) training has been used as the go-to control signal for BCI protocols that aim to alter cortical organization, with modest therapeutic effect (Buch et al., 2008; Ramos-Murguialday et al., 2013). SMR training may also be useful for normalizing SMR activity to produce more normal subsequent movements (McFarland et al., 2015), but this approach has not yet been tested in people with stroke.

Although there has been much speculation as to the capacity of electroencephalographic (EEG) based BCI technology to contribute to the rehabilitation of motor function, there is limited empirical data suggesting that volitional control of EEG activity can modify motor behavior. In this work, we hypothesize that 1) people with stroke can obtain control of an EEG-based SMR-amplitude BCI, given visual feedback, and 2) volitional modulation of pre-movement SMR amplitude immediately before a finger extension task can alter motor performance, measured as movement onset latency and maximum extension torque. In a previous study, we trained eight (N=8) unimpaired participants to control SMR during movement preparation in a similar manner to this study (McFarland et al., 2015). Following successful BCI training, participants were required to modulate SMR amplitude to initiate a motor task. Movement onset latency was significantly reduced when participants decreased their pre-movement SMR amplitude. Here we present a pilot study to test the ability of people with chronic hand paresis after stroke to control such a BCI and its potential effects on motor performance.

7.3 METHODS

7.3.1 PARTICIPANTS

We recruited individuals who had experienced a single stroke at least six months previously, which had spared the ipsilesional precentral gyrus, (i.e. whose stroke was subcortical or cortical sparing primary motor area), and who had a significant but not total deficit of finger motor function, defined as a Box and Blocks Test (BBT) score between 1 and 25. The resulting eight (N=8) participants were all male, aged 44-83 (mean 59.5 +/- SD 11.8),

with BBT score at baseline between 1-22 (mean 12.0 +/- 8.5). All participants were naïve to brain-computer interface training and achieved a satisfactory score (minimum 24) on the Montreal Cognitive Assessment (MoCA). All participants provided written informed consent and the study was approved by the Institutional Review Board of UC Irvine.

7.3.2 Protocol

Participants engaged in four weeks of training, undergoing three days of training per week using the FINGER robotic exoskeleton (Taheri et al., 2014). Each day consisted of 8 3-minute runs, with an average total of 240 trials per day. The study was divided into three phases. Phases 1 and 3 lasted one week, and incorporated finger extension practice, while Phase 2 lasted two weeks and focused solely on SMR control (Fig. 1). Phase 1 identified one or more SMR features in the EEG during the preparatory period that correlated with the go/nogo condition of the finger extension movement trial. Phase 2 trained users to increase or decrease the amplitude of these SMR features using visual feedback only, without attempting to move the fingers. Phase 3 combined the SMR regulation of Phase 2 with the movement of Phase 1 to evaluate the effects of achieving control of the pre-movement SMR feature on an immediately ensuing finger extension movement attempt.

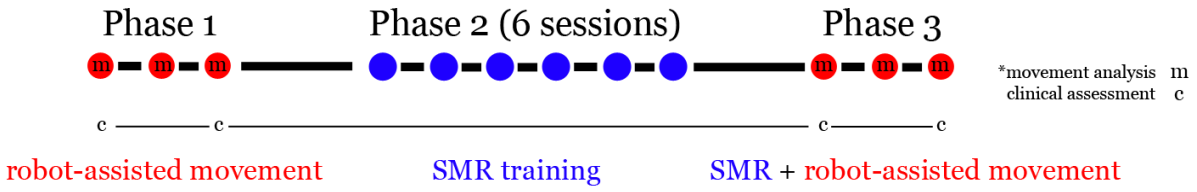

Fig. 1. Timeline of study. Each dot represents one session/day of training. Each group of three dots represents one week of training (4 weeks total). Red sessions indicate robot-assisted movement trials and blue sessions indicate BCI/visual feedback only sessions. Phases 1 and 3 had three sessions each, while phase 2 had six sessions. Clinical assessments of upper extremity movement ability were conducted at the beginning and end of phases 1 and

3.

7.3.3 Phase 1 – Identification of SMR features

During Phase 1, we aimed to identify participant-specific SMR features that predicted the intent to try to extend the fingers as quickly and forcefully as possible. Participants sat in a chair facing a 24" 1920x1080 monitor 1.5 m away while EEG was recorded. Participants completed a Go/NoGo task cued on the monitor. "Go" trials required them to extend the index finger only, the middle finger only, or both fingers together. On these trials, robot assistance was provided by the Finger Individuating Grasp Exercise Robot (FINGER) (Taheri et al., 2012). FINGER can assist flexion/extension of the index and middle fingers along a naturalistic grasping/release trajectory, and was used to record position, acceleration, and force at the proximal and middle phalanxes of the index and middle fingers to calculate torque at the metacarpophalangeal (MCP) joint. These data were sampled at 1000Hz and sub-sampled/recorded at 64Hz. On the "Go" trials, the robot only assisted the user after they reached a finger extension force threshold, requiring the participant to initiate each trial of their own volition. Assistance was given primarily to assist participants in completing finger extension movements that they couldn't normally complete on their own. Assistance forces were based on a position (PD) controller that corrected user movement towards a minimum-jerk trajectory that would complete a full extension movement in 0.5 s. Thus, if the user lagged the trajectory, the robot would assist them. However, if the user exceeded the trajectory, the robot would slow them down. We did not observe a slowing effect in any of the participants in this study.

Movement conditions were randomized between 1) no-movement (i.e. "NoGo" condition), 2) index finger only, 3) middle finger only, and 4) both finger movement. All movements were attempted using the paretic hand. Each trial began with the fingers flexed. Extension of the index and/or middle fingers was cued during a warning phase by the colors of two circles on the monitor (Fig. 2a). During the 1 s period prior to movement, the participant received a yellow circle(s) for the to-be-extended finger(s) and a blue circle(s) for any finger(s) that were to remain flexed, i.e. no movement. During the response interval, yellow circles changed to green to cue extension ("Go" condition) and blue circles changed to red to cue the participants' finger to remain flexed ("NoGo" condition, Fig. 2b). The participant had 2 seconds to complete the response (Fig. 2c). The green circle would grow

with proper movement as a form of positive visual feedback. If the response was correct and the participant completed the movement, the circle turned white for 1 s (Fig. 2d). If the response was not correct, or 2 seconds expired, the screen went black for 1 sec. Fig. 2 also shows an example of the finger position response profile recorded from a single trial. After each movement, the robot returned the fingers to the flexed position and held the fingers there.

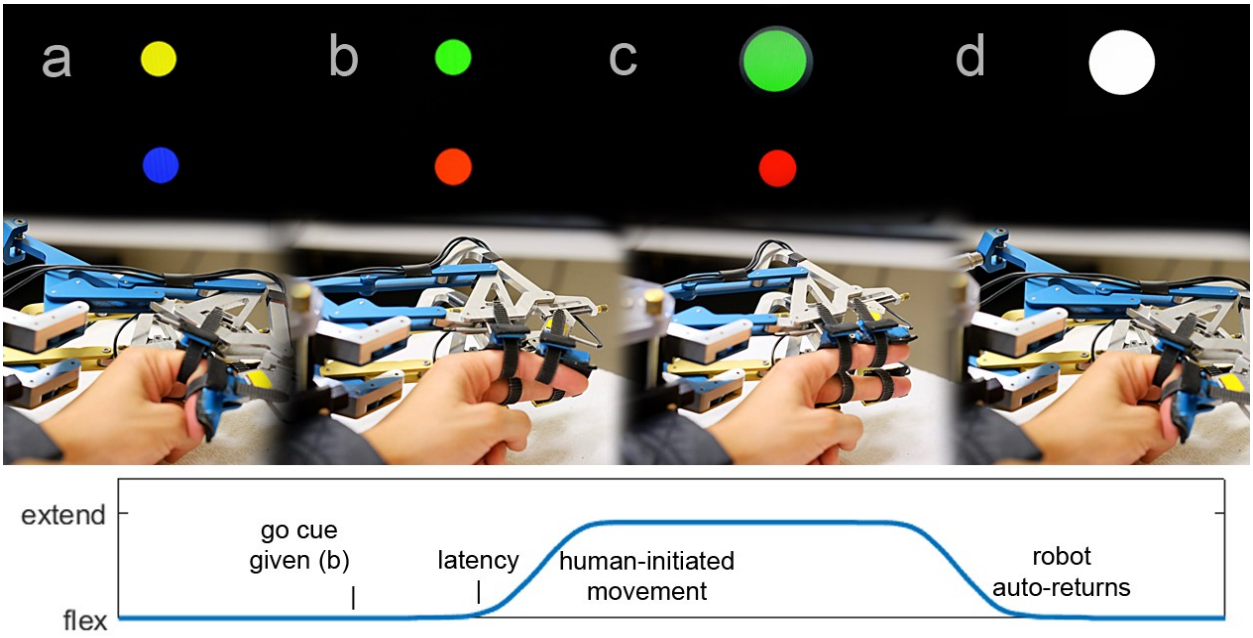

FIG. 2. PROGRESSION OF AN INDEX FINGER EXTENSION TRIAL DURING PHASE I. TOP: VISUAL CUES GIVEN TO THE PARTICIPANT. BOTTOM: THE CORRESPONDING RESPONSE OF A PARTICIPANT USING FINGER. AN EXAMPLE MOVEMENT PROGRESSION CAN BE SEEN STARTING WITH A, AN INDEX MOVEMENT PREPARATION CUE (YELLOW CIRCLE), AND B, THE 'GO' CUE (GREEN DOT) AND THE CORRECT MOVEMENT RESPONSE (INDEX FINGER EXTENSION). IN C, THE PARTICIPANT'S CORRECT RESPONSE HAS ELICITED ROBOT ASSISTANCE FOR THE REMAINDER OF THE MOVEMENT. VISUAL FEEDBACK IS GIVEN IN THAT THE GREEN CIRCLE GROWS WITH FINGER POSITION. IN D, THE CUE TURNS WHITE INDICATING A PROPERLY EXECUTED MOVEMENT BEYOND A TARGET DISTANCE. AFTER THIS, THE PARTICIPANT WAS GIVEN VISUAL FEEDBACK ON THE LATENCY FROM GO CUE TO FINGER MOVEMENT INITIATION, WHICH THEY WERE INSTRUCTED TO MINIMIZE, AND THE ROBOT RETURNED THE PARTICIPANT'S FINGER BACK TO THE STARTING POSITION.

7.3.3.1 EEG DATA COLLECTION, PROCESSING, AND MODELING

EEG activity for the period between the two cues was analyzed to identify the SMR features, defined as the amplitude in a specific mu (8-12 Hz) or beta (18-30 Hz) frequency band at a specific location(s) over sensorimotor cortices – that best predicted movement in the "Go" condition versus the "NoGo" condition. EEG was recorded using 9-mm tin electrodes

embedded in a cap (ElectroCap, Inc.) at 16 scalp locations according to the modified 10-20 system of Sharbrough et al. (Sharbrough et al., 1991). The electrodes were referenced to the mastoid and re-referenced to a common average reference transform (McFarland et al., 1997). Their signals were amplified and digitized at 256 Hz by a g.USB. BCI operation and data collection were supported by the BCI2000 platform (Mellinger & Schalk, 2009; Schalk, McFarland, Hinterberger, Birbaumer, & Wolpaw, 2004). Spectral analyses were performed using the 16^{th}-order autoregressive algorithm described in McFarland and Wolpaw (McFarland & Wolpaw, 2008) and used in (McFarland et al., 2015). The amplitudes for 3-Hz spectral bands from 6-24 Hz were computed for 400-ms sliding windows updated every 50ms. Next, we used multiple regression models in the glmnet package from R (J. Friedman et al., 2010) to correlate potential SMR features (e.g. SMR amplitude at 6-9 Hz for electrode *C3*) with the warning cue value (Go vs. NoGo). We tested three regression models: Elastic Net with l_1 and l_2 regularization and Ordinary Least Squares, keeping the best result for each participant.

7.3.4 Phase 2 – Sensorimotor rhythm training

In Phase 2, participants were trained to gain volitional control of the SMR feature amplitude selected on the basis of the analysis of the Phase 1 data. Participants attended three sessions of Phase 2 training per week for two weeks (6 total sessions). Each session lasted approximately one hour, during which participants completed 8 x 3-minute runs of SMR training. Participants learned to increase or decrease the amplitude of the SMR feature identified in Phase 1 using visual feedback in the form of color change of a square on the monitor. Participants were instructed to explore different motor imagery scenarios, e.g. finger movement, until they found a strategy that allowed them to control the BCI. For each trial, the starting color of the 5.1 cm squares was randomly chosen to be yellow or blue. When the square appeared, the participant controlled the saturation of the colored square based on real-time feedback of their modulation of the SMR. For yellow squares, the participant was asked to maintain the SMR feature amplitude above a threshold value for 1 s. As the criterion approached threshold, the square would change color to a brighter yellow and finally to bright green for 0.5 s upon success (Fig. 3). In blue-target trials, participants were asked to maintain the SMR feature amplitude below a threshold value for 1 s. As the criterion

approached threshold, the square would turn to a brighter yellow and finally to a bright green for 0.5 s upon success.

FIG. 3. PROGRESSION OF A PHASE 2 TRIAL. PARTICIPANTS LEARNED TO INCREASE SMR FEATURES ON YELLOW TARGETS AND DECREASE SMR FEATURES ON BLUE TARGETS GIVEN VISUAL FEEDBACK: A YELLOW TARGET APPEARS IN A, PROMPTING THE PARTICIPANT TO MODULATE THEIR SMR FEATURE AMPLITUDE. THE PARTICIPANT APPROACHED THE SMR CRITERION IN B, AND SUCCESSFULLY REACHED THE TARGET IN C, RESULTING IN A GREEN SQUARE/POSITIVE FEEDBACK. THE SCREEN GOES BLANK FOR 2.5 S AFTER FEEDBACK IN D. IF THE PARTICIPANT DID NOT REACH THE SMR CRITERION OR MODULATED THEIR SMR FEATURE IN THE WRONG DIRECTION, THE SCREEN GOES BLANK, AS IN D, WITHOUT SHOWING THE GREEN BOX, AND A NEW TRIAL STARTS AFTER A 2.5 S PERIOD.

Although all participants were given feedback on SMR regulation, the specific spatiospectral location of the SMR was participant-dependent as determined from their Phase 1 data. We selected the spatiospectral locations that maximized the predictive capacity of our models for each participant. Spatiospectral locations of SMR features (up to 3) for each participant can be seen in Table 1.

7.3.5 PHASE 3 – SMR-TRIGGERED MOVEMENT PERFORMANCE

Phase 3 consisted of three sessions spread over the one week immediately following the conclusion of Phase 2. During Phase 3, participants were given multimodal feedback on their ability to volitionally modulate SMR amplitude. Like Phase 2, participants were initially presented with a colored square that was color-saturated by proper SMR feature modulation. When the participants reached the feature threshold, a movement trial was immediately cued. Like Phase 1, the robot actively maintained a constant position, thus resisting movement, allowing for isometric torque to be measured. Once the participant initiated a movement (i.e. reached the force threshold) robot assistance was activated.

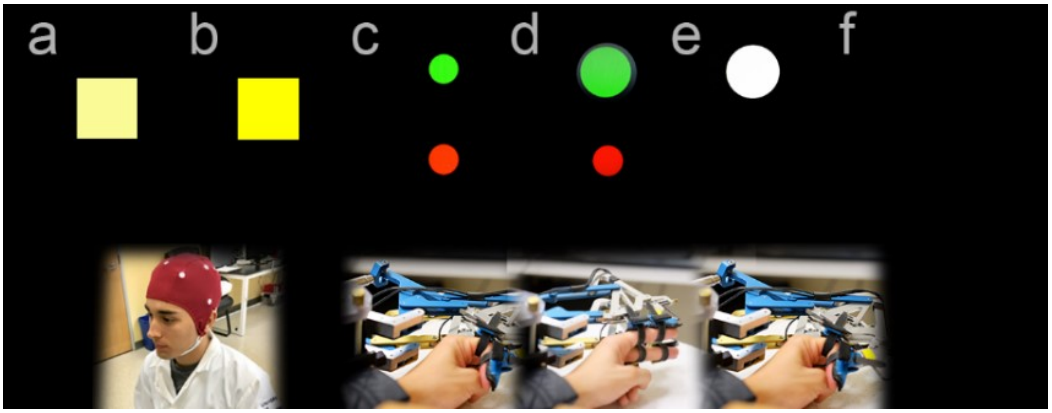

FIG. 4. PROGRESSION OF A PHASE 3 TRIAL. PARTICIPANTS MODULATED THEIR SMR FEATURE PER THE STIMULUS IN A, WHICH MAY HAVE BEEN A YELLOW (DOWN-REGULATION) OR BLUE (UP-REGULATION) SQUARE. AS THE PARTICIPANT SUCCESSFULLY GENERATED THE APPROPRIATE SMR (B), THE SQUARE GREW BRIGHTER. WHEN THE PARTICIPANT SUCCESSFULLY REACHED THE SMR CRITERION, THE MOVEMENT STIMULI WERE PRESENTED, INSTRUCTING THE PARTICIPANT TO FLEX THE INDEX OR MIDDLE FINGER, OR BOTH, USING GREEN CIRCLES (C). OTHERWISE, THE SCREEN WENT BLANK. IN D, THE PARTICIPANT'S CORRECT RESPONSE INITIATE INDEX FINGER EXTENSION ELICITED ROBOT ASSISTANCE FOR THE REMAINDER OF THE MOVEMENT. VISUAL FEEDBACK OF MOVEMENT PROGRESS WAS GIVEN IN THAT THE GREEN CIRCLE GREW WITH INCREASING FINGER EXTENSION POSITION. IN E, THE CUE TURNED WHITE INDICATING A PROPERLY EXECUTED MOVEMENT. IN F, THE SCREEN WENT BLANK BETWEEN TRIALS FOR 2.5 S AND THE ROBOT RETURNED THE PARTICIPANT'S FINGER BACK TO THE STARTING POSITION.

During Phase 3, we collected two primary measures of movement performance: latency to movement onset and maximum MCP torque. Latency to movement onset was defined as the amount of time it took the participant to initiate movement in the robot, i.e. exceed the force threshold that triggered robot assistance. Torque about the metacarpophalangeal joint (MCP torque) was calculated based on the forces measured by transducers placed at the proximal and middle finger joints of the index and middle fingers. Here, we report maximum MCP torque, calculated as the maximum MCP torque on an individual trial in the extension direction, normalized to the maximum torque across all trials. Thus, MCP torque is reported as a value 0-1.

7.4 RESULTS

7.4.1 PHASE 1 – IDENTIFICATION OF SMR FEATURES

Phase 1 data were collected to identify participant-specific SMR features that could maximally predict the movement intention of the participant, i.e. if they were about to move

or not. We successfully generated models for all eight participants that correlated SMR features with the Go-NoGo response condition in the training data from the first two sessions (R values ranged 0.156-0.783, mean R=0.5341, $p<0.05$ for 8/8 participants and $p<0.01$ for 7/8 participants). These models generalized well to test data from the third session (R values ranged 0.078-0.772, mean R=0.481, $p<0.05$ for 7/8 participants and $p<0.01$ for 5/8 participants). For each participant, we selected the model that had the highest correlation to the response condition. The linear combination of these SMR features comprised the 'SMR Composite' signal, which is what we used in Phase 2 as a measure of SMR regulation. In other words, regulating the SMR composite score, a linear combination of the power at the SMR features identified for each person, directly affected the stimulus color during Phases 2 and 3. Table 1 shows, for each participant, up to three SMR features that had the largest weights in the regression models. Note that all channels are bipolar referenced to *Cz*.

Table 1: SMR features and phase 2 accuracy for each subject

Subject	Impaired	Channel	Frequency (Hz)	Channel	Frequency (Hz)	Channel	Frequency (Hz)	Percent Correct
A	R	C3	18, 24	C4	18-24	CP4	12, 24	**82.4**
B	L	CP3	18-24	CP4	12, 24	-	-	**73.6**
C	R	C3	21	CP3	12, 21-24	CP4	12, 21	40
D	L	C4	12, 15	CP3	12	CP4	18	47.7
E	R	CP3	18	-	-	-	-	**74.5**
F	R	C3	21	C4	12, 21	-	-	**76.6**
G	L	C3	21	C4	12, 21	-	-	**72.7**
H	R	C3	15, 18	C4	18, 21	CP3	3, 18	**68.5**

7.4.2 Phase 2 – Sensorimotor rhythm training

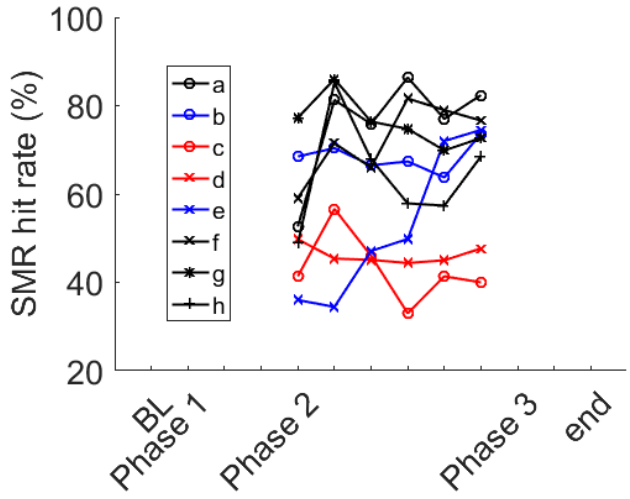

Fig. 5. BCI hit rate across Phase 2 sessions for all participants. All but two participants (c and d, in red) learned to reliably control the BCI. Two participants (b and e, in blue) exhibited broad spatiospectral patterns indicative of non-EEG BCI control.

The purpose of Phase 2 was for the participants to learn to volitionally modulate the SMR feature identified for them in Phase 1 using visual feedback (Fig. 3). Table 1 shows the percent correct on the last day of Phase 2 training. Six out of eight participants achieved BCI hit rates significantly above chance level (mean 74.8%, t-test vs. chance level across participants $p < 0.01$), and are bolded in Table 1. Individualized topographies and spectra for the last Phase 2 training day are shown in Fig. 6. Participants a, c, d, g, and h showed correlated activity (i.e. activity that correlated with the instruction to increase or decrease the feature) contralateral to their impaired hand. Participant f showed correlated activity centered about *Cz*, with less lateralization. Peak correlations were most often in the beta band for these participants, although the exact spatiospectral locations of the maximum correlation varied across individuals. Participants b and e showed broad spatial distribution and broadband spectral correlation to the SMR condition, suggesting the use of non-EEG artifacts. The proctors for this study noted that participants b and e exhibited symptoms of severe hypertonia and both participants would shrug their shoulders or tense their neck involuntarily during the recording session, which may have led to this putative EMG contamination of the EEG signals.

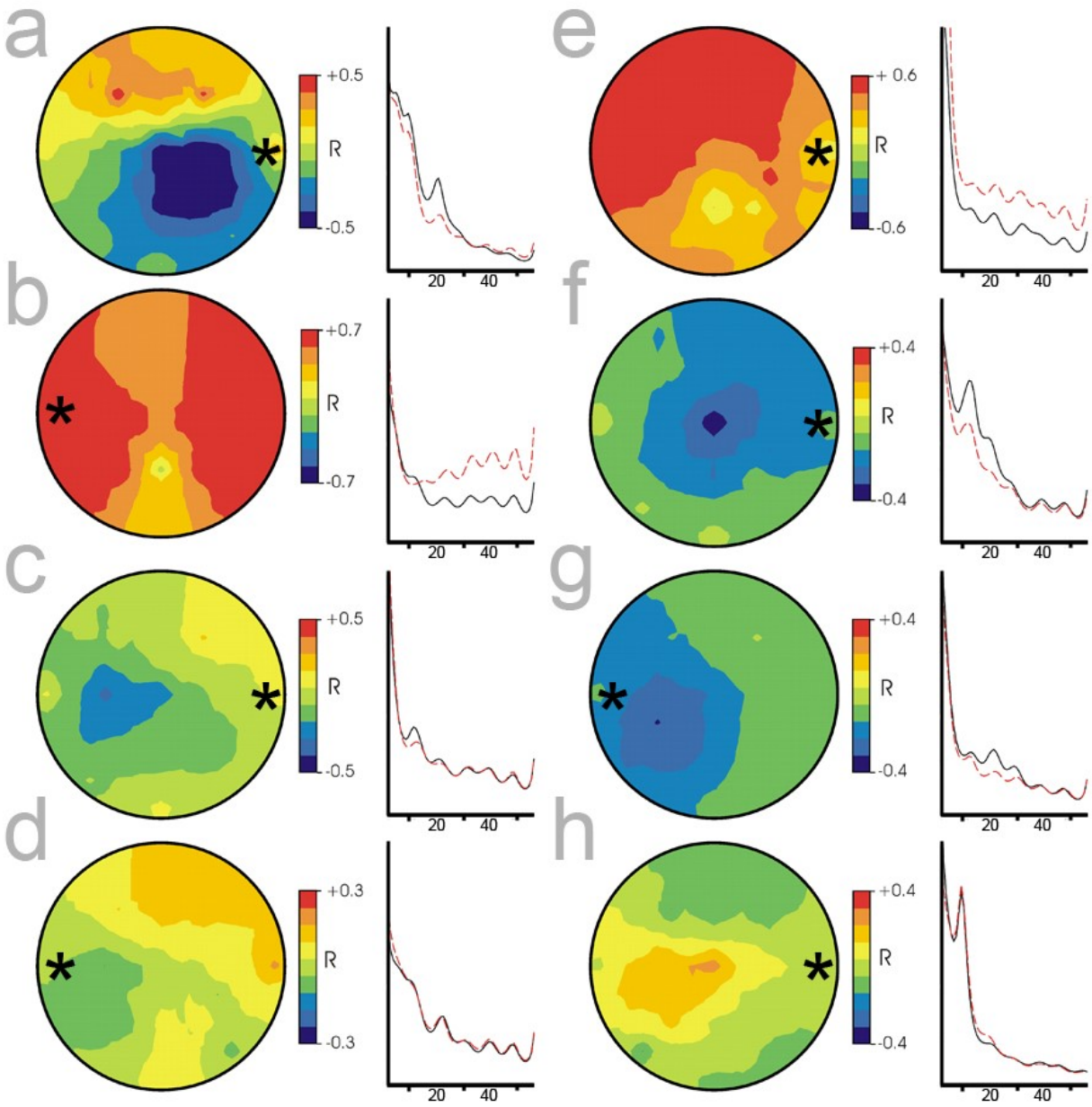

FIG. 6. TOPOGRAPHIES AND SPECTRA OF THE CORRELATION BETWEEN THE SMR FEATURE AMPLITUDE AND THE TARGET CONDITION, SMR DOWN-REGULATION VS. SMR UP-REGULATION. DATA ARE SHOWN FOR EACH PARTICIPANT, A THROUGH H, TAKEN AT THE LAST PHASE 2 SESSION. ASTERISKS DENOTE THE STROKE-AFFECTED HEMISPHERE.

7.4.3 PHASE 3 – SMR-TRIGGERED MOVEMENT PERFORMANCE

The purpose of Phase 3 was to combine the overt movement of Phase 1 with the SMR feature modulation of Phase 2 to elucidate the effects of pre-movement SMR feature modulation on movement performance in people with stroke. Like Phase 1, the participants modulated their SMR feature up or down corresponding to a visual cue on the monitor. Once they reached a threshold, a finger extension task was immediately cued (Fig. 4). We quantified three movement performance measures: latency to movement onset, maximum flexion torque at the MCP joint, and latency to the maximum flexion torque at the MCP joint. We restrict our analysis here to four participants. We exclude participants b and e who showed broad spatiospectral control of the BCI, suggesting the use of non-EEG artifacts. We also exclude participants c and d, who did not learn to control the BCI.

The four participants with reliable narrow-band BCI control at the end of Phase 2 (a, f, g, and h) showed significantly reduced SMR amplitude during blue targets. We performed two-way ANOVAs for each dependent motor performance measure (latency to movement initiation, latency to maximum MCP extension torque, and maximum MCP extension torque) and participant where the finger target (index, middle, both) and SMR condition (increase, decrease) served as independent variables. **Latency**: Three of four participants showed significantly lower latency to movement initiation for all finger targets when they reduced their SMR compared to when they increased their SMR (Fig. 8), participants a, g, h, $p < 0.05$; participant f, $p=0.40$). Two of four participants showed significantly lower latencies to maximum MCP torque in for all finger targets when they reduced their SMR (participants a, g, $p<0.01$; participant f, $p=0.49$; participant h, $p=0.09$). **MCP Torque**: Three of four participants showed significantly higher MCP torques when they reduced their SMR, with an interaction effect with finger condition. Post-hoc tests revealed that two participants showed significantly higher torques in individuated (index, middle) finger extensions when they reduced their SMR (participant a, index $p=0.012$, middle $p<0.01$; participant h, index $p=0.017$, middle $p<0.01$). The other participant showed significantly higher torques in coordinated (both) finger extensions when they reduced their SMR (participant g, both $p=0.04$).

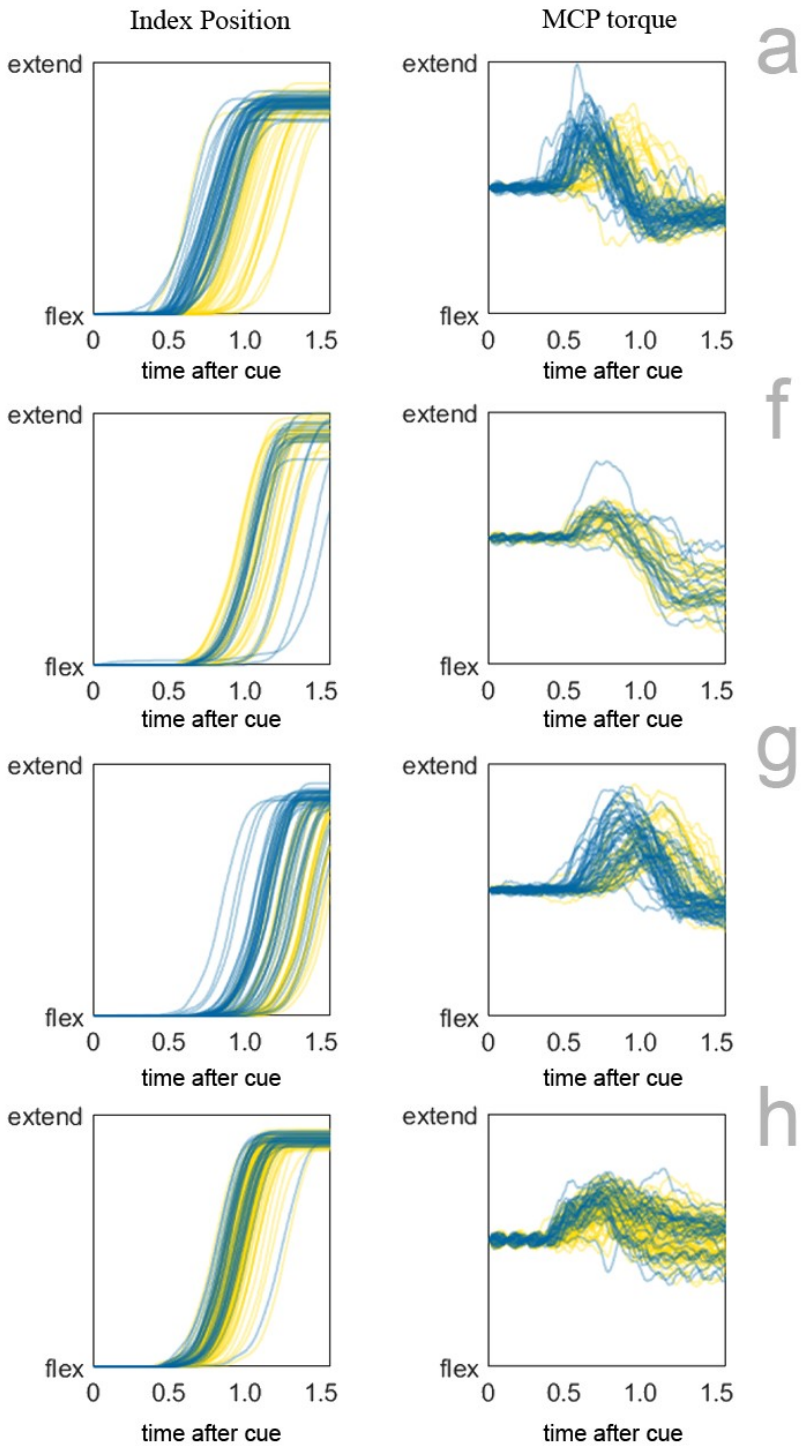

FIG. 7. ALL PHASE 3 INDEX FINGER MOVEMENTS FROM PARTICIPANTS A, F, G, AND H. INDEX FINGER POSITION (LEFT) AND NORMALIZED MCP TORQUE (RIGHT) ARE PLOTTED VS. TIME WHERE T=0 CORRESPONDS TO THE MOVEMENT CUE. YELLOW TRACES REPRESENT RESPONSES TO YELLOW STIMULI (INCREASED SMR) AND BLUE TRACES REPRESENT RESPONSES TO BLUE STIMULI (DECREASED SMR). MOVEMENT LATENCIES WERE SIGNIFICANTLY SHORTER FOR A, G, AND H WHEN THEY DECREASED THEIR PRE-MOVEMENT SMR VS. WHEN THEY INCREASED THEIR SMR. MCP TORQUES WERE SIGNIFICANTLY HIGHER FOR PARTICIPANTS A AND G WHEN THEY DECREASED THEIR SMR.

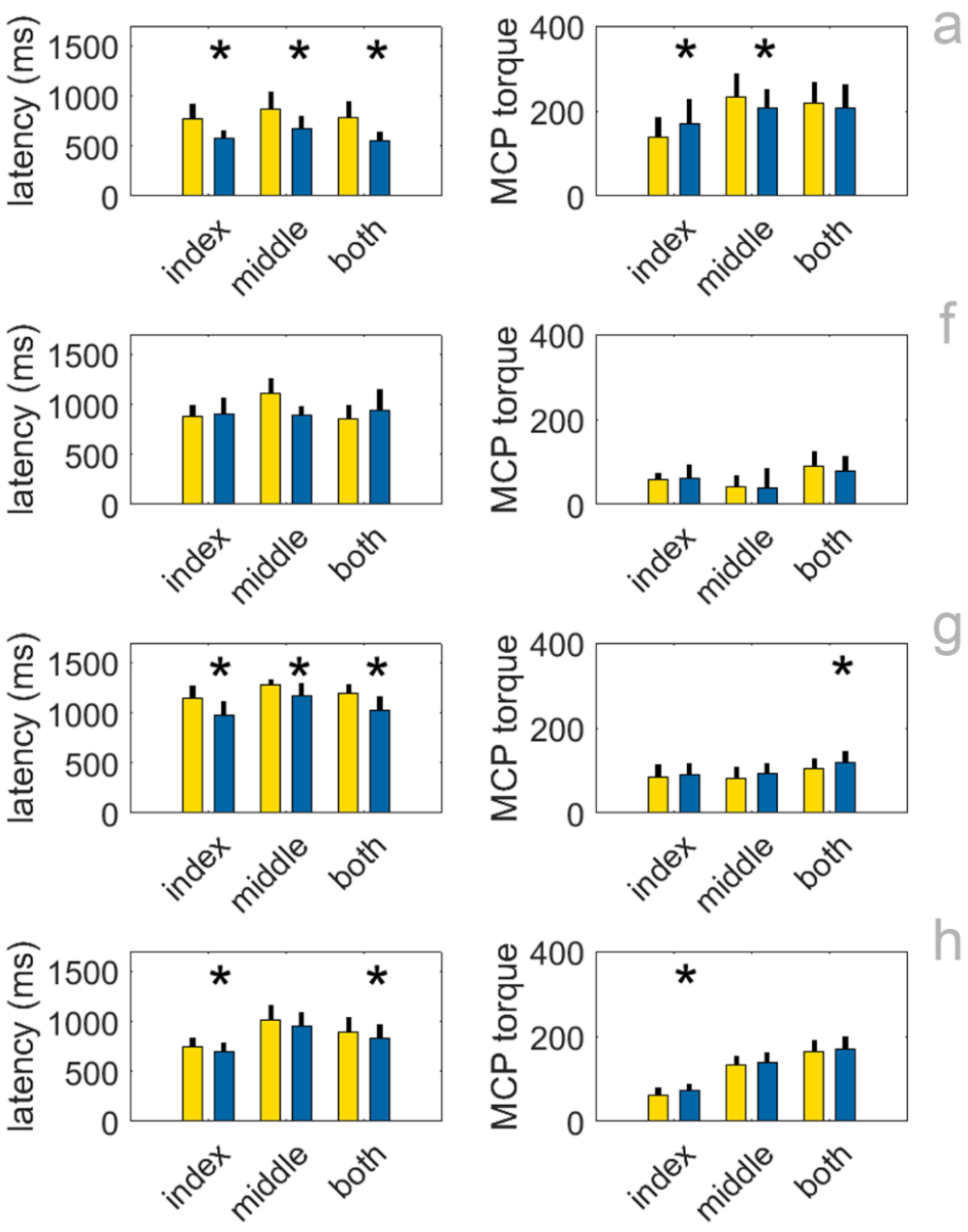

FIG. 8. PHASE 3 MOTOR PERFORMANCE COMPARISON FROM EXAMPLE PARTICIPANTS A (TOP), F, G, AND H (BOTTOM). LATENCY TO MOVEMENT ONSET (LEFT) AND MAXIMUM TORQUE (RIGHT) ARE PRESENTED WITH EACH MOVEMENT STIMULUS, I.E. INDEX FINGER, MIDDLE FINGER, OR TWO-FINGER MOVEMENT ACROSS SMR STIMULI (YELLOW & BLUE, I.E. INCREASE SMR & DECREASE SMR). STARS REPRESENT SIGNIFICANCE ($P<0.05$) AND BLACK BARS REPRESENT STANDARD ERROR. PARTICIPANTS A AND G SHOWED SIGNIFICANTLY SHORTER LATENCIES FOR ALL THREE FINGER STIMULI, AND PARTICIPANT H FOR INDEX AND BOTH FINGER STIMULI, WHEN THEY REDUCED THEIR SMR (BLUE). PARTICIPANT A HAD SIGNIFICANTLY HIGHER TORQUES IN THEIR INDEX FINGER AFTER REDUCING SMR, BUT LOWER TORQUES WITH THE MIDDLE FINGER. PARTICIPANT G HAD HIGHER TORQUE DURING TWO-FINGER MOVEMENTS ONLY AND PARTICIPANT H HAD HIGHER TORQUE DURING INDEX-FINGER MOVEMENTS ONLY.

7.4.4 Clinical Findings

The primary clinical outcome measure of this study was the Box & Blocks Test (BBT) (Radomski & Latham, 2008). Mean BBT score at screening was 14.3 +/- 10.4. For comparison, the average score for an unimpaired individual of this age group is 70.9 +/- 8.4 (Mathiowetz, Volland, Kashman, & Weber, 1985). We observed no significant effects of age, days-post-stroke, type of stroke (hemorrhagic/ischemic), or dominant hand on BBT score. We measured the change in BBT score as the difference in the score at the end of therapy compared to the mean of the values at screening and session 1. The mean change in BBT score after therapy was 4.3 +/- 4.5 with a minimum and maximum change of 0 and 12, respectively. The mean Box & Blocks change in participants that gained control of the BCI was 6.3 compared to 2.3 in those that did not learn to control the BCI or did so with broadband spatiospectral activity indicative of non-EEG control. However, the difference between groups was not significant (t-test, p=0.58).

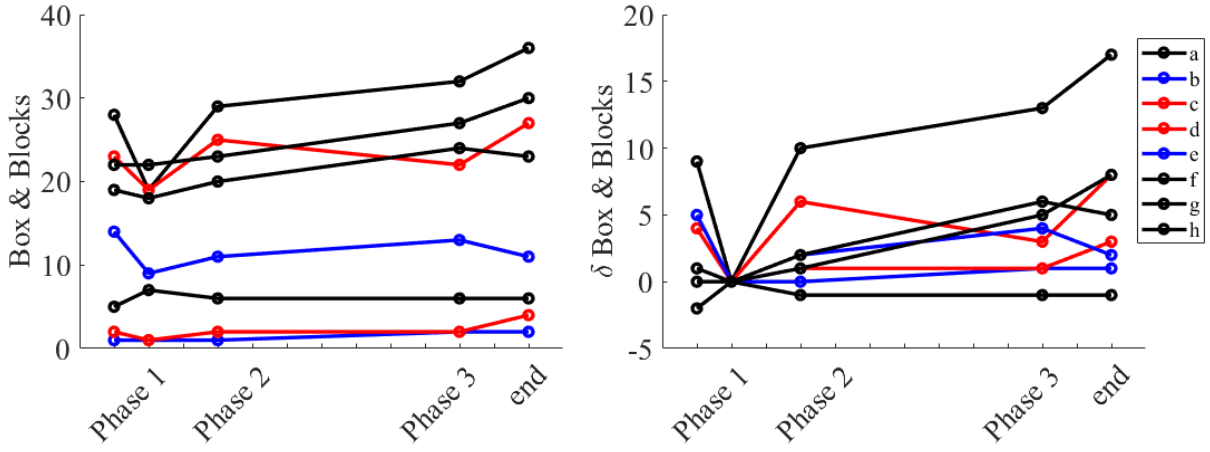

Fig. 9. Box & Blocks scores for each participant taken at baseline and the beginning and ends of phases 1 and 3. Raw scores (left) and change in score from session 1 (right) are shown. Participants that gained reliable narrow-band control of the BCI are shown in black. Participants C and D, who did not gain control of the BCI, are shown in red. Participants B and E, who used broadband activity to control the BCI, are shown in blue.

BBT score at screening predicted the change in BBT score over the course of training for all participants (R^2=0.63, p=0.019). The strength of this effect was significantly improved by limiting the model to the participants with BCI control (Fig. 10, R^2=0.99,

p=0.005). Participants with higher function had significantly better motor outcomes following the BCI-based training.

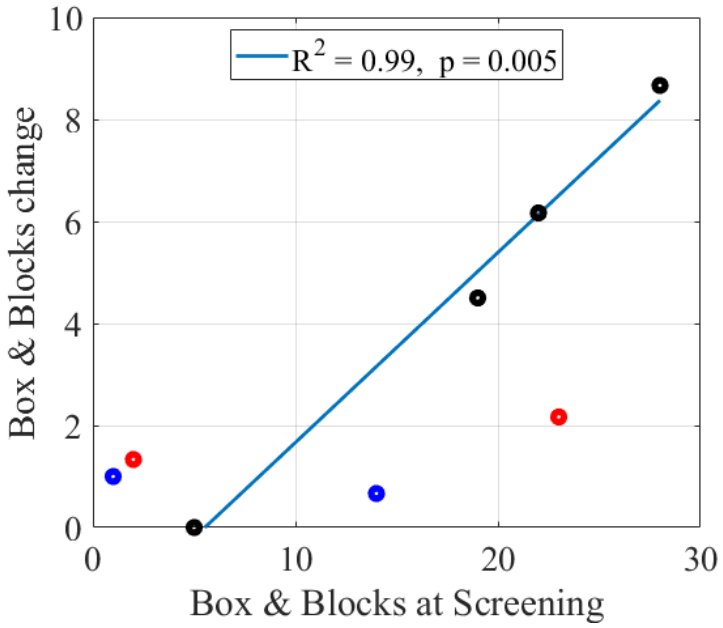

FIG. 10. BOX & BLOCKS, AS MEASURED AT THERAPY SCREENING, PREDICTED A CHANGE IN BOX & BLOCKS AFTER THERAPY, MEASURED AS THE CHANGE IN SCORE AT THE END OF THERAPY COMPARED TO THE AVERAGE OF THE BASELINE AND SESSION 1 SCORE. HIGHER BOX & BLOCKS SCORES AT BASELINE PREDICTED LARGER GAINS IN BOX & BLOCKS SCORE AFTER THERAPY. PARTICIPANTS C AND D, WHO DID NOT GAIN CONTROL OF THE BCI, ARE SHOWN IN RED. PARTICIPANTS B AND E, WHO USED BROADBAND ACTIVITY TO CONTROL THE BCI, ARE SHOWN IN BLUE.

7.5 DISCUSSION

BCI systems have been proposed, and are attracting increasing interest, to enhance rehabilitation protocols in people with motor impairment after a neurologic injury (Ang & Guan, 2013; Daly & Wolpaw, 2008). However, studies that examine the effects of BCI training for motor rehabilitation in people with stroke are limited. Most use muscle stimulation or orthotic assistance with the goal to improve sensory feedback that might improve motor outcome (Ang & Guan, 2013). To the extent that poor motor preparation can also limit subsequent motor function, training pre-movement SMR may improve motor performance. Here, we build on the results of (McFarland et al., 2015) to evaluate SMR control to improve preparation for subsequent movement in people with stroke.

7.5.1 Pre-movement SMR after stroke

Normative physiological SMR modulation includes a down-regulation of power in the mu (8-13 Hz) and beta (13-30 Hz) frequency bands preceding movement, a phenomenon known as event-related desynchronization (ERD) (Pfurtscheller & Aranibar, 1977; Pfurtscheller & Lopes da Silva, 1999). Seven of the eight participants in this study exhibited clear ERD patterns. However, the spatial representation of this signal was more broadly distributed (Fig. 6, participants a, c, d, f, g, h) than the results of previous work in unimpaired individuals (McFarland et al., 2015). This is a known phenomenon; movement related signals are often more spatially distributed in people with stroke (Cramer et al., 1997). These signals are also known to be significantly smaller in people with stroke than in those without impairment (Fu et al., 2006). Despite these confounding effects of stroke, we showed that we can predict the willing intent to move in a person with chronic stroke over the course of multiple EEG recording sessions and with similar success rates to our previous work in people without neurologic injury (McFarland et al., 2015).

7.5.2 SMR-based BCIs

Ultimately, the effectiveness of SMR-based BCIs depends on whether the underlying brain activity that produces pre-movement changes in SMR affects subsequent motor behavior. Pre-movement SMR desynchronization (Pfurtscheller & Aranibar, 1977) and post-movement rebound (Pfurtscheller, Neuper, Brunner, & da Silva, 2005) are understood to be a correlate of motor preparation (Krusienski, McFarland, Principe, & Wolpaw, 2012) and execution. Furthermore, SMR desynchronization increases motor cortex excitability (Pichiorri et al., 2011), which is thought to be beneficial for motor rehabilitation (Pomeroy et al., 2011). However, SMR's origins in the nervous system, and whether pre-movement SMR affects subsequent motor behavior, are less clear. SMR changes are an effect of a distributed process of the nervous system including premotor and motor cortices, subcortical, and spinal centers (O. Cohen, Sherman, Zinger, Perlmutter, & Prut, 2010). Resting SMR is thought to reflect motor inhibition (Pfurtscheller, 1992), a view consistent with its decrease leading up to movement and increase after movement. However, SMR may not be tied directly and uniquely to motor preparation but is also involved in preparation for

upcoming sensory information, evidenced by its modulation before passive movements elicited by an orthosis (Formaggio et al., 2013; S. L. Norman et al., 2016).

BCIs have been proposed as a possible method to enhance rehabilitation training by using operant conditioning to normalize brain states or couple normal brain states to sensory feedback. SMR operant conditioning has been used to control external devices that assist the users' movements with the expectation that the temporal coupling of more normal SMR activity to more normal sensory feedback of the device could induce Hebbian/activity-dependent plasticity in the CNS (Buch et al., 2008). For example, Ramos-Murguialday et al. used ERD as a contingent control signal for robotic therapy and found modest improvements in motor outcome compared to a control group (Ramos-Murguialday et al., 2013). Another strategy is for patients to produce more normal SMR with the assumption that normal SMR activity could also produce more normal movement (Khanna & Carmena, 2017; Rozelle & Budzynski, 1995). The implication of this approach is that people with stroke can learn, given feedback, to improve their preparation for movement. The sequential nature of the SMR and movement task used in this study is in contrast to the dual and parallel SMR and movement tasks used in other studies (Boulay et al., 2011; Ramos-Murguialday et al., 2013). Dual tasks such as these may interfere with each other, making them difficult for people with neurologic injury (Pashler, 1994). This study, for the first time in people with stroke, aims to answer whether normalizing pre-movement-associated EEG features can alter subsequent motor performance.

7.5.3 SMR TRAINING CAN AFFECT MOVEMENT PERFORMANCE

Khanna et al. recorded neural activity while three macaques performed a neurofeedback task in which they modulated their beta oscillatory power before executing an arm reaching task (Khanna & Carmena, 2017). The authors found that reaches preceded by reduced beta power had significantly less latency than those preceded by an increase in beta power. In (McFarland et al., 2015), we recorded neural activity while eight unimpaired people performed neurofeedback task in which they modulated their SMR activity before executing a joystick-based cursor-movement task with their hands. We found that movements preceded by reduced SMR power had significantly less latency than those

preceded by an increase in beta power, a result consistent with (Khanna & Carmena, 2017). The end goal of such studies is to provide insight into the mechanisms of motor performance from the brain level such that they might enhance training in a rehabilitation intervention and therefore improve restoration of useful motor function to people with neurologic injuries. Building on (McFarland et al., 2015) we set out to explore the efficacy of such a paradigm in impaired people.

In this study, six of eight people gained control of the BCI by the end of phase 2. Of those six, two exhibited broad spatiospectral control, suggesting non-EEG control of the BCI. Thus, the remaining four participants gained volitional, narrow-band control of the BCI and could be further investigated for changes in movement performance. We found that, for three out of these four people, modulating SMR amplitude during movement preparation altered subsequent movement performance. Participants' movements made after decreasing SMR amplitude were initiated with less latency compared to movements made after increasing SMR, in accordance with previous work (Khanna & Carmena, 2017; McFarland et al., 2015). In addition to these results, we also recorded measures of force at the proximal and middle phalanxes of the index and middle finger. We calculated the torque at the metacarpophalangeal joint, finding that two of the four participants had significantly higher extension torques when they had decreased SMR before the movement. In addition to improving latencies for the first time in people with stroke, these results also show, for the first time, that people can produce more forceful movement by decreasing their SMR before movement.

7.5.4 BCI & ROBOT TRAINING COULD IMPROVE MOVEMENT RECOVERY AFTER STROKE

The primary purpose of this study was methodological in nature: to explore the effects of modulating pre-movement SMR on subsequent motor performance. In addition to these results, we also performed clinical evaluations at screening, sessions 1, 3, 10, and 12. None of the participants showed a decline in function, and we saw an average increase of 4.3 blocks, which is a modest increase. Although the improvement in Box & Blocks score was higher for the four participants who had narrow-band control of the BCI (6.3) than in the four who did not (2.3), this result was not significant, meriting further investigation, ideally

with a larger sample size and a sham control group similar to (Ramos-Murguialday et al., 2013).

BCI has been suggested as a potential therapy for people with stroke, with an emphasis on people with more severe paralysis. In this study, we found that Box & Blocks score positively correlated with the change in Box & Blocks score over the course of training (Fig. 10, R^2=0.99, p=0.005). That is, people with higher functional scores at screening had better functional outcome. BCIs that interface with robot assisted movement therapy may be subject to the same constraints as robot therapy alone when considering their therapeutic efficacy, i.e. users must enter the therapy with sufficient function to utilize the robot.

7.5.5 Limitations

It was thought to best serve our study to select patients with an intact somatosensory cortex to not confound the EEG readings with such superficial damage. This decision was deemed necessary to prevent technical confounders. However, stroke patients with hemiparesis must have had damage either cortically or subcortically. Thus, the necessity to target patients with subcortical damage may create some unpredictable variability in response to therapies that could enhance cortical plasticity events. As brain imaging techniques improve, it may be possible to analyze the specific area where subcortical damage has occurred, e.g. internal capsule vs. thalamus, to better categorize patients' response to neuroplasticity-based therapies.

The majority (six of eight) of participants in this study gained volitional control of the BCI. However, two participants had severe hypertonia and were unable to completely relax during the BCI trials. Although they gained control of the BCI, it is likely that muscle activity obscured the EEG signals on enough trials to discredit their results. This is an important limitation in this type of BCI, where its utility may be limited for users with severe hypertonia.

This is the first test of SMR based training of pre-movement brain states to improve subsequent motor performance in people with stroke. However, the sample size of this study was small and only three participants improved their motor function, as measured by the robot. Longitudinal assessment of motor learning was not evaluated here. Increases in

clinical outcome, measured by the Box & Blocks Assessment, were modest but encouraging. Although this study provided evidence for this methodology to be feasible in people with stroke, its efficacy as a therapy is not yet clear. To examine clinical efficacy, future work would benefit from use of a larger sample size and a control group of people with stroke who receive sham BCI therapy with dose-matched robot assisted movement.

7.6 CONCLUSION

BCI-based training protocols for movement therapy are of growing interest. Training SMR features associated with movement performance has been shown to be a viable protocol in unimpaired people. This approach has further shown potential to improve motor performance immediately after desynchronizing individualized SMR features. In this study, we trained individualized SMR features in people with stroke and explored the effects of SMR modulation on subsequent movement performance. We found that people with stroke can learn to control this type of BCI and that it does affect movement performance. Specifically, we showed for the first time in people with stroke that decreasing SMR amplitude before movement produces quicker and more forceful movements. Although sample size was limited (N=8), a moderate therapeutic effect was observed, amplified in participants who entered the study with more residual motor function.

CHAPTER 8: POTENTIAL FOR LOW-COST DEVICES AND IN-HOME BCI-ROBOT THERAPY

Note: Portions of this chapter have been published as:

Aguilar, C., Shanta, O., Tran, T., Reinkensmeyer, D.J., & Norman, S. (2015, October). Towards a Low-Cost Alternative for BCI-aided Neurorehabilitation: A Comparison of the Emotiv Epoc to a Clinical EEG System. American Society of Neurorehabilitation 2015 Annual Meeting Abstracts.

Norman, S.L., Sarigul-Klijn, Y., & Reinkensmeyer, D.J. (2016, April). Design of a Wearable Robot to Enable Bimanual Manipulation after Stroke. Southern California Robotics Symposium 2016.

8.1 INTRODUCTION

Brain-computer interfacing (BCI) is a form of human-machine interaction with potential to enhance rehabilitation therapy after neurologic injuries. The most common method used to capture data in BCI is electroencephalography (EEG). In EEG, electrodes embedded in a non-invasive cap detect electrical signals over the user's scalp. The BCI then decodes these signals to control an external device, such as a wheelchair or exoskeleton robot. Although EEG has proven useful for neurorehabilitation, typical systems are very expensive, limiting their use to clinical and research settings. In recent years, low-cost alternatives, such as the Epoc by Emotiv©, have targeted widespread use of BCI, including bringing BCI into the home. In this chapter, I explore the potential of the Emotiv Epoc as a low-cost EEG headset for in-home use.

Individuals with hemiparesis after stroke often cannot use their hands together to achieve bimanual functions, as they lack the ability to extend the fingers in one hand. Static exoskeletons, such as FINGER described in this document, are useful in a clinical setting but are too expensive and difficult to operate to be viable as a commercial system. Indeed, adoption of rehabilitation exoskeleton robotics for commercial use is limited (Dollar & Herr, 2008), especially for the upper extremity (Lo & Xie, 2012). In recent years, wearable hand orthoses have gained popularity, and could potentially facilitate a path from the clinic to people's homes for orthotic devices (Bos et al., 2016).

Wearable robots could potentially enable finger extension after stroke, a key impaired function, but most previous devices are bulky and focus on multiple finger assistance and hard-wired control schemes (Bos et al., 2016). However, all degrees of

freedom in the hand are not lost. In this document, we have explored people with chronic stroke's ability to flex their fingers and the difficulty they incur to extend their fingers. In this chapter, I also present a wearable Robotic Hand Extension Device (RHED) that combines the user's residual capacity for finger flexion with robot assistance to enable extension in the user's thumb and index finger.

8.2 TOWARDS LOW-COST EEG: A COMPARISON OF THE EMOTIV EPOC TO A CLINICAL EEG SYSTEM

8.2.1 INTRODUCTION

Brain computer interface (BCI) technology records and translates neurophysiological signals to communicate with an external device (Birbaumer & Cohen, 2007). EEG, a non-invasive technique, records electrical activity at the scalp using dry electrodes, wet electrodes in a salt-water solution, or electrolyte gel injected into electrode sites. A commonly used EEG corollary to movement intention is a reduction of amplitude in the mu (8-12 Hz) and beta (13-30 Hz) frequency bands located in the sensorimotor and premotor cortices, a phenomenon called Event-Related Desynchronization (ERD) (Pfurtscheller & Lopes da Silva, 1999), and is commonly used in BCI applications as a control signal, e.g. (Ramos-Murguialday et al., 2013). ERD is robust, but smaller in amplitude for those with neurologic impairment (Fu et al., 2006). It is therefore important to be able to reliably detect changes in the sensorimotor rhythm (SMR) such as ERD for the purposes of BCI-assisted neurorehabilitation.

Despite promising results from past studies to improve BCI rehabilitation methods (Ramos-Murguialday et al., 2013), the cost of clinical EEG recording devices make them less accessible to the end-user and limit their use in developing countries or in-home therapies. Several low-cost EEG-based BCI alternatives are currently available on the market. One such device is the EPOC headset by Emotiv Inc. ©. The Emotiv EPOC is one of the first commercially available BCI systems intended for both impaired and unimpaired users and can be purchased at a starting cost of $399 as of this writing. The EPOC has 14 dry electrodes that record electrical activity at the scalp and transmits wirelessly to a receiver unit

connected to a standard computer. Its open license and access to raw data allow for flexible implementations and modulations of the acquired data, providing the technical possibility to use it for EEG-based BCIs.

There has been caution exercised in promoting the Emotiv EPOC to acquire significant EEG modulations (Duvinage et al., 2012). However, some studies have shown optimistic results acquiring well-studied event related brain signals. A key study demonstrated the ability of the Emotiv EPOC headset to successfully acquire event-related synchronization (ERS) modulations during motor imagery experiments (Vamvakousis & Ramirez). Another such study showed success of this device in a hybrid BCI paradigm that navigated a virtual humanoid robot in a computerized maze (Choi & Jo, 2013).

Here, we aim to investigate the potential for the EPOC, a dry electrode system, to detect ERD in a robot assisted environment. We directly compare the results of the EPOC to a clinical grade EEG recording system: the EGI Clinical Geodesic system, consisting of an EEG hydrocel cap with 256 Ag-Ag electrodes.

8.2.2 METHODS

The EPOC consists of 14 dry electrodes and samples at 128 Hz, while the EGI uses 256 electrodes and samples at 1000 Hz. The headset consists of 14 active electrodes and 2 reference electrodes. Electrode position for the Emotiv EPOC is based on the International 10-20 locations (*AF3, F7, F3, FC5, T7, P7, O1, O2, P8, T8, FC6, F4, F8, AF4*). A map of the EGI system's electrode placement, which uses the International 10-10 system, can be seen in Fig. 1. Channel selection for this EGI headset in this experiment was based on consideration of our previous study's (Ch. 4) results. Essentially, a combination of electrodes overlying *C4* and *CPz* that exhibited time-locked motor behavior was selected for analysis (see Fig. 3). The 256-channel electrode map of the EGI Clinical Geodesic hydrocel EEG System also includes the electrodes that are used by the Emotiv EPOC, highlighted in red. We used the Emotiv Research Edition software to store raw EEG data captured by the EPOC headset. The data was up-sampled using linear interpolation from 128 Hz to 1000 Hz to match the sampling frequency of the EGI Clinical Geodesic Hydrocel EEG System. The remainder of the data processing chain is described in detail in Chapter 4.3.4 and in (S. L. Norman et al., 2016).

We collected data from six (N=6) unimpaired subjects (4 right-handed, 5 Female) using their left hand to play a musical computer game, similar to Guitar Hero ©. Participants completed the same experiment described in (S. L. Norman et al., 2016) and here in Chapter 4. Participants received robotic assistance from the Finger Individuated Grasping Exercise Robot (FINGER) (Taheri et al., 2014). We used a two factor, two level factorial design where the factors were robot assistance (on or off) and overt motor activity by the subject (active or passive) resulting in 4 experimental conditions. Participants completed a total of 62 trials in each condition. We investigated the ability of each EEG system to reliably detect Event Related Desynchronization (ERD), a commonly used signal for BCI-contingent robot therapy. ERD refers to the reduction in amplitude of mu (8-13 Hz) oscillations over the sensorimotor cortex, known to precede both overt and imagined movement.

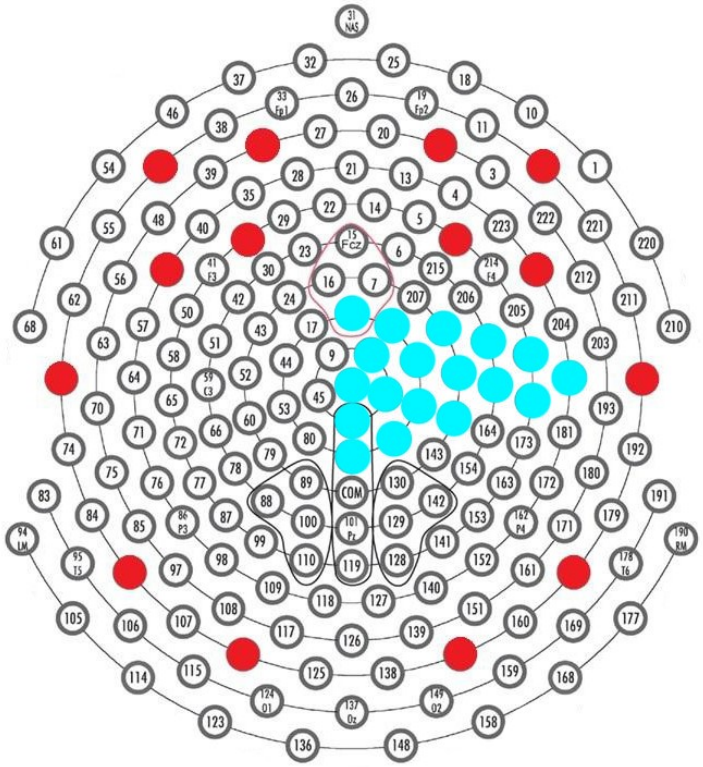

FIG. 1. A MAP OF THE EGI CLINICAL SYSTEM'S ELECTRODE PLACEMENT. A MAPPING OF THE EMOTIV EPOC'S ELECTRODE PLACEMENT (RED) AND THE EGI CHANNEL SELECTION HAVE BEEN SUPERIMPOSED (BLUE) OVER THE MAPPING FOR COMPARISON.

8.2.3 Results

The more expensive clinical-grade EGI system detected significant ERD in all subjects and all conditions where movement took place when compared to passive recording, i.e. the passive-passive condition (t-test, $p < 0.01$). The less expensive EPOC detected ERD for only one subject when the participant was active (within-subject MANOVA, $p = 0.0383$). The magnitude of ERD was also significantly greater with the EGI headset than with the Epoc (t-test, active subject, $p < 0.01$).

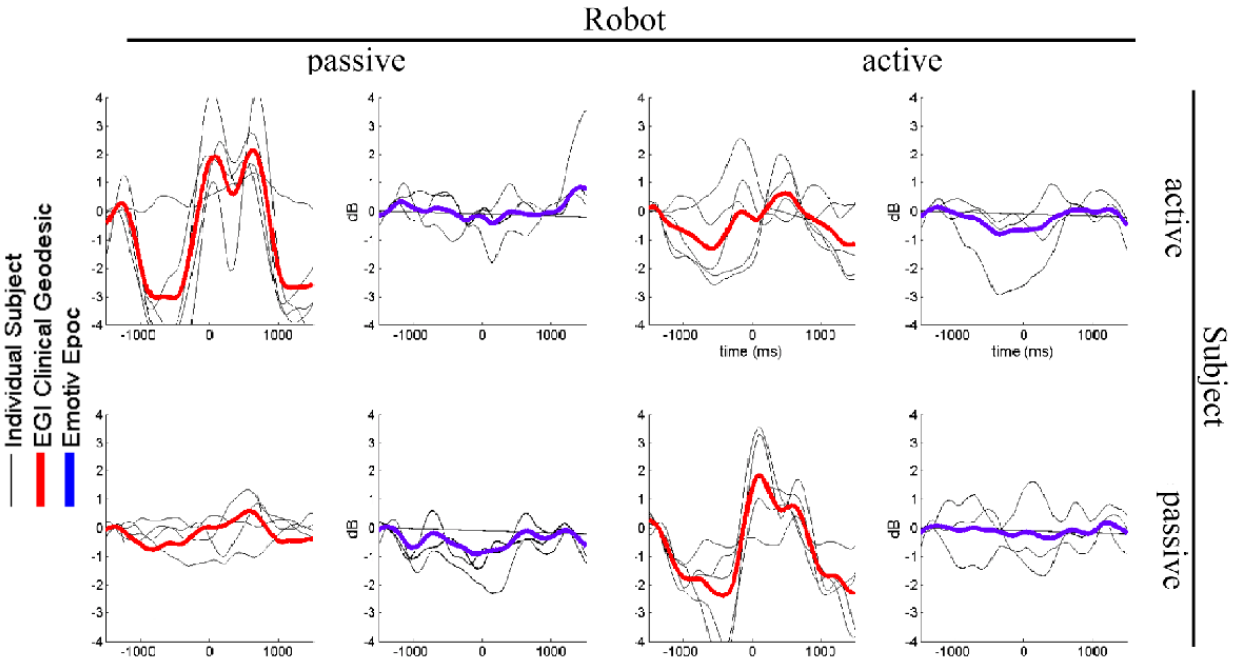

Fig. 2. A comparison of the sensorimotor mu rhythm (8-12 Hz) measured by the EGI Clinical Geodesic System and the Emotiv EPOC. Results are shown for all participants and conditions in a 3 s epoch surrounding the target time ($\tau=0$). Significant ERD signals precede movement onset in the clinical recordings in all except the passive-passive condition. Only one participant exhibited significant ERD as recorded by the Emotiv system

8.2.4 Discussion

The importance of the sensorimotor cortex in neurorehabilitation means that any EEG system used for BCI must reliably detect motor signals such as ERD. The 14 channels of the EPOC do not adequately cover the scalp, most closely approaching sensorimotor cortex with electrodes at *F3/F4* and *FC5/FC6*. It is likely that the EPOC detected ERD in these nearby

channels in one subject through volume conduction, as evidenced by the reduction in ERD magnitude. Although the EPOC shows promise in its ability to detect raw EEG, its electrode placement meant it was unable to reliably detect ERD, thus limiting its potential for applications in robotically assisted therapy.

8.3 DESIGN OF A WEARABLE ROBOT TO ENABLE BIMANUAL MANIPULATION AFTER STROKE

8.3.1 INTRODUCTION

Finger extension is a common movement impairment after stroke, the leading cause of disability in the United States (Muntner, Garrett, Klag, & Coresh, 2002; Trombly et al., 1986). People with stroke often resort to compensatory strategies using the unimpaired limb, but most tasks require at-least some degree of bilateral function (e.g. the impaired hand stabilizes a piece of paper while the other hand writes) (Bailey, Klaesner, & Lang, 2014). Because activities of daily living often require bilateral actions, grasping function in the impaired hand is paramount to quality of life. In recent years, declining cost and size in assistive robotics have made them increasingly attractive for use by people with impairment. However, many of the existing robotic-assistive devices for people with stroke remain impractical for day-to-day use (Heo, Gu, Lee, Rhee, & Kim, 2012). In this section, we introduce the design of the Robotic Hand Extension Device, or "RHED".

8.3.2 DESIGN AND METHODS

We designed RHED to capitalize on the user's residual flexion ability by limiting actuation to solely extension. This allows the device to be simple, lightweight, and low-cost, ideal attributes for a wearable device. The user is uninhibited during flexion, encouraging dexterity in coordinated grasping tasks. However, when the user struggles to achieve full extension, RHED uses a unique cable assembly to transmit extension forces to the fingers remotely from actuators located on the forearm. Flexible/incompressible cable sheaths allow for wrist manipulation without causing cable slack. This allows RHED to facilitate finger and thumb extension without limiting the freedom of the wrist and remaining finger joints or inhibiting flexion in any of the fingers or thumb when the device is slack.

FIG. 3: EXAMPLE OF A BIMANUAL TASK USING RHED.

Many wearable assistance devices have relied on agonist/antagonist muscle activation via electromyography (EMG) or force-based intention sensing (Heo et al., 2012; Wege & Zimmermann, 2007). However, people with stroke typically display abnormal muscle synergies, including coactivation of the flexor/extensor pair and inability to produce positive extension force, making these approaches suboptimal (Trombly et al., 1986). Additionally, past research has shown that rewarding abnormal synergies with robotic movement can result in their cementation through reinforcement learning (Dipietro et al., 2007). For RHED, we use the unimpaired hand as a means of controlling three discrete grip strategies for the impaired hand. The user wears a magnetic ring on the unimpaired hand and a three-axis magnetometer on the robot/impaired arm. A simple wave of the unimpaired hand in one of three gesture commands results in the extension of the thumb and index finger, or a combination thereof (Fig. 4).

$$posture = max\,index\left(\begin{bmatrix}\vec{F}\cdot\vec{F}_1\\ \vec{F}\cdot\vec{F}_2\\ \vec{F}\cdot\vec{F}_3\end{bmatrix}\right)\cdot\left(\left|\vec{F}\right| \geq F_{threshold}\right) \quad (1)$$

Equation 1 defines the next posture as an integer from one to three, where $\vec{F_1} \perp \vec{F_2} \perp \vec{F_3}$. If the ring is sufficiently close to the sensor ($\left|\vec{F}\right| \geq F_{threshold}$), the controller compares the current magnetic field $\vec{F}$ to three posture definitions $\vec{F}_i$ using their dot product. e index of the maximum value results in a value of one, two, or three, which results in the corresponding posture (numbered in Fig. 4). A field below threshold results in a value of zero and the default hand posture (flexion/posture 0, Fig. 4).

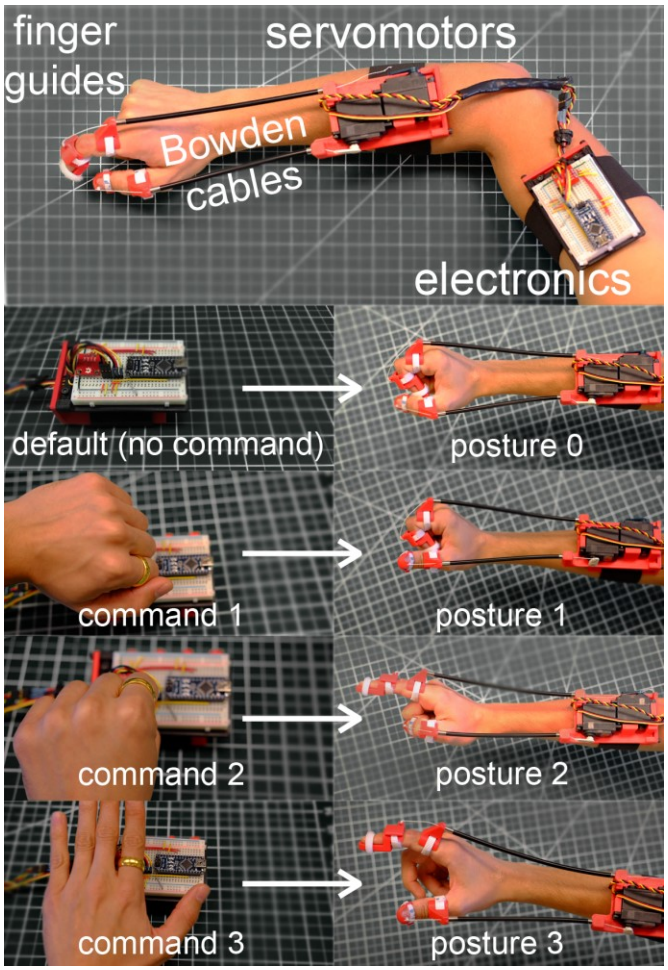

FIG. 4: TOP, THE ROBOTIC HAND EXOSKELETON DEVICE (RHED). LEFT, AN EXAMPLE OF THE THREE DISCRETE COMMAND GESTURES. RIGHT, FOUR RESULTING GRIP POSTURES PER INPUT COMMAND. POSTURE 0 IS UNASSISTED.

As a special consideration for people with spasticity after stroke, the device was designed to be donned and doffed using only the unimpaired hand. People with spasticity typically exhibit difficulty with one-piece designs such as gloves, as it is difficult to extend the impaired fingers to a position in which to don the device. We designed finger joint cable guides attached by hook-and-loop straps. The guides attach to the proximal/middle phalanxes of the index finger and the proximal/distal phalanxes of the thumb. Rapid prototyping methods made individualized guides possible, allowing for comfort and ease of use.

8.3.3 Discussion

A primary design goal of RHED was to exceed the passive flexion torques of the user's fingers to allow extension that could support bilateral movement tasks. A statics analysis showed that RHED applies a minimum torque about the proximal interphalangeal joint that is greater than the maximum passive torque calculated by Kamper et al. in people with stroke (Kamper, Harvey, Suresh, & Rymer, 2003). This was verified in preliminary tests where RHED was capable of extending unimpaired subjects' index finger and thumb while they maintained a flexion force. The device can be seen assisting the non-dominant hand in extension to complete a supporting role in a bimanual functional task in Fig. 1. This is just one example of many daily tasks that would now possible with an assistive device like RHED.

CHAPTER 9: SUMMARY OF THE PRIMARY FINDINGS OF THIS DISSERTATION

The primary contribution of this research was to elucidate the mechanisms behind BCI and robot-assisted movement and how one might affect the other in the context of developing BCI-robot therapy protocols to restore movement in people with stroke. First, I developed a novel computational model to investigate the conditions under which targeted plasticity, such as can be provided by a BCI, might optimize motor learning after a neurologic injury. I also applied the model to study the interaction between strength and coordination recovery after a stroke. Next, in a study with unimpaired people, I investigated a key potential confound of BCI-contingent robot-assisted therapy, showing that the robot assistance can cause ERD even when the participant is passive, a condition unhelpful for promoting motor learning. In Chapter 5, I identified a potential methodology to avoid this confound, which is to design robotic therapy games that require choice then to monitor frontal activity to detect engagement in the games. In Chapter 6, I present two pilot studies that tested methodological considerations for the experimental design and system parameters for a different approach to BCI-robot therapy – which is to require the participant to learn to volitionally control pre-movement brain states. The crux of this work lies in Chapter 7, where I presented the findings of a clinical study in eight people with stroke who underwent 12 days of training with this approach to BCI-robot therapy. Four of eight participants learned to control pre-movement brain state, and by doing so could modulate their finger movement ability – a result never before found for individuals with a stroke. I identified potential clinical benefits of the training, as well. Finally, I presented low-cost alternatives for BCI signal acquisition and wearable robot actuation in the context of this technology's future translation into people's homes.

Investigations into targeted neuroplasticity approaches that use BCI technology and robot assistance have experienced significant growth and promising results. Yet, they have struggled to reach their full potential, in part due to the difficulty and cost of testing new hypotheses in a clinical setting. Computational models of motor learning are therefore useful for predicting principles of adaptive plasticity during motor rehabilitation. In this work, I presented a novel computational model that employs a simplified corticospinal (CS) neural

network with inherent stochastic noise to simulate finger extension force recovery after stroke. The network predicted several experimental observations of motor recovery after stroke including exponential recovery, latent residual capacity, and a broad reorganization of motor activity after a neurologic injury.

Latent residual capacity, i.e. additional capacity for motor performance that the network could not easily access, appeared after a stroke followed by a dose of normal movement practice. Residual capacity is difficult for reinforcement learning to access without extrinsic assistance because the optimization of high-variability cells, i.e. cells that can learn quickly, can block the optimization of low-variability, i.e. slow-learning, cells that may have significant capacity to improve overall network performance. This result suggests ways in which brain networks may possess capacity to generate significant improvements that current rehabilitation is not yet capable of revealing. Thus, a primary contribution of this work was in predicting how to exploit residual capacity through targeted neuroplasticity interventions.

After a simulated stroke that affected finger extension, the network also produced abnormal cortical reorganization, including bilateral activation for unilateral movement, a result consistent with imaging data (Cramer & Crafton, 2006; Cramer et al., 1997; Grefkes & Fink, 2011). The model was then subject to normal movement practice interdigitated with targeted plasticity training wherein feedback was given on the summed activity of a targeted population of ipsilesional cells. This training restored more unilateral activation in the ipsilesional hemisphere for a unilateral motor task, improving overall force recovery. Furthermore, the model revealed that targeting these areas on 20% of trials, and giving normal movement practice for the remaining trials, maximized motor recovery. In preparing the methodology of a BCI-robot therapy protocol, we took these results into consideration. For example, during the experiments described in Chapters 6 and 7, we limited the spatial areas to target to the sensorimotor cortices.

We used a similar computational neurorehabilitation model to gain insight into the interaction between strength and coordination recovery after a stroke with the goal of informing future therapeutic protocols. This model replicated the nonlinear relationship

between strength and coordination observed in clinical recovery data for a finger force production task (Xu et al., 2016), and a bilateral wheelchair propulsion task. The primary finding of the model was that a neurologic injury such as stroke can cause a tradeoff between strength and coordination, a tradeoff that doesn't exist for an uninjured network. That is, before an injury, the neural resources in the brain related to focal control of muscles are plentiful and therefore capable of producing both forceful and coordinated movements. Although training one or the other might alter their progress in learning, an uninjured brain can produce satisfactory results for both task types. After a stroke, these focal neural resources are more scarce, and the simulated brain is incapable of learning both strength and coordination in fast simultaneous succession. Thus, robotic movement therapy devices can be an elegant aid for maximizing functional recovery, by adaptively mitigating the effects of over- or under-training strength or coordination. The tasks described in the lead up to, and in, the BCI-robot protocol described in this work attempt to balance strength and coordination training. For example, we developed an admittance controller for FINGER to be used in the experiments described in Chapters 6 & 7. Thus, the participant had to generate significant force (to trigger robot assistance), and had to do so with finger individuation, e.g. they could not move the non-cued finger or else the robot would not assist them. Although we do not systematically compare the therapeutic results of this type of training vs. pure individuation or pure strength training in this work, we felt that this approach struck a balance between strength and coordination training appropriate for the BCI-robot protocol being tested.

A common EEG corollary for movement intention is the reduction in mu (8-13 Hz) and beta (13-30 Hz) oscillation amplitude over the sensorimotor cortex that precedes movement-onset, a phenomenon referred to as event-related desynchronization (ERD). BCI therapy has been suggested to have potential in improving motor outcome, wherein an ERD-contingency triggers robot-assisted movements (Ramos-Murguialday et al., 2013). In Chapter 4, we investigated ERD as an a priori brain state that we could potentially target in a future BCI-robot therapy protocol. Specifically, we investigated how ERD changed as a function of audio-visual stimuli, overt movement from the participant, and robotic assistance. Overt movement by the subject caused ERD, whether the robot assisted the finger

movement or not. The primary finding of this work was that ERD was also present when the subjects remained passive and the robot moved their fingers. This ERD occurred in anticipation of the passive finger movement with similar onset timing as for the overt movement conditions. These results demonstrated that the brain generates an anticipatory ERD in expectation of a robot-imposed but predictable movement. This finding became an important caveat in developing a BCI-contingent robot therapy protocol. First, we attempted to use data-driven methods to find a way around this limiting factor, which I describe in Chapter 5. We aimed to classify active vs. passive movements in an offline data set with the goal of eventually moving to a real-time classification system. In applying these techniques to a data set of 12 people performing active and passive movements, we could predict patient engagement in the task with 75.9% accuracy on an individual trial basis. Although these results were encouraging, these were under ideal conditions and in unimpaired participants. Due to the confounding nature of stroke on neuroimaging and the underlying brain mechanisms, these accuracies might worsen in people with stroke. For these reasons, we did not pursue this method of classification for an online application. In a secondary exploratory analysis, we applied principal component analysis to discern the spatiotemporal patterns associated with each condition, e.g. passive vs. active. We found that, during active movements, the first principal component, which described 83% of the variance in the signal, was focused in prefrontal cortex. This finding was not present in passive movements, whose first principal component (57% of the variance) was an ERD signal over the contralateral sensorimotor cortex. These findings lent insight into the normative neurophysiological progression of planning for an intended movement, a process consistent with clinical findings (Frith et al., 1991). Thus, one potential method of mitigating the effects of the anticipatory ERD described in (S. L. Norman et al., 2016) is to involve a substantial decision-making task to a BCI-robot protocol. Indeed, we included a finger-matching task, both cued and un-cued, in Chapter 6.2 to investigate its effects on a BCI protocol. Although not implemented here, future work might also consider prefrontal activation patterns to detect patient engagement in real time.

Chapters 6 and 7 develop the methodology for, and implement a novel BCI-robot therapy protocol for the first time in people with stroke. In previous work, my colleagues

had shown that learning to control pre-movement SMR activity can modulate reaction time of the ensuing movement in unimpaired people (Boulay et al., 2011; McFarland et al., 2015). Thus, the questions remained: Can we also affect reaction time in a similar BCI protocol for individuated finger movements? Can we extend such a protocol to people with stroke? Would such a protocol have potential as a therapeutic intervention for people with movement disability after a stroke? In Chapter 6, I answer the first two questions. We then used these findings to guide the development of the BCI methodology which I present in Chapter 7.

First, we found that, in adults without motor impairment, training pre-movement SMR activity affected subsequent movement performance in a finger individuated task. This reinforced our task selection for a BCI-robot protocol. We also investigated several secondary methodological considerations. We found that our models had comparable performance in cued and uncued movements. We also found that bipolar channels performed better than Laplacian channels. Thus, when we designed the BCI methodology I describe in Chapter 7, we used bipolar channels. In a second pilot study, we investigated a similar BCI-robot protocol in people with chronic movement disability after stroke. The primary finding of this work was that we could predict the willing intent to move in people with stroke using an SMR-based BCI protocol over the course of multiple sessions. We also found that finger individuated extension movements generalized across multiple recording sessions better than flexion movements. These results provided the basis for the methodology of the BCI-robot protocol presented in Chapter 7.

Finally, we put the culmination of all the findings presented thus far to the test. In Chapter 7, I presented a BCI-robot therapy protocol as a potential rehabilitation tool for stroke. Eight participants with chronic hemiparesis of the hand completed 12 days of an EEG-based BCI-robot training protocol using the FINGER exoskeleton. The efficacy of such a protocol depends on its ability to modulate movement behavior in people with stroke. Until this point, we had only tested the full protocol – training pre-movement SMR to modulate subsequent motor performance – in unimpaired people. This study showed that people with stroke could learn to control their SMR. Specifically, six of eight participants achieved reliable control of the BCI, although two showed evidence of contamination from EMG signals.

Following BCI training, decreasing pre-movement SMR amplitude decreased movement latency, a novel finding in people with stroke. Furthermore, we also showed, for the first time (in people with- or without a stroke), that people can produce more forceful movement, i.e. higher extension torques about the MCP joint, by decreasing pre-movement SMR amplitude. In summary, a BCI-robot protocol, properly implemented, can positively affect subsequent motor performance in people with stroke. Although this study was not designed as a therapeutic intervention, we did find modest improvements in clinical scores of hand function, and these improvements were larger for those subjects who had achieved brain-control. These results merit further investigation of BCI-robot training in a rehabilitation context for people with movement disability after stroke ■

REFERENCES

Ada, L., Dorsch, S., & Canning, C. G. (2006). Strengthening interventions increase strength and improve activity after stroke: a systematic review. *Australian Journal of Physiotherapy, 52*(4), 241-248.

Alegre, M., Labarga, A., Gurtubay, I., Iriarte, J., Malanda, A., & Artieda, J. (2002). Beta electroencephalograph changes during passive movements: sensory afferences contribute to beta event-related desynchronization in humans. *Neuroscience letters, 331*(1), 29-32.

Anderson, R. W., Omidvar, O., & Dayhoff, J. (1997). Random-walk learning: A neurobiological correlate to trial-and-error. *Progress in Neural Networks, Ablex, Norwood, NJ*.

Ang, K. K., & Guan, C. (2013). Brain-computer interface in stroke rehabilitation. *Journal of Computing Science and Engineering, 7*(2), 139-146.

Bai, O., Mari, Z., Vorbach, S., & Hallett, M. (2005). Asymmetric spatiotemporal patterns of event-related desynchronization preceding voluntary sequential finger movements: a high-resolution EEG study. *Clinical Neurophysiology, 116*(5), 1213-1221.

Bailey, R. R., Klaesner, J. W., & Lang, C. E. (2014). An accelerometry-based methodology for assessment of real-world bilateral upper extremity activity. *PloS one, 9*(7), e103135.

Bailey, R. R., Klaesner, J. W., & Lang, C. E. (2015). Quantifying real-world upper-limb activity in nondisabled adults and adults with chronic stroke. *Neurorehabilitation and Neural Repair, 29*(10), 969-978.

Barreca, S., Wolf, S. L., Fasoli, S., & Bohannon, R. (2003). Treatment interventions for the paretic upper limb of stroke survivors: a critical review. *Neurorehabilitation and Neural Repair, 17*(4), 220-226.

Baur, K., Klamroth-Marganska, V., Giorgetti, C., Fichmann, D., & Riener, R. (2016). *Performance-based viscous force field adaptation in upper limb strength training for stroke patients.* Paper presented at the Biomedical Robotics and Biomechatronics (BioRob), 2016 6th IEEE International Conference on.

Birbaumer, N., & Cohen, L. G. (2007). Brain–computer interfaces: communication and restoration of movement in paralysis. *The Journal of physiology, 579*(3), 621-636.

Blakemore, S.-J., Wolpert, D., & Frith, C. (2000). Why can't you tickle yourself? *Neuroreport, 11*(11), R11-R16.

Blakemore, S. J., Goodbody, S. J., & Wolpert, D. M. (1998). Predicting the consequences of our own actions: the role of sensorimotor context estimation. *The Journal of Neuroscience, 18*(18), 7511-7518.

Blankertz, B., Dornhege, G., Krauledat, M., Müller, K.-R., & Curio, G. (2007). The non-invasive Berlin brain–computer interface: fast acquisition of effective performance in untrained subjects. *NeuroImage, 37*(2), 539-550.

Bos, R. A., Haarman, C. J., Stortelder, T., Nizamis, K., Herder, J. L., Stienen, A. H., & Plettenburg, D. H. (2016). A structured overview of trends and technologies used in dynamic hand orthoses. *Journal of neuroengineering and rehabilitation, 13*(1), 62.

Boulay, C., Sarnacki, W., Wolpaw, J., & McFarland, D. (2011). Trained modulation of sensorimotor rhythms can affect reaction time. *Clinical Neurophysiology, 122*(9), 1820-1826.

Broderick, J., Brott, T., Kothari, R., Miller, R., Khoury, J., Pancioli, A., . . . Shukla, R. (1998). The Greater Cincinnati/Northern Kentucky Stroke Study Preliminary first-ever and total incidence rates of stroke among blacks. *Stroke, 29*(2), 415-421.

Buch, E., Weber, C., Cohen, L. G., Braun, C., Dimyan, M. A., Ard, T., . . . Fourkas, A. (2008). Think to move: a neuromagnetic brain-computer interface (BCI) system for chronic stroke. *Stroke, 39*(3), 910-917.

Buonomano, D. V., & Merzenich, M. M. (1998). Cortical plasticity: from synapses to maps. *Annual review of neuroscience, 21*(1), 149-186.

Buzsáki, G., & Mizuseki, K. (2014). The log-dynamic brain: how skewed distributions affect network operations. *Nature Reviews Neuroscience, 15*(4), 264-278.

Calautti, C., & Baron, J.-C. (2003). Functional neuroimaging studies of motor recovery after stroke in adults. *Stroke, 34*(6), 1553-1566.

Calautti, C., Jones, P. S., Naccarato, M., Sharma, N., Day, D., Bullmore, E., . . . Baron, J.-C. (2010). The relationship between motor deficit and primary motor cortex hemispheric activation balance after stroke: longitudinal fMRI study. *Journal of Neurology, Neurosurgery & Psychiatry*, jnnp. 2009.190512.

Calautti, C., Naccarato, M., Jones, P. S., Sharma, N., Day, D. D., Carpenter, A. T., . . . Baron, J.-C. (2007). The relationship between motor deficit and hemisphere activation balance after stroke: a 3T fMRI study. *NeuroImage, 34*(1), 322-331.

Cassim, F., Monaca, C., Szurhaj, W., Bourriez, J.-L., Defebvre, L., Derambure, P., & Guieu, J.-D. (2001). Does post-movement beta synchronization reflect an idling motor cortex? *Neuroreport, 12*(17), 3859-3863.

Choi, B., & Jo, S. (2013). A Low-Cost EEG System-Based Hybrid Brain-Computer Interface for Humanoid Robot Navigation and Recognition. *PloS one, 8*(9), e74583.

Christopher deCharms, R. (2008). Applications of real-time fMRI. *Nature Reviews Neuroscience, 9*(9), 720-729.

Christopher deCharms, R., Maeda, F., Glover, G. H., Ludlow, D., Pauly, J. M., Soneji, D., . . . Mackey, S. C. (2005). Control over brain activation and pain learned by using real-time functional MRI. *Proceedings of the National Academy of Sciences of the United States of America, 102*(51), 18626-18631.

Cohen, L. G., Celnik, P., Pascual-Leone, A., Corwell, B., Faiz, L., Dambrosia, J., . . . Catalá, M. D. (1997). Functional relevance of cross-modal plasticity in blind humans. *Nature, 389*(6647), 180-183.

Cohen, M. X. (2014). *Analyzing Neural Time Series Data: Theory and Practice*.

Cohen, O., Sherman, E., Zinger, N., Perlmutter, S., & Prut, Y. (2010). Getting ready to move: transmitted information in the corticospinal pathway during preparation for movement. *Current opinion in neurobiology, 20*(6), 696-703.

Cox, R. W., Jesmanowicz, A., & Hyde, J. S. (1995). Real-Time Functional Magnetic Resonance Imaging. *Magnetic resonance in medicine, 33*(2), 230-236.

Cramer, S. C., & Crafton, K. R. (2006). Somatotopy and movement representation sites following cortical stroke. *Experimental Brain Research, 168*(1-2), 25-32.

Cramer, S. C., Nelles, G., Benson, R. R., Kaplan, J. D., Parker, R. A., Kwong, K. K., . . . Rosen, B. R. (1997). A functional MRI study of subjects recovered from hemiparetic stroke. *Stroke, 28*(12), 2518-2527.

Cramer, S. C., Sur, M., Dobkin, B. H., O'Brien, C., Sanger, T. D., Trojanowski, J. Q., . . . Chen, D. (2011). Harnessing neuroplasticity for clinical applications. *Brain, 134*(6), 1591-1609.

Daly, J. J., & Wolpaw, J. R. (2008). Brain–computer interfaces in neurological rehabilitation. *The Lancet Neurology, 7*(11), 1032-1043.

Das, K., & Nenadic, Z. (2008). Approximate information discriminant analysis: A computationally simple heteroscedastic feature extraction technique. *Pattern Recognition, 41*(5), 1548-1557.

Das, K., & Nenadic, Z. (2009). An efficient discriminant-based solution for small sample size problem. *Pattern Recognition, 42*(5), 857-866.

Dean, A. (1981). The variability of discharge of simple cells in the cat striate cortex. *Experimental Brain Research, 44*(4), 437-440.

Derambure, P., Defebvre, L., Bourriez, J., Cassim, F., & Guieu, J. (1999). [Event-related desynchronization and synchronization. Reactivity of electrocortical

rhythms in relation to the planning and execution of voluntary movement]. *Neurophysiologie clinique= Clinical neurophysiology, 29*(1), 53-70.

Dipietro, L., Krebs, H. I., Fasoli, S. E., Volpe, B. T., Stein, J., Bever, C., & Hogan, N. (2007). Changing motor synergies in chronic stroke. *Journal of neurophysiology, 98*(2), 757-768.

Dollar, A. M., & Herr, H. (2008). Lower extremity exoskeletons and active orthoses: challenges and state-of-the-art. *IEEE Transactions on robotics, 24*(1), 144-158.

Dong, Y., Dobkin, B. H., Cen, S. Y., Wu, A. D., & Winstein, C. J. (2006). Motor cortex activation during treatment may predict therapeutic gains in paretic hand function after stroke. *Stroke, 37*(6), 1552-1555.

Duvinage, M., Castermans, T., Dutoit, T., Petieau, M., Hoellinger, T., Saedeleer, C. D., . . . Cheron, G. (2012). A P300-based quantitative comparison between the Emotiv Epoc headset and a medical EEG device. *Biomedical Engineering, 765*, 2012.2764-2071.

Fabiani, G. E., McFarland, D. J., Wolpaw, J. R., & Pfurtscheller, G. (2004). Conversion of EEG activity into cursor movement by a brain-computer interface (BCI). *Neural Systems and Rehabilitation Engineering, IEEE Transactions on, 12*(3), 331-338.

Faisal, A. A., Selen, L. P., & Wolpert, D. M. (2008). Noise in the nervous system. *Nature Reviews Neuroscience, 9*(4), 292-303.

Feigin, V. L., Forouzanfar, M. H., Krishnamurthi, R., Mensah, G. A., Connor, M., Bennett, D. A., . . . Truelsen, T. (2014). Global and regional burden of stroke during 1990–2010: findings from the Global Burden of Disease Study 2010. *The Lancet, 383*(9913), 245-255.

Fok, S., Schwartz, R., Wronkiewicz, M., Holmes, C., Zhang, J., Somers, T., . . . Leuthardt, E. (2011). *An EEG-based brain computer interface for rehabilitation and restoration of hand control following stroke using ipsilateral cortical physiology.* Paper presented at the Engineering in Medicine and Biology Society, EMBC, 2011 Annual International Conference of the IEEE.

Formaggio, E., Storti, S. F., Galazzo, I. B., Gandolfi, M., Geroin, C., Smania, N., . . . Manganotti, P. (2014). Time–Frequency Modulation of ERD and EEG Coherence in Robot-Assisted Hand Performance. *Brain topography*, 1-12.

Formaggio, E., Storti, S. F., Galazzo, I. B., Gandolfi, M., Geroin, C., Smania, N., . . . Manganotti, P. (2013). Modulation of event-related desynchronization in robot-assisted hand performance: brain oscillatory changes in active, passive and imagined movements. *J Neuroeng Rehabil, 10*, 24.

Fregni, F., & Pascual-Leone, A. (2007). Technology insight: noninvasive brain stimulation in neurology—perspectives on the therapeutic potential of rTMS and tDCS. *Nature Clinical Practice Neurology, 3*(7), 383-393.

French, B., Thomas, L. H., Leathley, M. J., Sutton, C. J., McAdam, J., Forster, A., . . . Watkins, C. L. (2007). Repetitive task training for improving functional ability after stroke. *The Cochrane Library*.

Friedman, J., Hastie, T., & Tibshirani, R. (2010). Regularization paths for generalized linear models via coordinate descent. *Journal of statistical software, 33*(1), 1.

Friedman, N., Chan, V., Reinkensmeyer, A. N., Beroukhim, A., Zambrano, G. J., Bachman, M., & Reinkensmeyer, D. J. (2014). Retraining and assessing hand movement after stroke using the MusicGlove: comparison with conventional hand therapy and isometric grip training. *Journal of neuroengineering and rehabilitation, 11*(1), 76.

Frith, C. D., Friston, K., Liddle, P., & Frackowiak, R. (1991). Willed action and the prefrontal cortex in man: a study with PET. *Proceedings of the Royal Society of London B: Biological Sciences, 244*(1311), 241-246.

Fu, M. J., Daly, J. J., & Cavusoglu, M. C. (2006). *Assessment of EEG event-related desynchronization in stroke survivors performing shoulder-elbow movements.* Paper presented at the Robotics and Automation, 2006. ICRA 2006. Proceedings 2006 IEEE International Conference on.

Grefkes, C., & Fink, G. R. (2011). Reorganization of cerebral networks after stroke: new insights from neuroimaging with connectivity approaches. *Brain*, awr033.

Gresham, G., Duncan, P., Stason, W., Adams, H., Adelman, A., Alexander, D., . . . Granger, C. (1995). Post-Stroke Rehabilitation. Rockville, MD: US Department of Health and Human Services. *Public Health Service, Agency for Health Care Policy and Research*.

Han, C. E., Arbib, M. A., & Schweighofer, N. (2008). Stroke rehabilitation reaches a threshold. *PLoS Comput Biol, 4*(8), e1000133.

Hashimoto, Y., Ushiba, J., Kimura, A., Liu, M., & Tomita, Y. (2010). Change in brain activity through virtual reality-based brain-machine communication in a chronic tetraplegic subject with muscular dystrophy. *BMC neuroscience, 11*(1), 1.

Heo, P., Gu, G. M., Lee, S.-j., Rhee, K., & Kim, J. (2012). Current hand exoskeleton technologies for rehabilitation and assistive engineering. *International Journal of Precision Engineering and Manufacturing, 13*(5), 807-824.

Hidler, J., Nichols, D., Pelliccio, M., Brady, K., Campbell, D. D., Kahn, J. H., & Hornby, T. G. (2009). Multicenter randomized clinical trial evaluating the effectiveness

of the Lokomat in subacute stroke. *Neurorehabilitation and Neural Repair, 23*(1), 5-13.

Hornby, T. G., Campbell, D. D., Zemon, D. H., & Kahn, J. H. (2005). Clinical and quantitative evaluation of robotic-assisted treadmill walking to retrain ambulation after spinal cord injury. *Topics in Spinal Cord Injury Rehabilitation, 11*(2), 1.

Hornby, T. G., Reinkensmeyer, D. J., & Chen, D. (2010). Manually-Assisted Versus Robotic-Assisted Body Weight− Supported Treadmill Training in Spinal Cord Injury: What Is the Role of Each? *PM&R, 2*(3), 214-221.

Hu, X. L., Tong, K.-y., Song, R., Zheng, X. J., & Leung, W. W. (2009). A comparison between electromyography-driven robot and passive motion device on wrist rehabilitation for chronic stroke. *Neurorehabilitation and Neural Repair, 23*(8), 837-846.

Ingemanson, M. L., Rowe, J. B., Chan, V., Wolbrecht, E. T., Cramer, S. C., & Reinkensmeyer, D. J. (2015). Use of a robotic device to measure age-related decline in finger proprioception. *Experimental Brain Research*, 1-11.

Israel, J. F., Campbell, D. D., Kahn, J. H., & Hornby, T. G. (2006). Metabolic costs and muscle activity patterns during robotic-and therapist-assisted treadmill walking in individuals with incomplete spinal cord injury. *Physical therapy, 86*(11), 1466-1478.

Jackson, P. L., Lafleur, M. F., Malouin, F., Richards, C., & Doyon, J. (2001). Potential role of mental practice using motor imagery in neurologic rehabilitation. *Archives of physical medicine and rehabilitation, 82*(8), 1133-1141.

KAAS, J., TAUB, E., & MISHKIN, M. (1991). Massive cortical reorganization after sensory deafferentation in adult macaques.

Kaelin-Lang, A., Sawaki, L., & Cohen, L. G. (2005). Role of voluntary drive in encoding an elementary motor memory. *Journal of neurophysiology, 93*(2), 1099-1103.

Kahn, L. E., Zygman, M. L., Rymer, W. Z., & Reinkensmeyer, D. J. (2006). Robot-assisted reaching exercise promotes arm movement recovery in chronic hemiparetic stroke: a randomized controlled pilot study. *Journal of neuroengineering and rehabilitation, 3*, 12.

Kamiya, J. (1969). Operant control of the EEG alpha rhythm and some of its reported effects on consciousness. *Altered states of consciousness. New York: Wiley, 1069*.

Kamper, D., Harvey, R., Suresh, S., & Rymer, W. (2003). Relative contributions of neural mechanisms versus muscle mechanics in promoting finger extension deficits following stroke. *Muscle & nerve, 28*(3), 309-318.

Kamper, D., & Rymer, W. (2001). Impairment of voluntary control of finger motion following stroke: role of inappropriate muscle coactivation. *Muscle & nerve, 24*(5), 673-681.

Kawato, M. (1999). Internal models for motor control and trajectory planning. *Current opinion in neurobiology, 9*(6), 718-727.

Khanna, P., & Carmena, J. M. (2017). Beta band oscillations in motor cortex reflect neural population signals that delay movement onset. *eLife, 6*.

Kim, S.-g., Ashe, J., Georgopoulos, A. P., Merkle, H., Ellermann, J., Menon, R., . . . Ugurbil, K. (1993). Functional imaging of human motor cortex at high magnetic field. *Journal of neurophysiology, 69*(1), 297-302.

King, C. E., Wang, P. T., McCrimmon, C. M., Chou, C. C., Do, A. H., & Nenadic, Z. (2015). The feasibility of a brain-computer interface functional electrical stimulation system for the restoration of overground walking after paraplegia. *Journal of neuroengineering and rehabilitation, 12*(1), 80.

King, C. E., Wang, P. T., Mizuta, M., Reinkensmeyer, D. J., Do, A. H., Moromugi, S., & Nenadic, Z. (2011). *Noninvasive brain-computer interface driven hand orthosis.* Paper presented at the Engineering in Medicine and Biology Society, EMBC, 2011 Annual International Conference of the IEEE.

Kiper, P., Szczudlik, A., Venneri, A., Stozek, J., Luque-Moreno, C., Opara, J., . . . Turolla, A. (2016). Computational models and motor learning paradigms: Could they provide insights for neuroplasticity after stroke? An overview. *Journal of the Neurological Sciences*.

Kleim, J. A., & Jones, T. A. (2008). Principles of experience-dependent neural plasticity: implications for rehabilitation after brain damage. *Journal of speech, language, and hearing research, 51*(1), S225-S239.

Klein, J., Spencer, S., Allington, J., Minakata, K., Wolbrecht, E., Smith, R., . . . Reinkensmeyer, D. (2008). *Biomimetic orthosis for the neurorehabilitation of the elbow and shoulder (BONES).* Paper presented at the Biomedical Robotics and Biomechatronics, 2008. BioRob 2008. 2nd IEEE RAS & EMBS International Conference on.

Krebs, H., Volpe, B., Aisen, M., & Hogan, N. (2000). Increasing productivity and quality of care: Robot-aided neuro-rehabilitation. *Journal of rehabilitation research and development, 37*(6), 639.

Krusienski, D. J., McFarland, D. J., Principe, J. C., & Wolpaw, E. (2012). BCI signal processing: feature extraction. *Brain–computer interfaces: principles and practice. Oxford University Press, New York*, 123-146.

Kwakkel, G., Kollen, B. J., & Krebs, H. I. (2007). Effects of robot-assisted therapy on upper limb recovery after stroke: a systematic review. *Neurorehabilitation and Neural Repair*.

Lang, C. E., DeJong, S. L., & Beebe, J. A. (2009). Recovery of thumb and finger extension and its relation to grasp performance after stroke. *Journal of neurophysiology, 102*(1), 451-459.

Lang, C. E., MacDonald, J. R., Reisman, D. S., Boyd, L., Kimberley, T. J., Schindler-Ivens, S. M., . . . Scheets, P. L. (2009). Observation of amounts of movement practice provided during stroke rehabilitation. *Archives of physical medicine and rehabilitation, 90*(10), 1692-1698.

Lang, C. E., & Schieber, M. H. (2003). Differential impairment of individuated finger movements in humans after damage to the motor cortex or the corticospinal tract. *Journal of neurophysiology, 90*(2), 1160-1170.

Lee, D., Port, N. L., Kruse, W., & Georgopoulos, A. P. (1998). Variability and correlated noise in the discharge of neurons in motor and parietal areas of the primate cortex. *Journal of neuroscience, 18*(3), 1161-1170.

Levin, M. F., Kleim, J. A., & Wolf, S. L. (2008). What do motor "recovery" and "compensation" mean in patients following stroke? *Neurorehabilitation and Neural Repair*.

Lewis, G. N., & Perreault, E. J. (2009). An assessment of robot-assisted bimanual movements on upper limb motor coordination following stroke. *IEEE Transactions on Neural Systems and Rehabilitation Engineering, 17*(6), 595-604.

Liao, K., Xiao, R., Gonzalez, J., & Ding, L. (2014). Decoding individual finger movements from one hand using human EEG signals. *PloS one, 9*(1), e85192.

Lo, H. S., & Xie, S. Q. (2012). Exoskeleton robots for upper-limb rehabilitation: State of the art and future prospects. *Medical engineering & physics, 34*(3), 261-268.

Lopez, A. D., Mathers, C. D., Ezzati, M., Jamison, D. T., & Murray, C. J. (2006). Global and regional burden of disease and risk factors, 2001: systematic analysis of population health data. *The Lancet, 367*(9524), 1747-1757.

Lotze, M., Braun, C., Birbaumer, N., Anders, S., & Cohen, L. G. (2003). Motor learning elicited by voluntary drive. *Brain, 126*(4), 866-872.

Lum, P., Reinkensmeyer, D., Mahoney, R., Rymer, W. Z., & Burgar, C. (2002). Robotic devices for movement therapy after stroke: current status and challenges to clinical acceptance. *Topics in stroke rehabilitation, 8*(4), 40-53.

Lum, P. S., Burgar, C. G., Shor, P. C., Majmundar, M., & Van der Loos, M. (2002). Robot-assisted movement training compared with conventional therapy techniques for the rehabilitation of upper-limb motor function after stroke. *Archives of physical medicine and rehabilitation, 83*(7), 952-959.

Lum, P. S., Burgar, C. G., Van der Loos, M., Shor, P., Majmundar, M., & Yap, R. (2005). *The MIME robotic system for upper-limb neuro-rehabilitation: results from a clinical trial in subacute stroke.* Paper presented at the Rehabilitation Robotics, 2005. ICORR 2005. 9th International Conference on.

Maciejasz, P., Eschweiler, J., Gerlach-Hahn, K., Jansen-Troy, A., & Leonhardt, S. (2014). A survey on robotic devices for upper limb rehabilitation. *Journal of neuroengineering and rehabilitation, 11*(1), 3.

Martin, P. I., Naeser, M. A., Theoret, H., Tormos, J. M., Nicholas, M., Kurland, J., . . . Pascual-Leone, A. (2004). *Transcranial magnetic stimulation as a complementary treatment for aphasia.* Paper presented at the Seminars in speech and language.

Mathiowetz, V., Volland, G., Kashman, N., & Weber, K. (1985). Adult norms for the Box and Block Test of manual dexterity. *American Journal of Occupational Therapy, 39*(6), 386-391.

Mazzoni, P., Andersen, R. A., & Jordan, M. I. (1991). A more biologically plausible learning rule for neural networks. *Proceedings of the National Academy of Sciences, 88*(10), 4433-4437.

McFarland, D. J., McCane, L. M., David, S. V., & Wolpaw, J. R. (1997). Spatial filter selection for EEG-based communication. *Electroencephalography and clinical neurophysiology, 103*(3), 386-394.

McFarland, D. J., Sarnacki, W. A., & Wolpaw, J. R. (2015). Effects of training pre-movement sensorimotor rhythms on behavioral performance. *Journal of neural engineering, 12*(6), 066021.

McFarland, D. J., & Wolpaw, J. R. (2008). Sensorimotor rhythm-based brain–computer interface (BCI): model order selection for autoregressive spectral analysis. *Journal of neural engineering, 5*(2), 155.

Mellinger, J., & Schalk, G. (2009). Using BCI2000 in BCI Research *Brain-Computer Interfaces* (pp. 259-279): Springer.

Miyai, I., Yagura, H., Hatakenaka, M., Oda, I., Konishi, I., & Kubota, K. (2003). Longitudinal optical imaging study for locomotor recovery after stroke. *Stroke, 34*(12), 2866-2870.

Müller-Putz, G., Daly, I., & Kaiser, V. (2014). Motor imagery-induced EEG patterns in individuals with spinal cord injury and their impact on brain–computer interface accuracy. *Journal of neural engineering, 11*(3), 035011.

Müller-Putz, G. R., Zimmermann, D., Graimann, B., Nestinger, K., Korisek, G., & Pfurtscheller, G. (2007). Event-related beta EEG-changes during passive and attempted foot movements in paraplegic patients. *Brain research, 1137*, 84-91.

Müller, G., Neuper, C., Rupp, R., Keinrath, C., Gerner, H., & Pfurtscheller, G. (2003). Event-related beta EEG changes during wrist movements induced by functional electrical stimulation of forearm muscles in man. *Neuroscience letters, 340*(2), 143-147.

Muntner, P., Garrett, E., Klag, M. J., & Coresh, J. (2002). Trends in stroke prevalence between 1973 and 1991 in the US population 25 to 74 years of age. *Stroke, 33*(5), 1209-1213.

Nakayashiki, K., Saeki, M., Takata, Y., Hayashi, Y., & Kondo, T. (2014). Modulation of event-related desynchronization during kinematic and kinetic hand movements. *Journal of neuroengineering and rehabilitation, 11*(1), 90.

Nelles, G., Spiekermann, G., Jueptner, M., Leonhardt, G., Müller, S., Gerhard, H., & Diener, H. C. (1999). Reorganization of sensory and motor systems in hemiplegic stroke patients. *Stroke, 30*(8), 1510-1516.

Nenadic, Z. (2007). Information discriminant analysis: Feature extraction with an information-theoretic objective. *Pattern Analysis and Machine Intelligence, IEEE Transactions on, 29*(8), 1394-1407.

Neuper, C., & Pfurtscheller, G. (2001). Evidence for distinct beta resonance frequencies in human EEG related to specific sensorimotor cortical areas. *Clinical Neurophysiology, 112*(11), 2084-2097.

Newell, A., & Rosenbloom, P. S. (1981). Mechanisms of skill acquisition and the law of practice. *Cognitive skills and their acquisition, 1*, 1-55.

Norman, S., Dennison, M., Wolbrecht, E., Cramer, S., Srinivasan, R., & Reinkensmeyer, D. (2016). Movement Anticipation and EEG: Implications for BCI-Contingent Robot Therapy.

Norman, S. L., Dennison, M., Wolbrecht, E., Cramer, S. C., Srinivasan, R., & Reinkensmeyer, D. J. (2016). Movement Anticipation and EEG: Implications for BCI-Contingent Robot Therapy. *IEEE Transactions on Neural Systems and Rehabilitation Engineering, 24*(8), 911-919.

Nudo, R. J. (2006). Plasticity. *NeuroRx, 3*(4), 420-427.

Page, S. J., Gater, D. R., & Bach-y-Rita, P. (2004). Reconsidering the motor recovery plateau in stroke rehabilitation. *Archives of physical medicine and rehabilitation, 85*(8), 1377-1381.

Pashler, H. (1994). Dual-task interference in simple tasks: data and theory. *Psychological bulletin, 116*(2), 220.

Pfurtscheller, G. (1992). Event-related synchronization (ERS): an electrophysiological correlate of cortical areas at rest. *Electroencephalography and clinical neurophysiology, 83*(1), 62-69.

Pfurtscheller, G., & Aranibar, A. (1977). Event-related cortical desynchronization detected by power measurements of scalp EEG. *Electroencephalography and clinical neurophysiology, 42*(6), 817-826.

Pfurtscheller, G., Krausz, G., & Neuper, C. (2001). Mechanical stimulation of the fingertip can induce bursts of β oscillations in sensorimotor areas. *Journal of clinical neurophysiology, 18*(6), 559-564.

Pfurtscheller, G., & Lopes da Silva, F. H. (1999). Event-related EEG/MEG synchronization and desynchronization: basic principles. *Clinical Neurophysiology, 110*(11), 1842-1857.

Pfurtscheller, G., Neuper, C., Brunner, C., & da Silva, F. L. (2005). Beta rebound after different types of motor imagery in man. *Neuroscience letters, 378*(3), 156-159.

Pfurtscheller, G., Stancak Jr, A., & Edlinger, G. (1997). On the existence of different types of central beta rhythms below 30 Hz. *Electroencephalography and clinical neurophysiology, 102*(4), 316-325.

Pfurtscheller, G., Zalaudek, K., & Neuper, C. (1998). Event-related beta synchronization after wrist, finger and thumb movement. *Electroencephalography and Clinical Neurophysiology/Electromyography and Motor Control, 109*(2), 154-160.

Pichiorri, F., Fallani, F. D. V., Cincotti, F., Babiloni, F., Molinari, M., Kleih, S., . . . Mattia, D. (2011). Sensorimotor rhythm-based brain–computer interface training: the impact on motor cortical responsiveness. *Journal of neural engineering, 8*(2), 025020.

Plow, E. B., Carey, J. R., Nudo, R. J., & Pascual-Leone, A. (2009). Invasive cortical stimulation to promote recovery of function after stroke a critical appraisal. *Stroke, 40*(5), 1926-1931.

Pomeroy, V., Aglioti, S. M., Mark, V. W., McFarland, D., Stinear, C., Wolf, S. L., . . . Fitzpatrick, S. M. (2011). Neurological principles and rehabilitation of action

disorders: rehabilitation interventions. *Neurorehabilitation and Neural Repair, 25*(5_suppl), 33S-43S.

Radomski, M. V., & Latham, C. A. T. (2008). *Occupational therapy for physical dysfunction*: Lippincott Williams & Wilkins.

Ramos-Murguialday, A., Schürholz, M., Caggiano, V., Wildgruber, M., Caria, A., Hammer, E. M., . . . Birbaumer, N. (2012). Proprioceptive feedback and brain computer interface (BCI) based neuroprostheses. *PloS one, 7*(10), e47048.

Ramos-Murguialday, A., Broetz, D., Rea, M., Läer, L., Yilmaz, Ö., Brasil, F. L., . . . Vyziotis, A. (2013). Brain–machine interface in chronic stroke rehabilitation: A controlled study. *Annals of neurology, 74*(1), 100-108.

Reinkensmeyer, D. J., Burdet, E., Casadio, M., Krakauer, J. W., Kwakkel, G., Lang, C. E., . . . Schweighofer, N. (2016). Computational neurorehabilitation: modeling plasticity and learning to predict recovery. *Journal of neuroengineering and rehabilitation, 13*(1), 1.

Reinkensmeyer, D. J., Emken, J. L., & Cramer, S. C. (2004). Robotics, motor learning, and neurologic recovery. *Annu. Rev. Biomed. Eng., 6*, 497-525.

Reinkensmeyer, D. J., Guigon, E., & Maier, M. A. (2012). A computational model of use-dependent motor recovery following a stroke: optimizing corticospinal activations via reinforcement learning can explain residual capacity and other strength recovery dynamics. *Neural Networks, 29*, 60-69.

Reinkensmeyer, D. J., Wolbrecht, E. T., Chan, V., Chou, C., Cramer, S. C., & Bobrow, J. E. (2012). Comparison of 3D, Assist-as-Needed Robotic Arm/Hand Movement Training Provided with Pneu-WREX to Conventional Table Top Therapy Following Chronic Stroke. *American journal of physical medicine & rehabilitation/Association of Academic Physiatrists, 91*(11 0 3), S232.

Riddle, C. N., Edgley, S. A., & Baker, S. N. (2009). Direct and indirect connections with upper limb motoneurons from the primate reticulospinal tract. *Journal of neuroscience, 29*(15), 4993-4999.

Rijntjes, M. (2006). Mechanisms of recovery in stroke patients with hemiparesis or aphasia: new insights, old questions and the meaning of therapies. *Current opinion in neurology, 19*(1), 76-83.

Rossiter, H. E., Boudrias, M.-H., & Ward, N. S. (2014). Do movement-related beta oscillations change after stroke? *Journal of neurophysiology, 112*(9), 2053-2058.

Rozelle, G. R., & Budzynski, T. H. (1995). Neurotherapy for stroke rehabilitation: A single case study. *Applied Psychophysiology and Biofeedback, 20*(3), 211-228.

Sanchez Jr, R., Wolbrecht, E., Smith, R., Liu, J., Rao, S., Cramer, S., . . . Reinkensmeyer, D. (2005). *A pneumatic robot for re-training arm movement after stroke: Rationale and mechanical design.* Paper presented at the Rehabilitation Robotics, 2005. ICORR 2005. 9th International Conference on.

Schalk, G., McFarland, D. J., Hinterberger, T., Birbaumer, N., & Wolpaw, J. R. (2004). BCI2000: a general-purpose brain-computer interface (BCI) system. *IEEE Transactions on biomedical engineering, 51*(6), 1034-1043.

Selinger, J. C., O'Connor, S. M., Wong, J. D., & Donelan, J. M. (2015). Humans can continuously optimize energetic cost during walking. *Current Biology, 25*(18), 2452-2456.

Sharbrough, F., Chatrian, G., Lesser, R., Lüders, H., Nuwer, M., & Picton, T. (1991). American electroencephalographic society guidelines for standard electrode position nomenclature. *J. clin. Neurophysiol, 8*(2), 200-202.

Sitaram, R., Ros, T., Stoeckel, L., Haller, S., Scharnowski, F., Lewis-Peacock, J., . . . Oblak, E. (2016). Closed-loop brain training: the science of neurofeedback. *Nature Reviews Neuroscience*.

Sitaram, R., Veit, R., Stevens, B., Caria, A., Gerloff, C., Birbaumer, N., & Hummel, F. (2012). Acquired control of ventral premotor cortex activity by feedback training an exploratory real-time fMRI and TMS study. *Neurorehabilitation and Neural Repair, 26*(3), 256-265.

Smith, B. W. (2017). Unexpected Elements of Human Force Control and Instances of Preservation after Severe Stroke: Implications for Optimality, Variability and Rehabilitation Technology.

Smith, B. W., Zondervan, D. K., Lord, T. J., Chan, V., & Reinkensmeyer, D. J. (2014). *Feasibility of a bimanual, lever-driven wheelchair for people with severe arm impairment after stroke.* Paper presented at the Engineering in Medicine and Biology Society (EMBC), 2014 36th Annual International Conference of the IEEE.

Soekadar, S. R., Witkowski, M., Birbaumer, N., & Cohen, L. G. (2014). Enhancing Hebbian learning to control brain oscillatory activity. *Cerebral cortex*, bhu043.

Soekadar, S. R., Witkowski, M., Mellinger, J., Ramos, A., Birbaumer, N., & Cohen, L. G. (2011). ERD-based online brain–machine interfaces (BMI) in the context of neurorehabilitation: optimizing BMI learning and performance. *IEEE Transactions on Neural Systems and Rehabilitation Engineering, 19*(5), 542-549.

Stančák Jr, A., Feige, B., Lücking, C. H., & Kristeva-Feige, R. (2000). Oscillatory cortical activity and movement-related potentials in proximal and distal movements. *Clinical Neurophysiology, 111*(4), 636-650.

Stein, J., Krebs, H. I., Frontera, W. R., Fasoli, S. E., Hughes, R., & Hogan, N. (2004). Comparison of two techniques of robot-aided upper limb exercise training after stroke. *American journal of physical medicine & rehabilitation, 83*(9), 720-728.

Stienen, A. H., Hekman, E. E., Van der Helm, F. C., Prange, G. B., Jannink, M. J., Aalsma, A. M., & Van der Kooij, H. (2007). *Dampace: dynamic force-coordination trainer for the upper extremities.* Paper presented at the Rehabilitation Robotics, 2007. ICORR 2007. IEEE 10th International Conference on.

Stinear, C. M., Barber, P. A., Smale, P. R., Coxon, J. P., Fleming, M. K., & Byblow, W. D. (2007). Functional potential in chronic stroke patients depends on corticospinal tract integrity. *Brain, 130*(1), 170-180.

Sulzer, J., Haller, S., Scharnowski, F., Weiskopf, N., Birbaumer, N., Blefari, M. L., . . . Goebel, R. (2013). Real-time fMRI neurofeedback: progress and challenges. *NeuroImage, 76*, 386-399.

Tacchino, G., Gandolla, M., Coelli, S., Barbieri, R., Pedrocchi, A., & Bianchi, A. M. (2016). EEG Analysis During Active and Assisted Repetitive Movements: Evidence for Differences in Neural Engagement. *IEEE Transactions on Neural Systems and Rehabilitation Engineering*.

Taheri, H., Rowe, J. B., Gardner, D., Chan, V., Gray, K., Bower, C., . . . Wolbrecht, E. T. (2014). Design and preliminary evaluation of the FINGER rehabilitation robot: controlling challenge and quantifying finger individuation during musical computer game play. *Journal of neuroengineering and rehabilitation, 11*(1), 10.

Taheri, H., Rowe, J. B., Gardner, D., Chan, V., Reinkensmeyer, D. J., & Wolbrecht, E. T. (2012). *Robot-assisted guitar hero for finger rehabilitation after stroke.* Paper presented at the Engineering in medicine and biology society (EMBC), 2012 annual international conference of the IEEE.

Tanji, J., Okano, K., & Sato, K. C. (1988). Neuronal activity in cortical motor areas related to ipsilateral, contralateral, and bilateral digit movements of the monkey. *Journal of neurophysiology, 60*(1), 325-343.

Teasell, R. W., Foley, N. C., Bhogal, S. K., & Speechley, M. R. (2003). An evidence-based review of stroke rehabilitation. *Topics in stroke rehabilitation, 10*(1), 29-58.

Thompson, A. K., Pomerantz, F. R., & Wolpaw, J. R. (2013). Operant conditioning of a spinal reflex can improve locomotion after spinal cord injury in humans. *The Journal of Neuroscience, 33*(6), 2365-2375.

Thompson, A. K., & Wolpaw, J. R. (2015). Targeted neuroplasticity for rehabilitation. *Progress in brain research, 218*, 157-172.

Trombly, C. A., Thayer-Nason, L., Bliss, G., Girard, C. A., Lyrist, L. A., & Brexa-Hooson, A. (1986). The effectiveness of therapy in improving finger extension in stroke patients. *American Journal of Occupational Therapy, 40*(9), 612-617.

Vamvakousis, Z., & Ramirez, R. Towards a Low Cost Mu-Rhythm Based BCI.

van der Lee, J. H., Snels, I. A., Beckerman, H., Lankhorst, G. J., Wagenaar, R. C., & Bouter, L. M. (2001). Exercise therapy for arm function in stroke patients: a systematic review of randomized controlled trials. *Clinical rehabilitation, 15*(1), 20-31.

van Steveninck, R. R. d. R., Lewen, G. D., Strong, S. P., Koberle, R., & Bialek, W. (1997). Reproducibility and variability in neural spike trains. *Science, 275*(5307), 1805-1808.

Veerbeek, J. M., Langbroek-Amersfoort, A. C., van Wegen, E. E., Meskers, C. G., & Kwakkel, G. (2016). Effects of Robot-Assisted Therapy for the Upper Limb After Stroke A Systematic Review and Meta-analysis. *Neurorehabilitation and Neural Repair*, 1545968316666957.

Veerbeek, J. M., van Wegen, E., van Peppen, R., van der Wees, P. J., Hendriks, E., Rietberg, M., & Kwakkel, G. (2014). What is the evidence for physical therapy poststroke? A systematic review and meta-analysis. *PloS one, 9*(2), e87987.

Volpe, B. T., Ferraro, M., Lynch, D., Christos, P., Krol, J., Trudell, C., . . . Hogan, N. (2005). Robotics and other devices in the treatment of patients recovering from stroke. *Current neurology and neuroscience reports, 5*(6), 465-470.

Volpe, B. T., Lynch, D., Rykman-Berland, A., Ferraro, M., Galgano, M., Hogan, N., & Krebs, H. I. (2008). Intensive sensorimotor arm training mediated by therapist or robot improves hemiparesis in patients with chronic stroke. *Neurorehabilitation and Neural Repair, 22*(3), 305-310.

Wagner, T., Valero-Cabre, A., & Pascual-Leone, A. (2007). Noninvasive human brain stimulation. *Annu. Rev. Biomed. Eng., 9*, 527-565.

Warzecha, A.-K., & Egelhaaf, M. (1999). Variability in spike trains during constant and dynamic stimulation. *Science, 283*(5409), 1927-1930.

Webster, B. R., Celnik, P. A., & Cohen, L. G. (2006). Noninvasive brain stimulation in stroke rehabilitation. *NeuroRx, 3*(4), 474-481.

Wege, A., & Zimmermann, A. (2007). *Electromyography sensor based control for a hand exoskeleton.* Paper presented at the Robotics and Biomimetics, 2007. ROBIO 2007. IEEE International Conference on.

Werfel, J., Xie, X., & Seung, H. S. (2005). Learning curves for stochastic gradient descent in linear feedforward networks. *Neural computation, 17*(12), 2699-2718.

Williams, R. J. (1992). Simple statistical gradient-following algorithms for connectionist reinforcement learning. *Machine learning, 8*(3-4), 229-256.

Witham, C. L., Fisher, K. M., Edgley, S. A., & Baker, S. N. (2016). Corticospinal Inputs to Primate Motoneurons Innervating the Forelimb from Two Divisions of Primary Motor Cortex and Area 3a. *Journal of neuroscience, 36*(9), 2605-2616.

Witten, D. M., Tibshirani, R., & Hastie, T. (2009). A penalized matrix decomposition, with applications to sparse principal components and canonical correlation analysis. *Biostatistics, 10*(3), 515-534.

Wolbrecht, E. T., Chan, V., Reinkensmeyer, D. J., & Bobrow, J. E. (2008). Optimizing compliant, model-based robotic assistance to promote neurorehabilitation. *Neural Systems and Rehabilitation Engineering, IEEE Transactions on, 16*(3), 286-297.

Wolpaw, J. R., Birbaumer, N., McFarland, D. J., Pfurtscheller, G., & Vaughan, T. M. (2002). Brain–computer interfaces for communication and control. *Clinical Neurophysiology, 113*(6), 767-791.

Wolpaw, J. R., Braitman, D. J., & Seegal, R. F. (1983). Adaptive plasticity in primate spinal stretch reflex: initial development. *Journal of neurophysiology, 50*(6), 1296-1311.

Wolpaw, J. R., & Carp, J. S. (2006). Plasticity from muscle to brain. *Progress in neurobiology, 78*(3), 233-263.

Wolpaw, J. R., & Tennissen, A. M. (2001). Activity-dependent spinal cord plasticity in health and disease. *Annual review of neuroscience, 24*(1), 807-843.

Wolpert, D. M., Ghahramani, Z., & Jordan, M. I. (1995). An internal model for sensorimotor integration. *SCIENCE-NEW YORK THEN WASHINGTON-*, 1880-1880.

Wu, C.-Y., Hsieh, Y.-W., Lin, K.-C., Chuang, L.-L., Chang, Y.-F., Liu, H.-L., . . . Wai, Y.-Y. (2010). Brain reorganization after bilateral arm training and distributed constraint-induced therapy in stroke patients: a preliminary functional magnetic resonance imaging study. *Chang Gung Med J, 33*(6), 628-638.

Wu, H. G., Miyamoto, Y. R., Castro, L. N. G., Ölveczky, B. P., & Smith, M. A. (2014). Temporal structure of motor variability is dynamically regulated and predicts motor learning ability. *Nature neuroscience, 17*(2), 312-321.

Wyrwicka, W., & Sterman, M. B. (1968). Instrumental conditioning of sensorimotor cortex EEG spindles in the waking cat. *Physiology & Behavior, 3*(5), 703-707.

Xu, J., Ejaz, N., Hertler, B., Branscheidt, M., Widmer, M., Faria, A. V., . . . Celnik, P. A. (2016). Recovery of hand function after stroke: separable systems for finger strength and control. *bioRxiv*, 079269.

Yozbatiran, N., & Cramer, S. C. (2006). Imaging motor recovery after stroke. *NeuroRx, 3*(4), 482-488.

Yuan, H., & He, B. (2014). Brain-Computer Interfaces Using Sensorimotor Rhythms: Current State and Future Perspectives.

Yuan, H., Perdoni, C., & He, B. (2010). Relationship between speed and EEG activity during imagined and executed hand movements. *Journal of neural engineering, 7*(2), 026001.

Zackowski, K., Dromerick, A., Sahrmann, S., Thach, W., & Bastian, A. (2004). How do strength, sensation, spasticity and joint individuation relate to the reaching deficits of people with chronic hemiparesis? *Brain, 127*(5), 1035-1046.

Zemke, A. C., Heagerty, P. J., Lee, C., & Cramer, S. C. (2003). Motor cortex organization after stroke is related to side of stroke and level of recovery. *Stroke, 34*(5), e23-e26.

Zou, H., & Hastie, T. (2005). Regularization and variable selection via the elastic net. *Journal of the Royal Statistical Society: Series B (Statistical Methodology), 67*(2), 301-320.